Mediators of Inflammation

The Immunome in Inflammatory Bowel Disease

Lead Guest Editor: Amedeo Amedei
Guest Editors: Alessio Fasano, Francesco Giudici, and Edda Russo

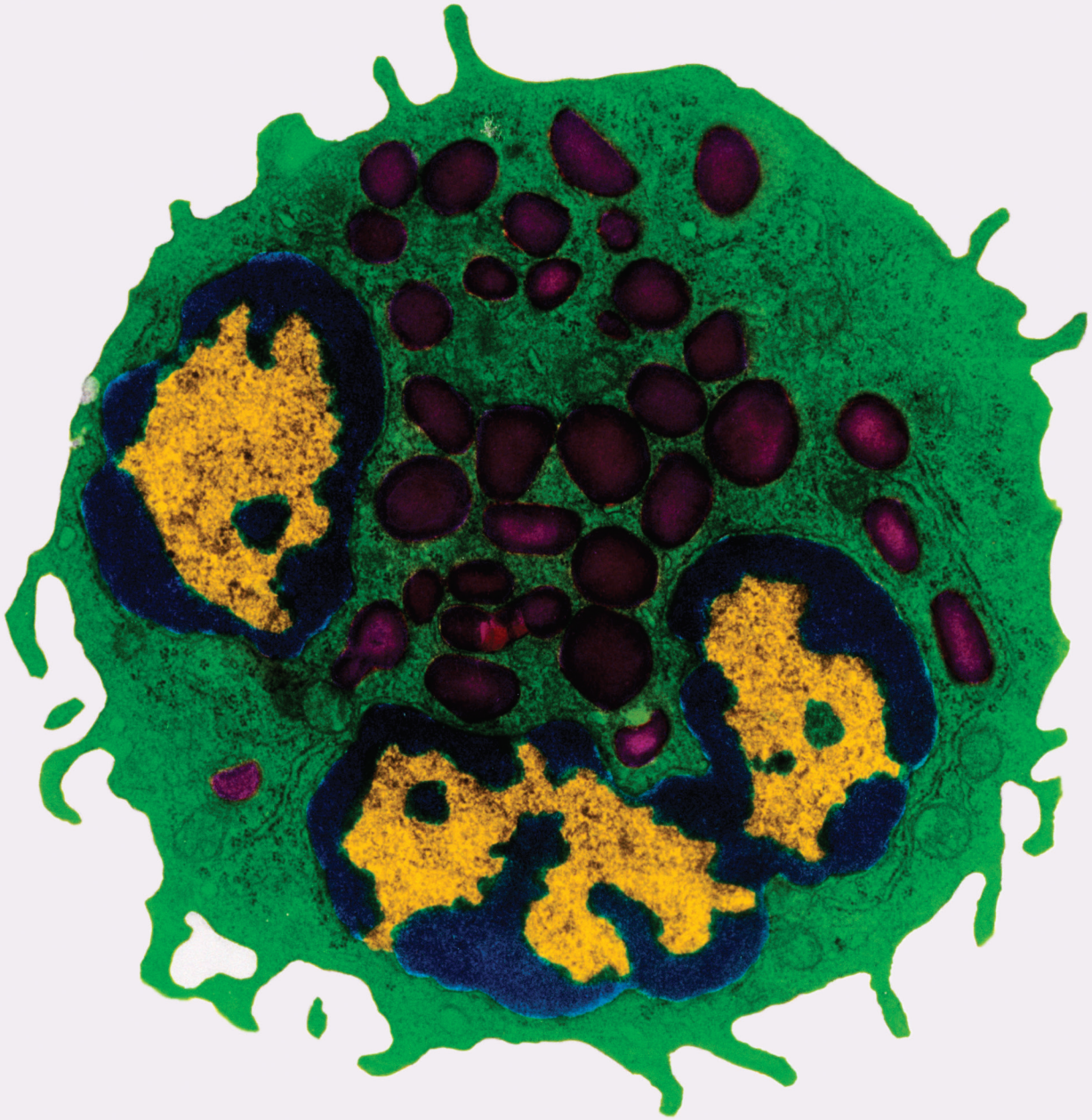

The Immunome in Inflammatory Bowel Disease

Mediators of Inflammation

The Immunome in Inflammatory Bowel Disease

Lead Guest Editor: Amedeo Amedei
Guest Editors: Alessio Fasano, Francesco Giudici, and Edda Russo

Contents

Effect and Mechanism of TL1A Expression on Epithelial-Mesenchymal Transition during Chronic Colitis-Related Intestinal Fibrosis
Jia Wenxiu, Yang Mingyue, Han Fei, Luo Yuxin, Wu Mengyao, Li Chenyang, Song Jia, Zhang Hong, David Q. Shih, Stephan R. Targan, and Zhang Xiaolan
Research Article (21 pages), Article ID 5927064, Volume 2021 (2021)

Xi Lei San Attenuates Dextran Sulfate Sodium-Induced Colitis in Rats and TNF-α-Stimulated Colitis in CACO2 Cells: Involvement of the NLRP3 Inflammasome and Autophagy
Zhang Tao, Xiaoqing Zhou, Yan Zhang, Wenfeng Pu, Yi Yang, Fuxia Wei, Qian Zhou, Lin Zhang, Zhonghan Du, and Ji Wu
Research Article (12 pages), Article ID 1610251, Volume 2021 (2021)

Long-Term Follow-Up, Association between CARD15/NOD2 Polymorphisms, and Clinical Disease Behavior in Crohn's Disease Surgical Patients
Francesco Giudici, Tiziana Cavalli, Cristina Luceri, Edda Russo, Daniela Zambonin, Stefano Scaringi, Ferdinando Ficari, Marilena Fazi, Amedeo Amedei, Francesco Tonelli, and Cecilia Malentacchi
Research Article (11 pages), Article ID 8854916, Volume 2021 (2021)

Mica Can Alleviate TNBS-Induced Colitis in Mice by Reducing Angiotensin II and IL-17A and Increasing Angiotensin-Converting Enzyme 2, Angiotensin 1-7, and IL-10
Mengdie Shen, Bibi Zhang, Mengyao Wang, Li'na Meng, and Bin Lv
Research Article (8 pages), Article ID 3070345, Volume 2020 (2020)

Hindawi
Mediators of Inflammation
Volume 2021, Article ID 5927064, 21 pages
https://doi.org/10.1155/2021/5927064

Research Article

Effect and Mechanism of TL1A Expression on Epithelial-Mesenchymal Transition during Chronic Colitis-Related Intestinal Fibrosis

Jia Wenxiu,[1] **Yang Mingyue**,[1] **Han Fei**,[1] **Luo Yuxin**,[1] **Wu Mengyao**,[1] **Li Chenyang**,[1] **Song Jia**,[1] **Zhang Hong**,[1] **David Q. Shih**,[2] **Stephan R. Targan**,[2] **and Zhang Xiaolan**[1]

[1]*Department of Gastroenterology, The Second Hospital of Hebei Medical University, Hebei Key Laboratory of Gastroenterology, Hebei Institute of Gastroenterology, No. 80 Huanghe Road, Yuhua District, Shijiazhuang, Hebei, China*
[2]*F. Widjaja Foundation Inflammatory Bowel and Immunobiology Research Institute, Cedars-Sinai Medical Center, Los Angeles, CA, USA*

Correspondence should be addressed to Zhang Xiaolan; xiaolanzh@126.com

Received 19 April 2020; Revised 30 March 2021; Accepted 28 May 2021; Published 25 June 2021

Academic Editor: Edda Russo

Background and Aims. Recent evidences reveal that epithelial to mesenchymal transition (EMT) exacerbates the process of intestinal fibrosis. Tumor necrosis factor-like ligand 1A (TL1A) is a member of the tumor necrosis family (TNF), which can take part in the development of colonic inflammation and fibrosis by regulating immune response or inflammatory factors. The purpose of this study was to elucidate the possible contribution of TL1A in onset and progression of intestinal inflammation and fibrosis through EMT. *Methods*. Colonic specimens were obtained from patients with inflammatory bowel disease (IBD) and control individuals. The expression levels of TL1A and EMT-related markers in intestinal tissues were evaluated. Furthermore, the human colorectal adenocarcinoma cell line, HT-29, was stimulated with TL1A, anti-TL1A antibody, or BMP-7 to assess EMT process. In addition, transgenic mice expressing high levels of TL1A in lymphoid cells were used to further investigate the mechanism of TL1A in intestinal fibrosis. *Results*. High levels of TL1A expression were detected in the intestinal specimens of patients with ulcerative colitis and Crohn's disease and were negatively associated with the expression of an epithelial marker (E-cadherin), while it was positively associated with the expression of interstitial markers (FSP1 and α-SMA). Transgenic mice with high expression of TL1A were more sensitive to dextran sodium sulfate and exhibited severe intestinal inflammation and fibrosis. Additionally, the TGF-β1/Smad3 pathway may be involved in TL1A-induced EMT, and the expression of IL-13 and EMT-related transcriptional molecules (e.g., ZEB1 and Snail1) was increased in the intestinal specimens of the transgenic mice. Furthermore, TL1A-induced EMT can be influenced by anti-TL1A antibody or BMP-7 *in vitro*. *Conclusions*. TL1A participates in the formation and process of EMT in intestinal fibrosis. This new knowledge enables us to better understand the pathogenesis of intestinal fibrosis and identify new therapeutic targets for its treatment.

1. Introduction

In patients with inflammatory bowel disease (IBD), recurrent intestinal inflammation triggers mucosal healing reactions, leading to extracellular matrix (ECM) deposition in the intestine to form intestinal fibrosis [1]. As many as one-third of patients with Crohn's disease (CD) develop end-stage fibrotic disease characterized by stenosis and organ failure [2, 3], and 80% of cases require surgical resection of the fibrotic intestinal tissue. Unfortunately, the recurrence rate is as high as 70% [4]. Ulcerative colitis (UC) has long been believed to be a nonfibrotic disease; however, recent studies have found a certain degree of submucosal fibrosis in almost all colon resection specimens from patients with UC [5–7]. Identifying effective treatment for intestinal fibrosis-induced by IBD has become the focus of investigations worldwide.

Myofibroblasts are important effector cells for the deposition of ECM in intestinal fibrosis, and their sources are varied

[8]. Exploration into the origins of myofibroblasts may provide an opportunity to develop effective treatments in intestinal fibrosis. An increasing number of studies indicate that epithelial to mesenchymal transition (EMT) is involved in intestinal fibrosis [9]. During this process, epithelial cells lose polarity as well as tight junctions, transform into interstitial cells, and produce a large amount of ECM deposited in the intestine, resulting in intestinal lumen narrowing [10]. Experiments with a transgenic mouse model with epithelial-driven expression of fluorescent reporters, indicate that about one-third of $FSP1^+$ fibroblasts are derived from intestinal epithelial cells [11]. EMT can also be observed *in vitro*. For example, rat intestinal epithelial cells (IEC-6) displayed an irregular polygonal shape in control medium but obtained a spindle-shaped morphology after exposure to TGF-β1 for seven days [11]. Another study showed that parathyroid hormone-like hormone (PTHLH) was capable of increasing vimentin and FSP1 expression and reducing E-cadherin expression in a concentration- and time-dependent manner. Furthermore, exposure to PTHLH leads to collagen deposition [12]. All of these studies suggest that EMT may be an important mechanism in the development of intestinal fibrosis.

The process of EMT is regulated by a complex cell signaling pathway and gene regulation. The TGF-β1/Smad3 pathway is the most classical pathway involving TGF-β1 [13]. However, exploring when and how it occurs may lead to effective treatment strategies for intestinal fibrosis. Genome-wide association studies (GWAS) have emphasized that the gene encoding tumor necrosis factor-like ligand 1A (TL1A) is associated with susceptibility to UC and CD and is upregulated in both UC and CD patients [14–16]. In recent years, studies have shown that TL1A participates in the development of intestinal inflammation and fibrosis [17, 18]. Moreover, mice with high expression of TLIA can develop spontaneous ileitis, proximal colitis, and even fibrosis, which is associated with elevated levels of fibrotic factor interleukin-13 (IL-13). Elevated secretion of IL-13 is tightly associated with the expression of TL1A in the transgenic mouse model described above [19, 20], and the fourth European Crohn's and Colitis Organisation (ECCO) guidelines state that the TGF-β1/Smad3 pathway activated by IL-13 is a central process in the formation of intestinal fibrosis [21].

Further study has shown that in colitic mice with adoptively transferred T cells, intestinal inflammation and fibrosis could be alleviated with the treatment of anti-TL1A antibodies, which reduce the expression of α-SMA and vimentin and inhibit the TGF-β1/smad3 pathway [22]. Recombinant human bone morphogenetic protein-7 (BMP-7), which belongs to the TGF-β superfamily, reverses TGF-β1-induced EMT in intestinal fibrosis both *in vitro* and *in vivo* [11].

Therefore, we hypothesized that TL1A promotes intestinal fibrosis by inducing EMT. In this study, we evaluated the correlation between TL1A expression and changes in EMT-related markers in patients with UC or CD. Furthermore, wild-type (WT) mice and TL1A transgenic (Tg) mice were used to establish a chronic colitis-associated intestinal fibrosis model. Moreover, HT-29 cells were stimulated with TL1A, anti-TL1A antibodies, and BMP-7, and the changes in EMT-related markers were evaluated. The effects and mechanisms of TL1A on EMT are discussed in order to bring forward new theoretical bases for the treatment of intestinal fibrosis.

2. Methods

2.1. Human Tissues. Twelve patients with UC (male/female: 6/6) and ten patients with CD (male/female: 4/6) were enrolled in this study from the Second Hospital of Hebei Medical University (Shijiazhuang, China). The diagnosis of IBD was based on standard clinical, endoscopic, radiological, and histological findings. Normal colonic samples were taken from 8 control individuals (male/female: 4/4), who underwent colonoscopy for other reasons and were found to be normal in examination and histology. The clinical characteristics and inflammatory markers of the three groups are shown in Tables 1 and 2. The age, sex, and other relevant markers of the three groups were matched. This study has been approved by the Ethics Committee of Hebei Medical University.

2.2. Mice and Treatment. LCK-CD2-TL1A-GFP-transgenic (Tg) mice overexpressing TL1A in lymphocytes, and wild-type (WT) mice applied in this study, were in the C57BL/6J genetic background. The Tg mice were brought from American Cedars-Sinai Medical Center and Immunology Research Center. All mice were matched by age (8–10 weeks), weight (20–22 g), and sex (female). The animals were housed under specified pathogen-free conditions. The genotypes of the mice used in this study were confirmed through PCR (Supplementary Figure 1). There were four experimental groups: the control/WT group ($n = 8$), the control/Tg group ($n = 8$), the dextran sodium sulfate (DSS)/WT group ($n = 8$), and the DSS/Tg group ($n = 10$). A chronic colitis-related intestinal fibrosis model was generated by the administration of DSS for three cycles. One cycle consisted of 2% DSS in drinking water for seven days followed by normal drinking water for two weeks. All experiments were carried out in accordance with the Ethics Committee of Hebei Medical University.

2.3. Evaluation of the Severity of Intestinal Inflammation. The general condition of the mice was observed daily, and the body weights were measured every four days. On the last day of modeling, disease activity index (DAI) scores were performed based on mouse body weight, stool characteristics, and fecal occult blood to assess colonic inflammation [23]. After the mice were euthanized, the colon was removed to record the length and weight, and used for further analyses. Tissue sections of 4 μm were cut from formalin-fixed paraffin-embedded colon tissue blocks and were dewaxed in xylene and rehydrated in graded alcohol washes, then stained with hematoxylin and eosin (H&E) staining to assess histopathological inflammation. Macroscopic scoring and microscopic scoring [24] were used to assess the histological damage. To further evaluate inflammatory cell infiltration, myeloperoxidase (MPO) activity was detected using the

Table 1: Patient characteristics of human samples.

	Controls ($n = 8$)	UC ($n = 12$)	CD ($n = 10$)
Mean age (year, range)	45.5 ± 9.68	40.25 ± 13.05	37.40 ± 12.55
Females	4 (50%)	6 (50%)	6 (60%)
Males	4 (50%)	6 (50%)	4 (40%)
Mean disease duration (year, range)	0	6.25 ± 2.14	6.80 ± 2.25
Disease activity			
No	8 (100%)	0 (0%)	0 (0%)
Low	0	3 (25%)	3 (30%)
Moderate	0	5 (41.67%)	5 (50%)
Strong	0	4 (33.33%)	2 (20%)

UC: ulcerative colitis; CD: Crohn's disease. Disease activity based on modified Mayo score. Data are expressed as mean ± SD.

Table 2: Inflammation markers in IBD patients and controls.

	Control ($n = 8$)	UC ($n = 12$)	CD ($n = 10$)
WBC ($/mm^3 \times 10^3$)	5.11 ± 0.85	7.16 ± 1.88*	6.95 ± 1.82*
hsCRP (mg/L)	1.35 ± 1.44	28.43 ± 34.23*	24.15 ± 22.61*
ESR (mm/h)	4.50 ± 2.14	23.41 ± 14.03**	20.90 ± 12.66**
HGB (g/L)	134.50 ± 13.44	119.42 ± 19.51	128.10 ± 19.30
NE ($/mm^3 \times 10^3$)	3.01 ± 0.60	4.45 ± 1.58*	3.54 ± 1.46
PLT	240.05 ± 61.72	270.61 ± 78.08*	355.53 ± 120.73
ALB	44.8 ± 52.89	36.00 ± 6.95**	37.53 ± 4.43**

WBC: white blood cell; hsCRP: high-sensitivity C-reactive protein; ESR: erythrocyte sedimentation rate; HGB: hemoglobin; NE: neutrophil; PLT: blood platelet; ALB: albumin. Data are expressed as mean ± SD. As compared to the control group: $^*P < 0.05$; $^{**}P \leq 0.01$; $^{***}P \leq 0.001$.

Myeloperoxidase Activity Assay Kit (Nanjing Jiancheng Bioengineering Institute, China).

2.4. Evaluation of Fibrosis and Chronic Wound Healing. Sirius red staining was conducted to evaluate collagen deposition in colonic tissue specimens embedded in paraffin. Furthermore, *Image-Pro Plus* software (IPP 6.0) was used to evaluate the percent of fibrotic area in IBD and control patients [12]. And fibrosis scoring criteria [25] (Supplementary Table 1) was used to evaluate the fibrosis level in mice. Next, the relative minimal and maximal thickness of submucosa were also calculated in mice [26]. In addition, a hydroxyproline assay was performed to assess collagen content in the colon tissues.

2.5. Cell Culture and Cell Viability Assay. The human HT-29 cell line was obtained from the Chinese Academy of Sciences Cell Bank (Shanghai, China) and cultured in McCoy's 5A medium with 10% fetal bovine serum, penicillin (100 units/ml), and streptomycin (100 μg/ml). Cells were grown at 37°C in a 5% CO_2 atmosphere. Cell Counting Kit-8 assay (CCK-8) was used to detect cell viability. HT-29 cells were seeded 100 μL per well at a density of 1×10^4 cells/well in 96-well plates. When the cell growth reaches logarithmic phase, serum-free media with different concentrations (0 ng/mL, 20 ng/mL, 50 ng/mL, 100 ng/mL, and 150 ng/mL) of TL1A replaced the complete culture medium. After incubating for 12, 24, 48, or 72 h, 10 μL CCK-8 was added to each well and incubated at 37°C for an additional 1 h. Then, the optical densities (OD) under 450 nm were recorded. Based on the results (Supplementary Figure 2), a concentration of 50 ng/mL of TL1A was applied in subsequent experiments.

2.6. Immunofluorescence Staining. Colonic tissues and HT-29 cells were treated with 0.5% Triton X-100 for permeability. After blocking with 10% goat serum, sections were incubated with primary antibodies (E-cadherin and FSP1) overnight at 4°C. The sections were then stained with secondary antibodies conjugated with either FITC or Cy3. Nuclei appeared blue with 4′6-diamidino-2-phenylindole (DAPI) staining (Beyotime, Shanghai, China). A laser scanning confocal microscope FV12-IXCOV (Olympus, Japan) were used to obtain images. The mean optical density of images was calculated through Image-Pro Plus software to analyze the positive expression.

2.7. Immunohistochemical Staining. Paraffin-embedded mucosal biopsy specimens and mice colonic tissues (4 μm thick sections) were incubated in antigen retrieval solution for 10 min at 95°C. After cooling at room temperature, peroxidases were inhibited with 3% H_2O_2 for 10 minutes. Sections were then treated with 10% goat serum for 30 minutes before incubating with primary antibodies (β-catenin, E-cadherin, α-SMA, FSP1, IL-13, TGF-β1, Smad3, Snail, and ZEB1). After washing with PBS three times for 10 minutes, sections were incubated with secondary antibodies for 30 minutes at

room temperature. Then, according to the manufacturer's protocol, sections were incubated with the DAB detection kit, then stained with H&E. Three fields of view (400x) of each slice are calculated through Image-Pro Plus software to analyze the positive expression. We obtained the mean optical density value of each group and produced a histogram to show the results.

2.8. Western Blot. Proteins from the WT and Tg mouse colonic specimens and HT-29 cells were extracted and concentrations were quantified by the BCA method. Total protein was separated on an SDS-PAGE gel system, then transferred to a PVDF membrane (0.22 μm, Millipore Corp., Billerica, MA, USA). The blot with separated proteins was incubating with primary antibodies (against collagen I, collagen III, β-catenin, E-cadherin, α-SMA, FSP1, IL-13, TGF-β1, Smad3, Snail1, ZEB1, and GAPDH) overnight at 4°C. After washing with Tris-buffered saline-Tween (TBST), the membranes were incubated with fluorescently labeled secondary antibody for 1 h at room temperature. The developed protein bands were quantified using ImageJ and normalized with GAPDH internal controls.

2.9. Real-Time Reverse Transcription-Polymerase Chain Reaction (RT-PCR). Total RNA was extracted from WT and Tg mouse colonic tissues or HT-29 cells following the manufacturer's guidelines and reversed transcribed into cDNA by PrimeScript qRT-PCR Kit (TaKaRa, China). The RT-PCR analysis was performed using SYBR® GreenER™ qPCR SuperMix kit (Invitrogen, Carlsbad, CA) on a 7500 Real-time system (Applied Biosystems, USA). Primer sequences are listed in Supplementary Table 2. GAPDH was used as an internal standard. Data were calculated by the comparative cycle threshold (CT) ($2^{-\Delta\Delta CT}$) method.

2.10. Quantification of Cytokines by Enzyme-Linked Immunosorbent Assay (ELISA). According to manufacturer's instructions, the expression levels of IL-13 and TGF-β1 in serum of WT mice and Tg mice were detected using an ELISA kit (R&D, Minneapolis, USA). Changes in absorbance were determined by spectrophotometry at 450 nm wavelength.

2.11. Statistical Analysis. Statistical analysis was performed using IBM SPSS Statistics 22.0 (SPSS Inc., Chicago, IL, USA). Data were represented as mean ± standard deviation (SD). The Kolmogorov-Smirnov test was used to test the normal distribution of quantitative data. If the data were normally distributed, one-way ANOVA and the Student-Newman-Keuls (SNK) post hoc tests were used to determine the statistical significance between multiple groups; if not, the Kruskal-Wallis test and the Nemenyi post hoc test were used. The relationship between continuous variables were represented by the Pearson correlation analysis. Differences were noted as significant at $^{*}P < 0.05$, $^{**}P < 0.01$, and $^{***}P < 0.001$.

3. Results

3.1. Evidence for Intestinal Fibrosis and EMT in Patients with IBD. Inflammation destroys the gastrointestinal epithelial barrier, and barrier dysfunction, in turn, causes further spread of inflammation. We collected serum and intestinal samples from 8 controls and 12 UC and 10 CD patients for this study. Serum inflammation marker high-sensitivity C-reactive protein (hsCRP), erythrocyte sedimentation rate (ESR), and white blood cell (WBC) were increased in IBD patients compared with the control group (Table 2). Further, H&E staining revealed that the colonic mucosa was intact in the control group, while erosions and ulcers appeared in the IBD group (Figure 1(a)). Sirius red staining, applied to evaluate collagen deposition and degree of fibrosis in UC and CD intestinal mucosa, revealed substantial collagen deposition as well as fibrotic alterations in the colon tissues of CD and UC patients compared with controls (Figure 1(a)). Fibrosis area was significantly higher in the UC and CD groups than in the control group (Figure 1(b)). To verify the occurrence of EMT, double-label immunofluorescence staining was performed to determine the colocalization of E-cadherin and FSP1. There were more double-positive cells detected in the colon tissues of UC and CD patients than in the control group (Figure 1(c)).

3.2. TL1A Expression Was Markedly Increased in IBD Colon and Correlated with Degree of Fibrosis and EMT-Related Markers. To explore the possible contribution of TL1A in IBD, the expression of TL1A was detected in colonic tissues from controls and patients with UC and CD by immunohistochemical staining. β-Catenin membrane staining in IBD patients was weaker than the control group, and more cells have nuclear staining, indicating that β-catenin has transcriptional activity (Figure 1(d)). While in healthy tissues, TL1A immunoreactivity was weak, while the majority of UC and CD patients displayed increased expression of TL1A in their colon tissues (Figure 1(d)). The mean optical density values of TL1A in the UC and CD groups were nearly 2-fold higher than that in the control group (Figure 1(d)). Next, the expression of epithelial cell marker E-cadherin, and myofibroblast markers FPS1 and α-SMA, was also assessed by immunohistochemical staining. E-cadherin expression stained more strongly in normal intestinal tissues than in UC and CD tissues (Figure 1(d)). In contrast, positive immunostaining for α-SMA and FPS1 exhibited increased intensity in UC and CD intestinal tissues. Altogether, these results confirm the appearance of EMT in IBD colon tissues (Figure 1(d)). Furthermore, the Pearson correlation and linear regression analyses were applied to explore the relationship between TL1A and EMT-related markers, which demonstrated that TL1A expression is negatively associated with E-cadherin expression (Figure 1(e)), while it is positively associated with nuclear localization of β-catenin, α-SMA, and FSP1 expression levels and fibrosis area (Figure 1(e)). Therefore, TL1A is likely to be involved in the EMT process in intestinal fibrosis.

3.3. Mice with High Expression of TL1A after DSS Induction Had More Severe Intestinal Inflammation. To further determine the contribution of TL1A in colonic inflammation, we

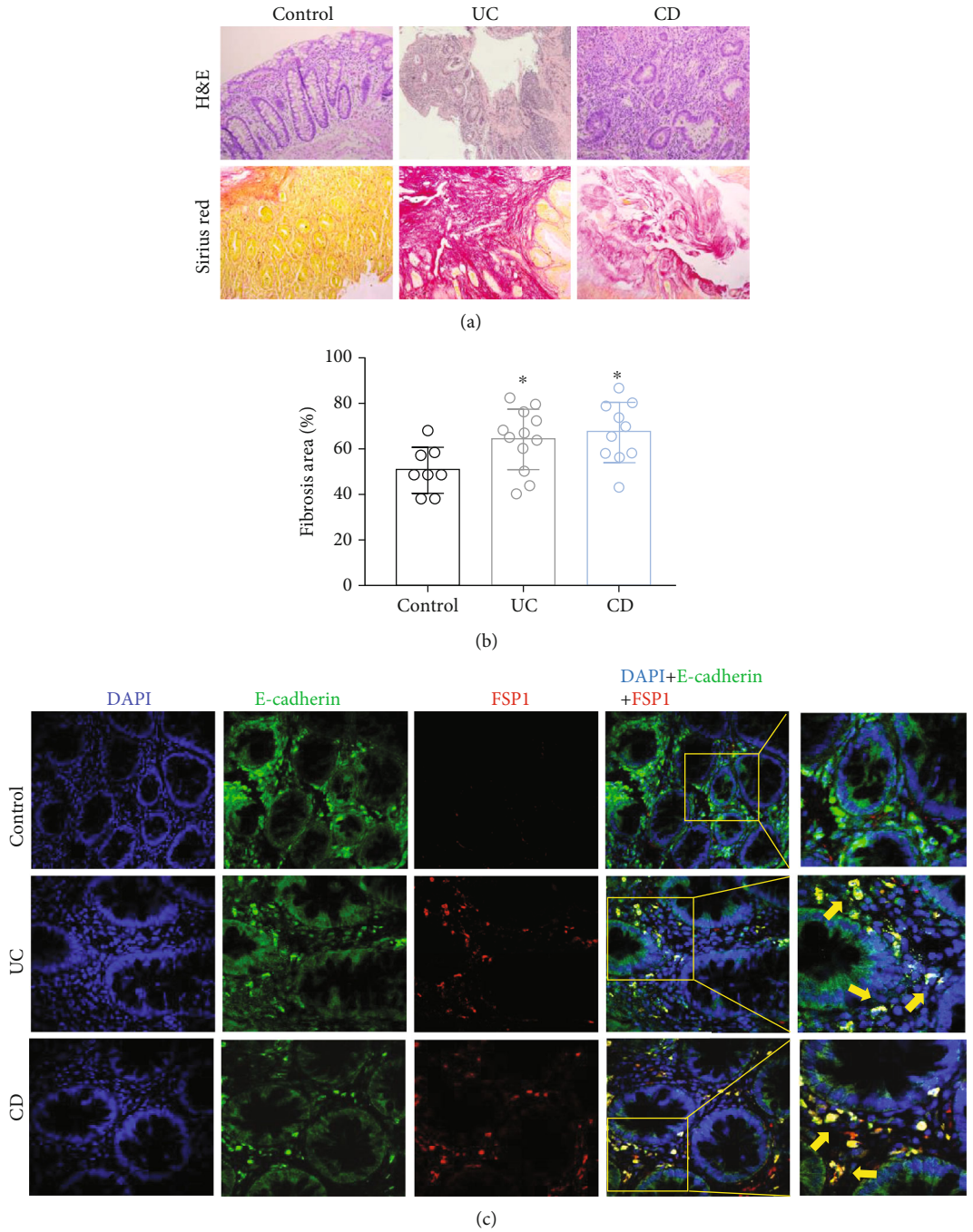

Figure 1: Continued.

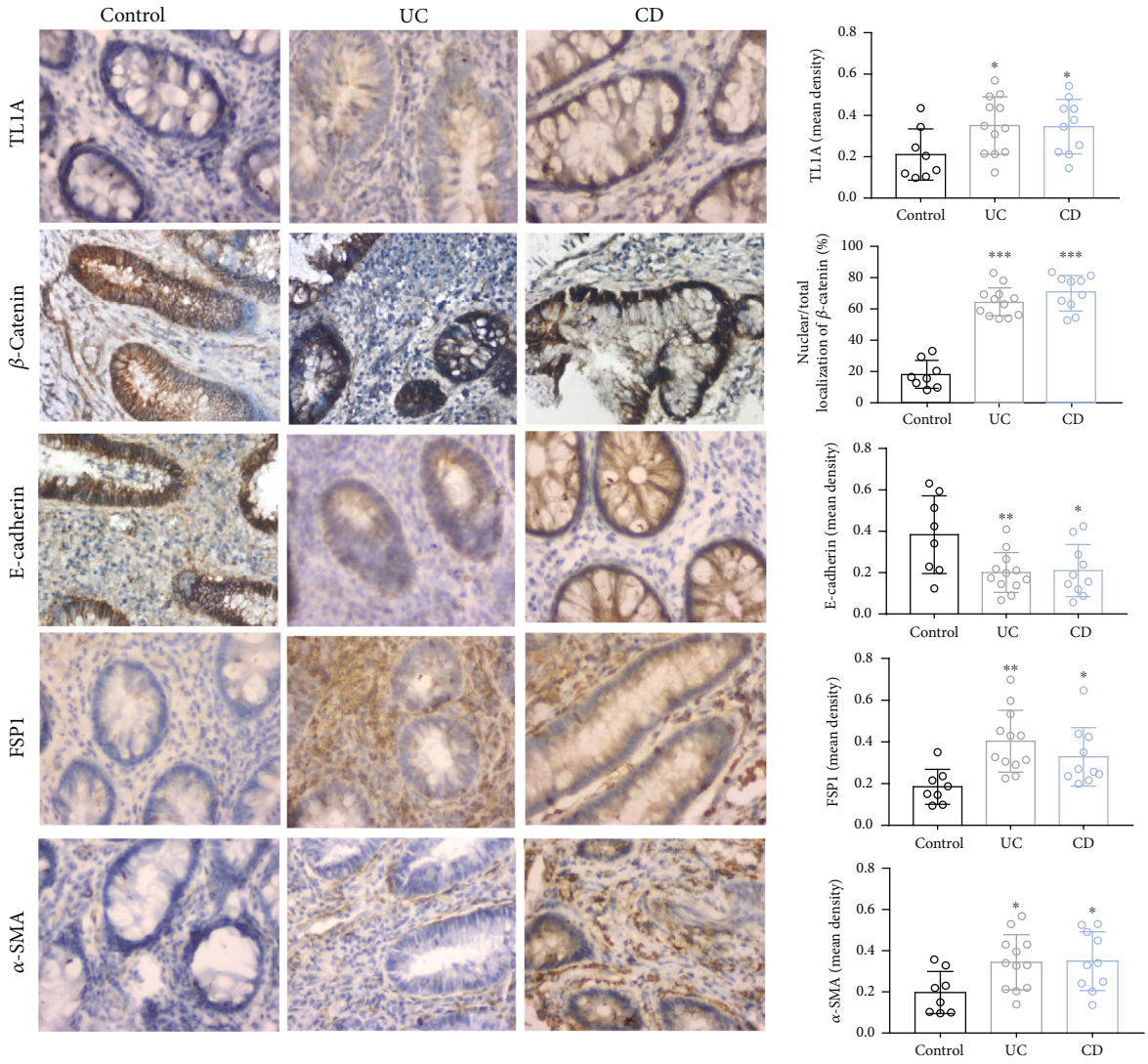

(d)

Figure 1: Continued.

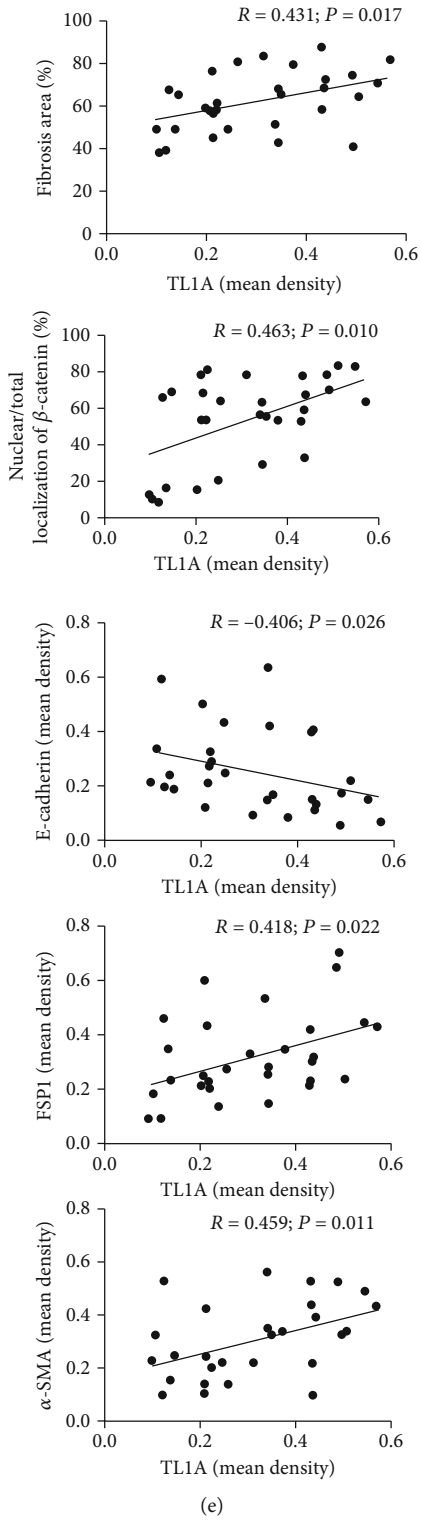

(e)

Figure 1: TL1A in colon tissue of patients with ulcerative colitis (UC) and Crohn's disease (CD) correlates with fibrosis score and EMT-related markers. Colon tissues from CD patients ($n = 10$), UC patients ($n = 12$), and controls ($n = 8$) were included. (a, b) Representative microscopic images of hematoxylin and eosin- (H&E-) stained paraffin-embedded colonic tissue samples (100x), and the quantitative determination of fibrosis area based on Sirius red staining (100x). (c) Immunofluorescence double staining. E-cadherin (green), α-SMA (red), and colocalization (yellow) in colon tissue samples of IBD patients and controls (400x). DAPI stains nuclei (blue). (d) Immunohistochemical staining of β-catenin, TL1A, E-cadherin, FSP1, and α-SMA in colon tissues of controls and IBD patients (400x), and mean density of nuclear localization of β-catenin and expressions of TL1A, FSP1, and α-SMA were increased in the UC and CD groups; however, the mean density of E-cadherin was decreased in the UC and CD groups. (e) Pearson's correlation and linear analysis. Data were given as mean ± standard deviation (SD). As compared to the control group: $^{*}P < 0.05$, $^{**}P \leq 0.01$, and $^{***}P \leq 0.001$.

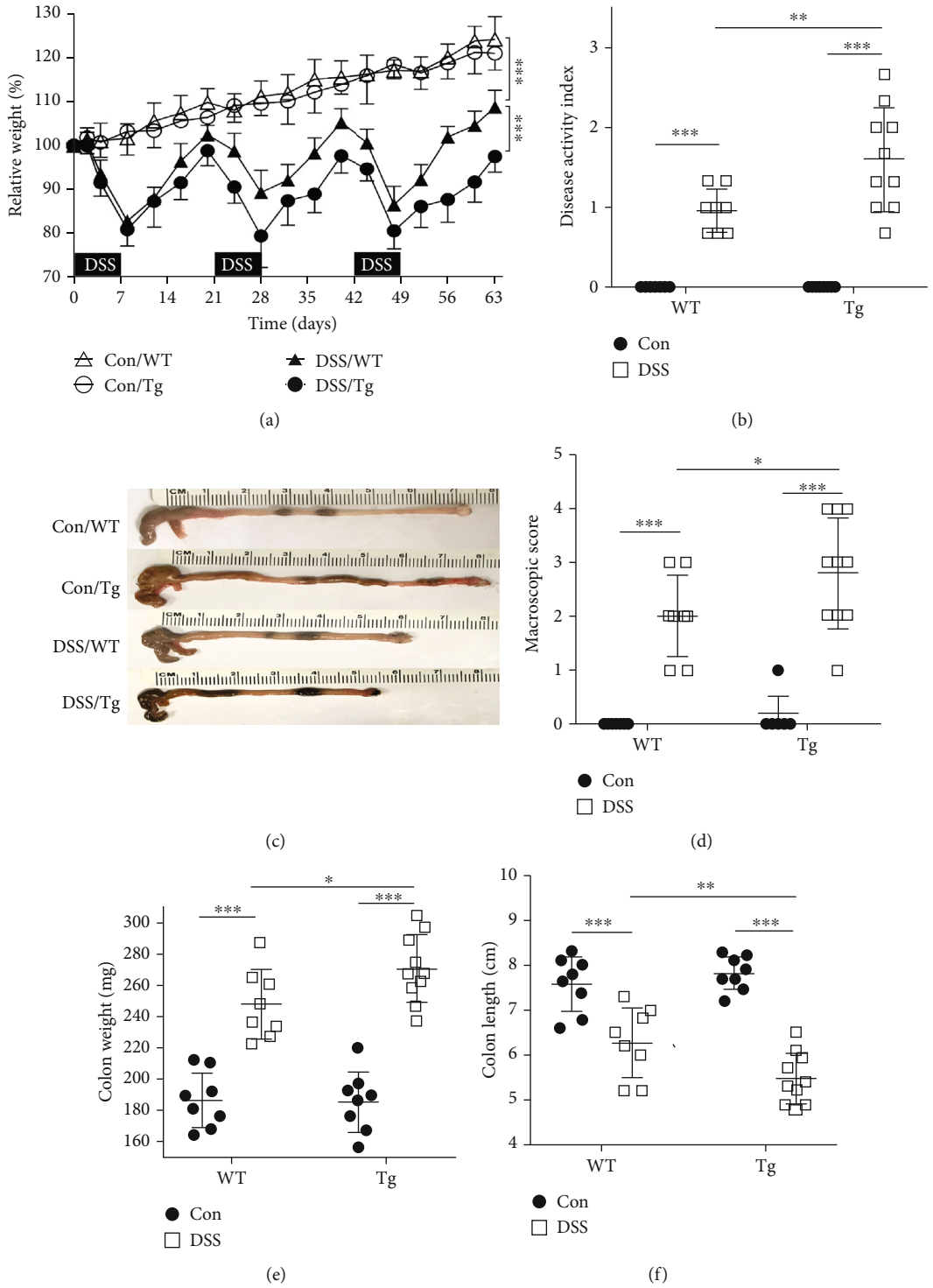

Figure 2: Continued.

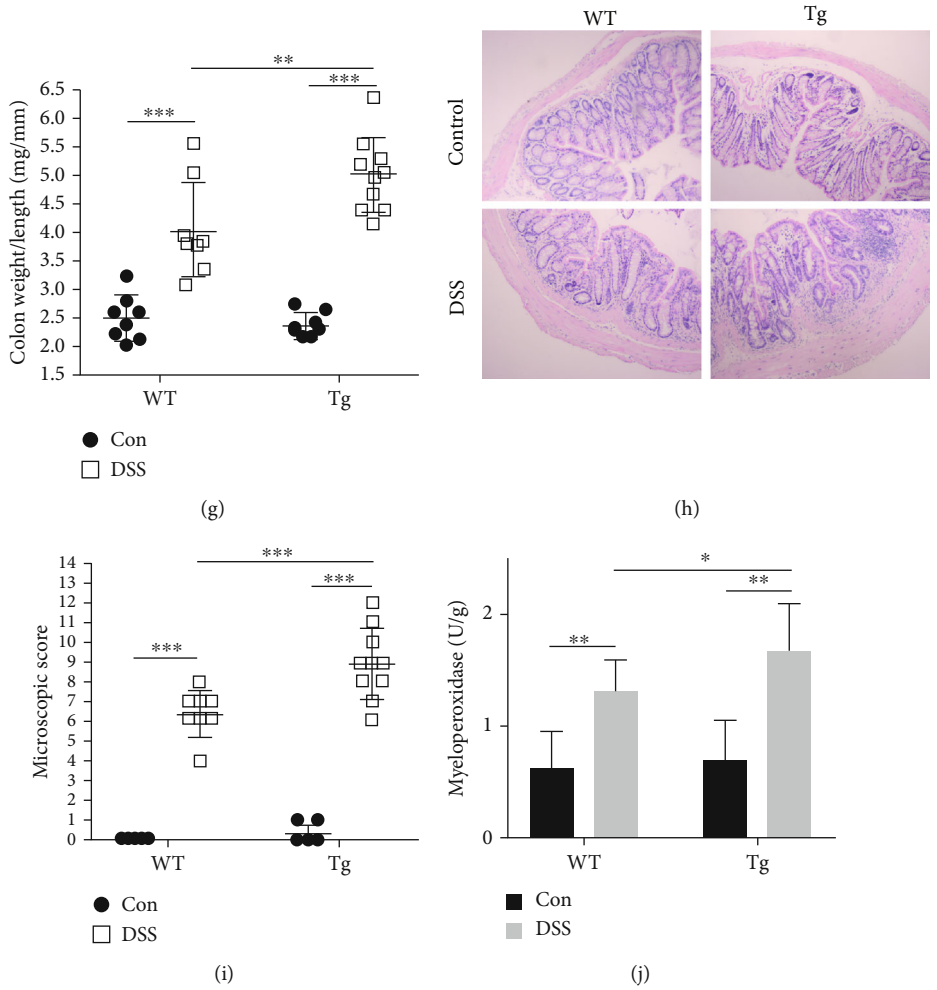

FIGURE 2: TL1A promotes colon inflammation in the DSS-induced intestinal fibrosis model. Transgenic (Tg) and wildtype (WT) mice were subjected to 2.0% dextran sulfate sodium (DSS) to generate an intestinal fibrosis model. There were four study groups: control/WT group ($n = 8$), control/Tg group ($n = 8$), DSS/WT group ($n = 8$), and DSS/Tg group ($n = 10$). (a) The percent change in body weight of mice during modeling. (b) Postmodeling disease activity index (DAI) based on body weight, stool characteristics, and fecal occult blood of mice. (c, d) Macroscopic damage and score. (e) Weight of colon. (f) Length of colon. (g) Colon weight/length ratio. (h) Representative images of H&E-stained colonic tissue sections of WT and Tg mice (100x). (i) Microscopic damage score. (j) Myeloperoxidase (MPO) activity. Data were given as mean ± standard deviation (SD). As compared to the control group: $^{*}P < 0.05$, $^{**}P \leq 0.01$, and $^{***}P \leq 0.001$.

divided WT mice and Tg mice each into two groups to administrate normal drinking water or 2% DSS as described above. After nine weeks, DAI scores and histopathological indicators were evaluated. During modeling, after drinking 2.0% DSS, the mice showed soft or loose, and visibly bloody stools, and a fluctuating decline in body weight, especially in the DSS/Tg group (Figure 2(a)). Meanwhile, the DAI score, which is performed based on mouse body weight, stool characteristics, and fecal occult blood increased more in the DSS/Tg group than in the DSS/WT group (Figure 2(b)). After the mice were euthanized, the colon was removed for macroscopic damage scoring. The control group (fed water without DSS) had no edema in the colon, while the intestinal mucosa of the DSS group showed hyperemic and edematous mucosa with thickening of the intestinal wall (Figure 2(c)). The macroscopic damage score in the DSS/Tg group was significantly higher than that in the DSS/WT group (Figure 2(d)). The DSS/Tg group had shorter colon length (Figure 2(f)), heavier colon weight (Figure 2(e)), and therefore, higher colon weight-to-length ratio (Figure 2(g)) than the DSS/WT group. These differences were statistically significant. H&E staining displayed that the colonic mucosal epithelium of the control group was intact and the glands were neatly arranged. However, in the DSS group, the colonic mucosal epithelium was destroyed, goblet cells were reduced or even missing, and neutrophils and lymphocytes had infiltrated the tissue (Figure 2(h)). The colonic microscopic damage score was significantly higher in the DSS/Tg group than that in the DSS/WT group (Figure 2(i)). MPO activity in the colon tissue reflects infiltration of inflammatory cells into the intestinal tissue. Compared with the DSS/WT group, MPO content was significantly increased in the DSS/Tg group (Figure 2(j)). The above results show that Tg mice with a high expression of TL1A are susceptible to inflammation in the colon.

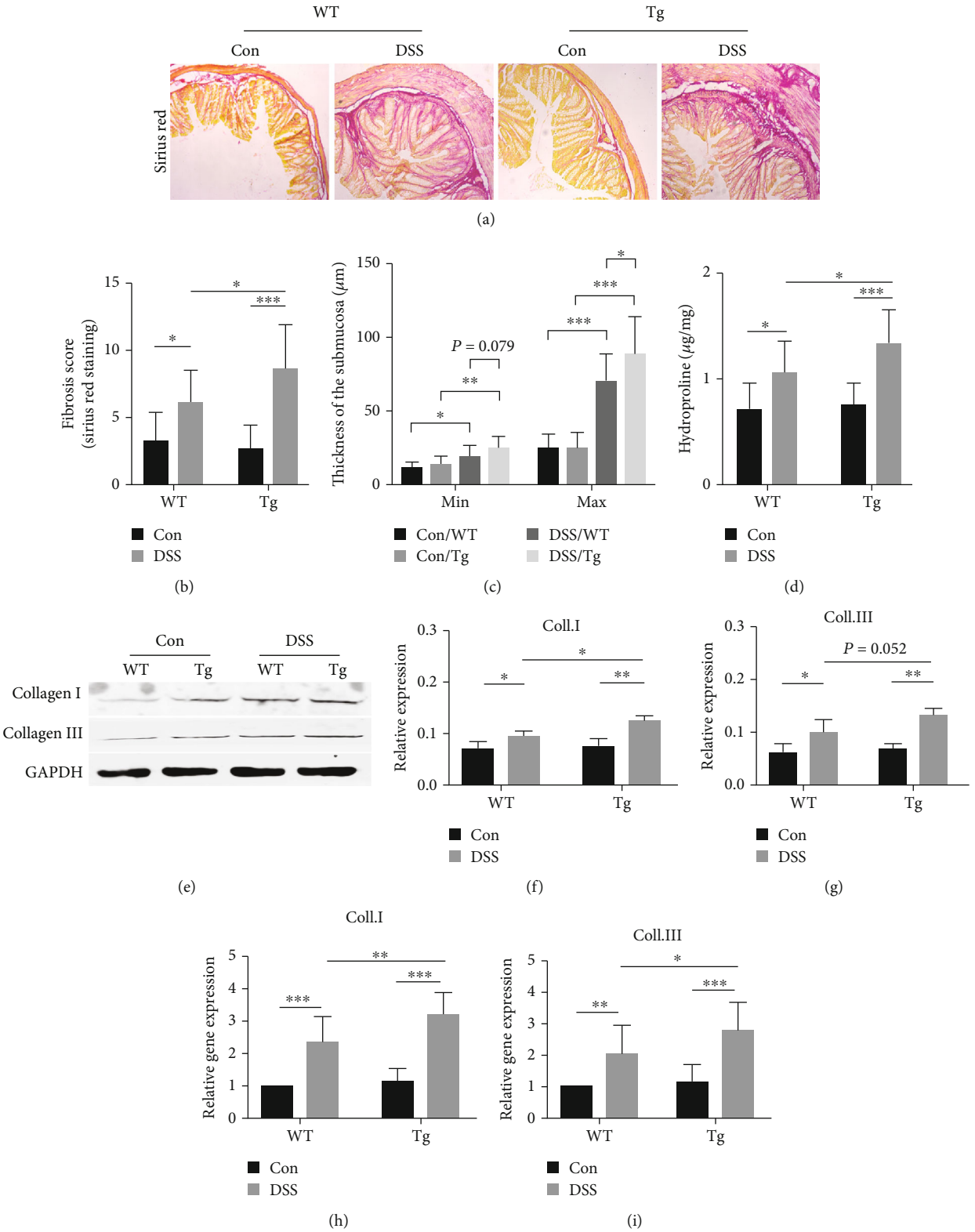

Figure 3: TL1A promotes colon fibrosis in the DSS-induced intestinal fibrosis model. (a) Sirius red staining of collagen deposition in colon from wild type and transgenic (Tg) mice overexpressing TL1A (100x). (b) Fibrosis scores reflect fibrotic alterations of colonic sections. (c) The relative minimal (min) and maximal (max) width of submucosa in mice. (d) Hydroxyproline content. (e–g) Western blot analysis of collagen I and collagen III in colonic tissues normalized with GAPDH. (h, i) RT-PCR detection of collagen I and collagen III mRNA. Data were given as mean ± standard deviation (SD). As compared to the control group: $^{*}P < 0.05$, $^{**}P \leq 0.01$, and $^{***}P \leq 0.001$.

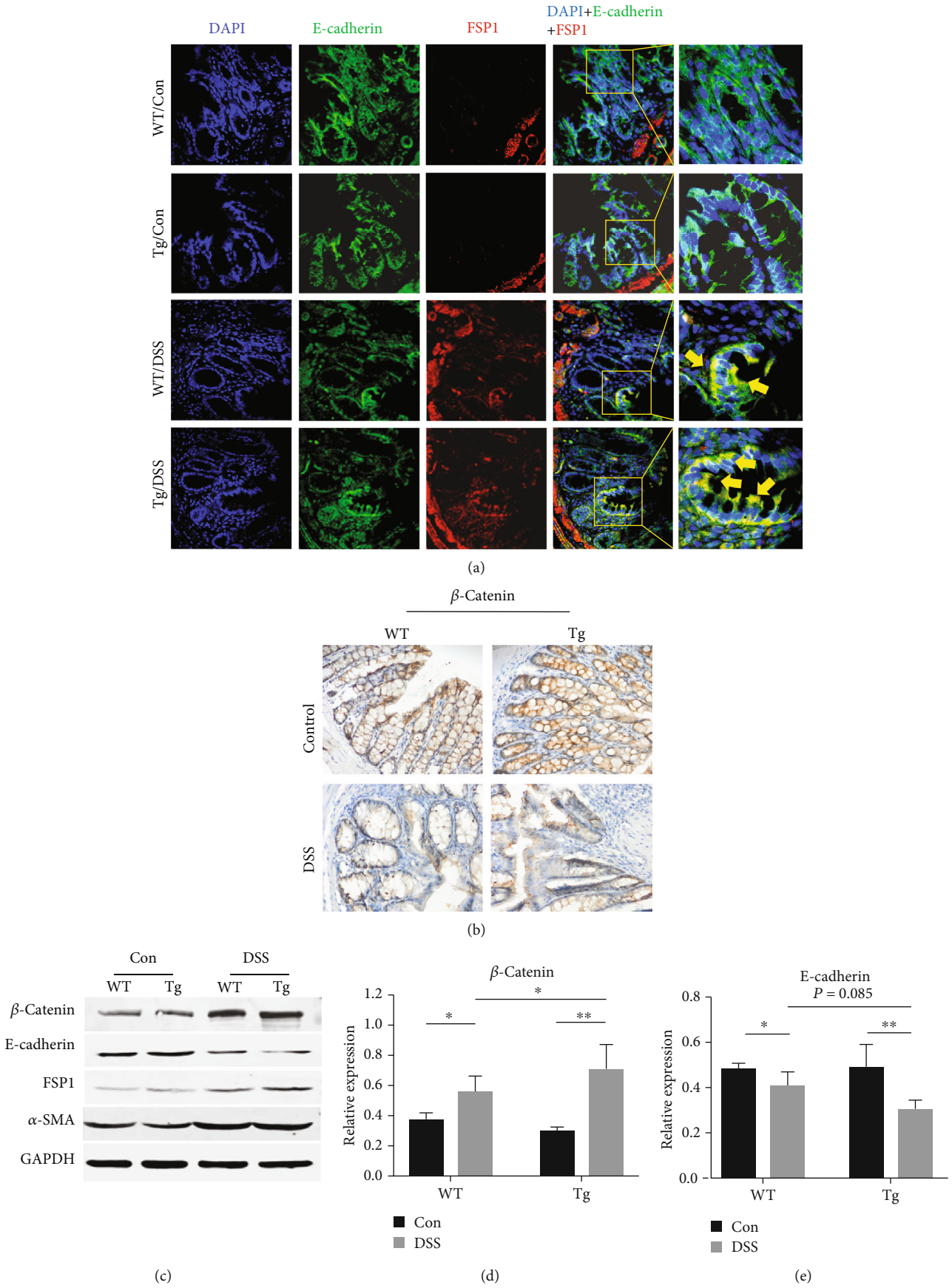

Figure 4: Continued.

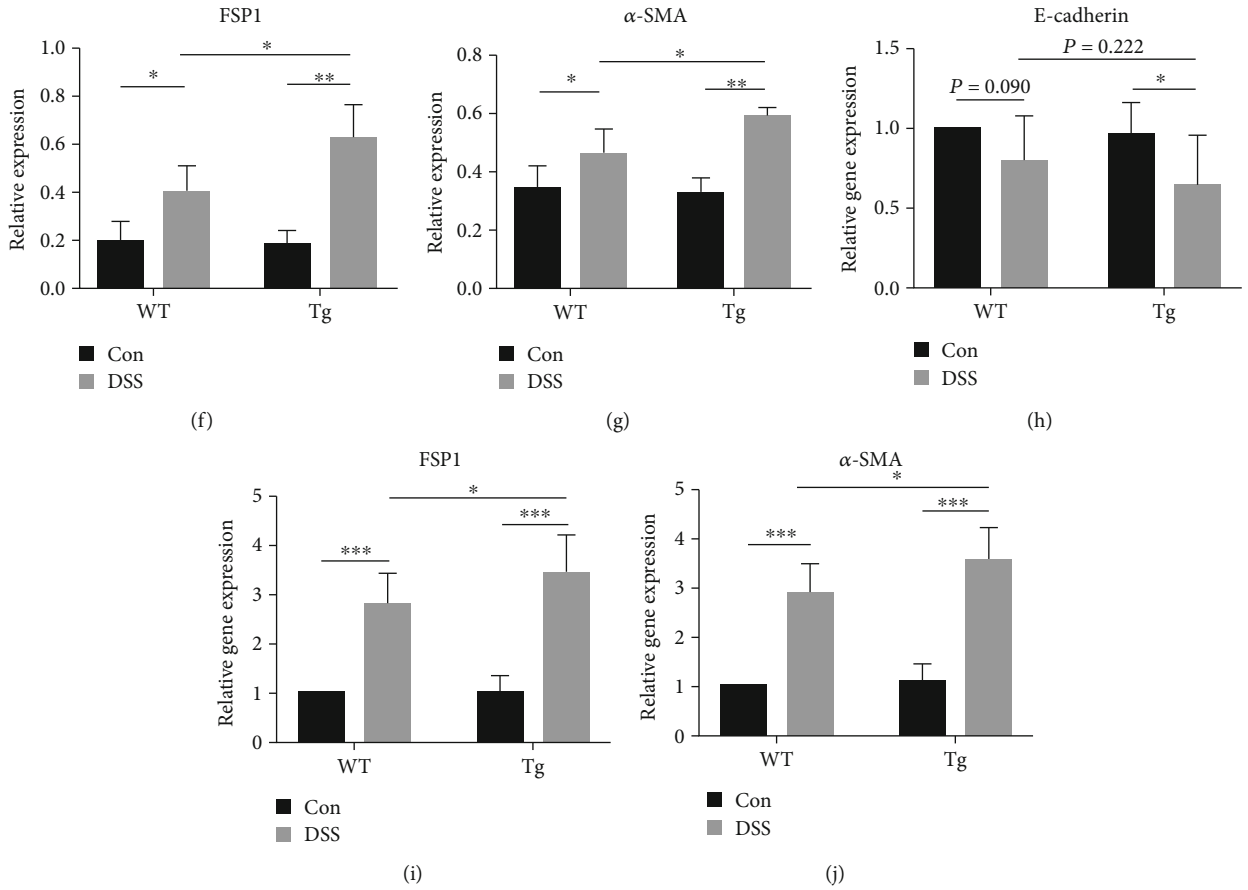

Figure 4: TL1A promotes EMT in the DSS-induced intestinal fibrosis model. (a) Immunofluorescence staining of colon tissue sections from wild type (WT) and transgenic (Tg) mice probed with antibodies against E-cadherin (green) and FSP1 (red) (400x). E-cadherin^{+}FSP1^{+} cells (yellow; reflects EMT). Nuclei are stained with DAPI (blue). (b) Immunohistochemical staining of β-catenin in colon tissues of mice groups (400x). (c–g) Western blot analysis of total protein of β-catenin, E-cadherin, α-SMA, and FSP1 in intestinal tissue, normalized with GAPDH. (h–j) RT-PCR analysis of E-cadherin, α-SMA, and FSP1 mRNA levels in the indicated groups. Data were given as mean ± standard deviation (SD). As compared to the control group: $^{*}P < 0.05$, $^{**}P \leq 0.01$, and $^{***}P \leq 0.001$.

3.4. Mice with High Expression of TL1A Had More Severe Intestinal Fibrosis. As previously reported, TL1A promoted intestinal fibrosis [22]. Sirius red staining showed that mice in the DSS group had a substantial amount of collagen deposition in colon tissues, especially in the DSS/Tg group (Figure 3(a)). Fibrotic alterations were quantified based on the fibrosis score according to the Supplementary Table 1. The DSS group showed a higher fibrosis score than the control group, and the DSS/Tg group had the highest score (Figure 3(b)). Compared with control group, the DSS group exhibited a significant increase in the minimum and maximum thickness of the submucosa (Figure 3(c)). The amount of hydroxyproline, one of the main components of collagen tissue, was significantly higher in DSS/Tg mice than in DSS/WT mice (Figure 3(d)). Collagen I and collagen III, components of ECM, are the main collagen fibers deposited when intestinal fibrosis occurs. Protein and mRNA levels of collagen I were greater in DSS/Tg mice than in DSS/WT mice (Figures 3(e), 3(f), and 3(h)) as were the mRNA levels of collagen III (Figure 3(i)). The protein levels of collagen III trended higher in the DSS/Tg group than in the DSS/WT group; however, this difference was not statistically significant (Figures 3(e) and 3(g)).

3.5. TL1A Promotes EMT In Vivo. EMT is a dynamic process during which cells can simultaneously express epithelial and mesenchymal markers, e.g., E-cadherin and FSP1, respectively. Therefore, the colocalization of these proteins was assessed. Immunofluorescence costaining showed that green fluorescent E-cadherin was apparently decreased in DSS mice, while red fluorescent FSP1 was apparently increased in DSS mice. Moreover, yellow fluorescence, representing E-cadherin and FSP1 colocalized expression, was stronger in DSS/Tg mice than in DSS/WT mice, indicating that TL1A participates in the EMT process (Figure 4(a)). Furthermore, immunohistochemical staining showed that β-catenin, which is a well-established marker for the onset of EMT, is no longer a membrane associated in the DSS group but localized in the cytoplasm or even in the nucleus (Figure 4(b)). Next, the levels of protein and mRNA expression of epithelial marker E-cadherin and interstitial markers FSP1 and α-SMA were determined by Western blot analysis and RT-

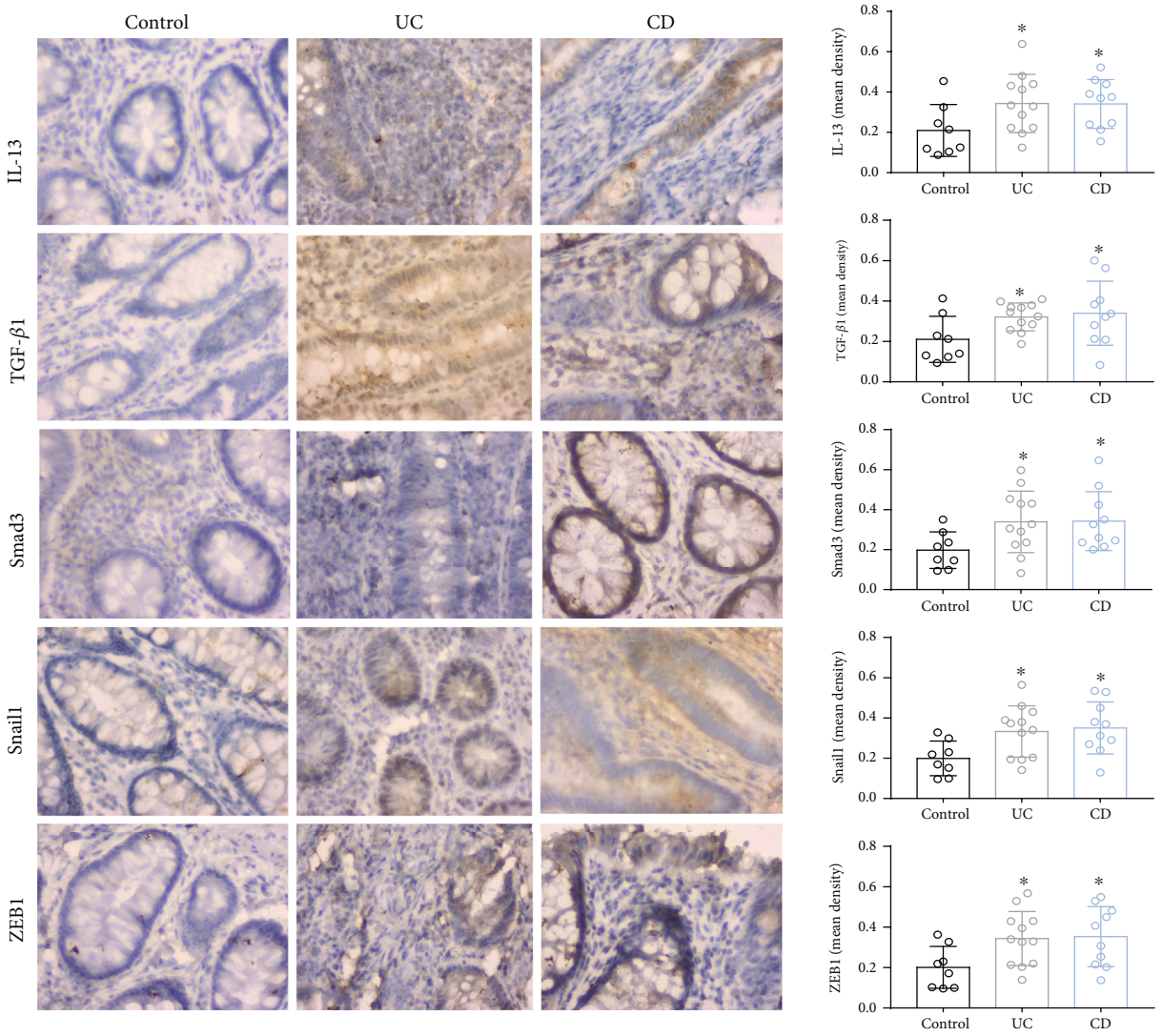

Figure 5: IL-13, TGF-β1, Smad3, and EMT-related transcriptional factor expression in IBD colon tissues. Immunohistochemical staining of IL-13, TGF-β1, Smad3, ZEB1, and Snail1 in intestinal tissues of controls, ulcerative colitis (UC), and Crohn's disease (CD) patients (400x). Data were given as mean ± SD. As compared to the control group: $^{*}P < 0.05$, $^{**}P \leq 0.01$, and $^{***}P \leq 0.001$.

PCR. There was no statistically significant difference in the protein and mRNA expression levels of E-cadherin between the DSS/WT group and the DSS/Tg group (Figures 4(c), 4(e), and 4(h)), while the total protein level of β-catenin, FSP1, and α-SMA expression levels were statistically increased in the DSS/WT group, especially in the DSS/Tg group (Figures 4(c), 4(d), 4(f), 4(g), 4(i), and 4(j)).

3.6. TL1A May Affect EMT through TGF-β/Smad3 Pathways in Patients with IBD. To explore the possible mechanism of TL1A regulation of EMT, colonic sections from control patients and patients with IBD were assessed for proteins of the TGF-β1/Smad3 pathway and EMT-related transcripts by immunohistochemical staining. Fibrogenic factor IL-13, TGF-β1, and Smad3 were found to be increased in UC and CD groups compared with the control group. The TGF-β1/Smad3 pathway is a classical way involved in EMT. The SMAD complex enters the nucleus and inhibits or activates target genes, such as Snail, ZEB, and basic helix-loop-helix (bHLH). Therefore, we tested the expression of ZEB1 and Snail1 and found that compared with control group, these two proteins were expressed higher in the UC and CD groups (Figure 5).

3.7. TL1A Induces EMT through TGF-β/Smad3 Pathways in the DSS-Induced Intestinal Fibrosis Model. Western blot analysis and RT-PCR were performed to explore the effects of TL1A in the DSS-induced intestinal fibrosis model. The TGF-β1 protein levels were greater in DSS/Tg mice than in DSS/WT mice; however, the difference was not statistically significant (Figures 6(a) and 6(c)), while IL-13, Smad3, Snail1, and ZEB1 protein expression was significantly higher in DSS/Tg mice than in DSS/WT mice (Figures 6(a), 6(b), 6(d), 6(e), and 6(f)). The mRNA levels of IL-13, Smad3, TGF-β1, and ZEB1 were significantly greater in DSS/Tg mice than that in DSS/WT mice (Figures 6(g), 6(h), 6(i), and 6(k)),

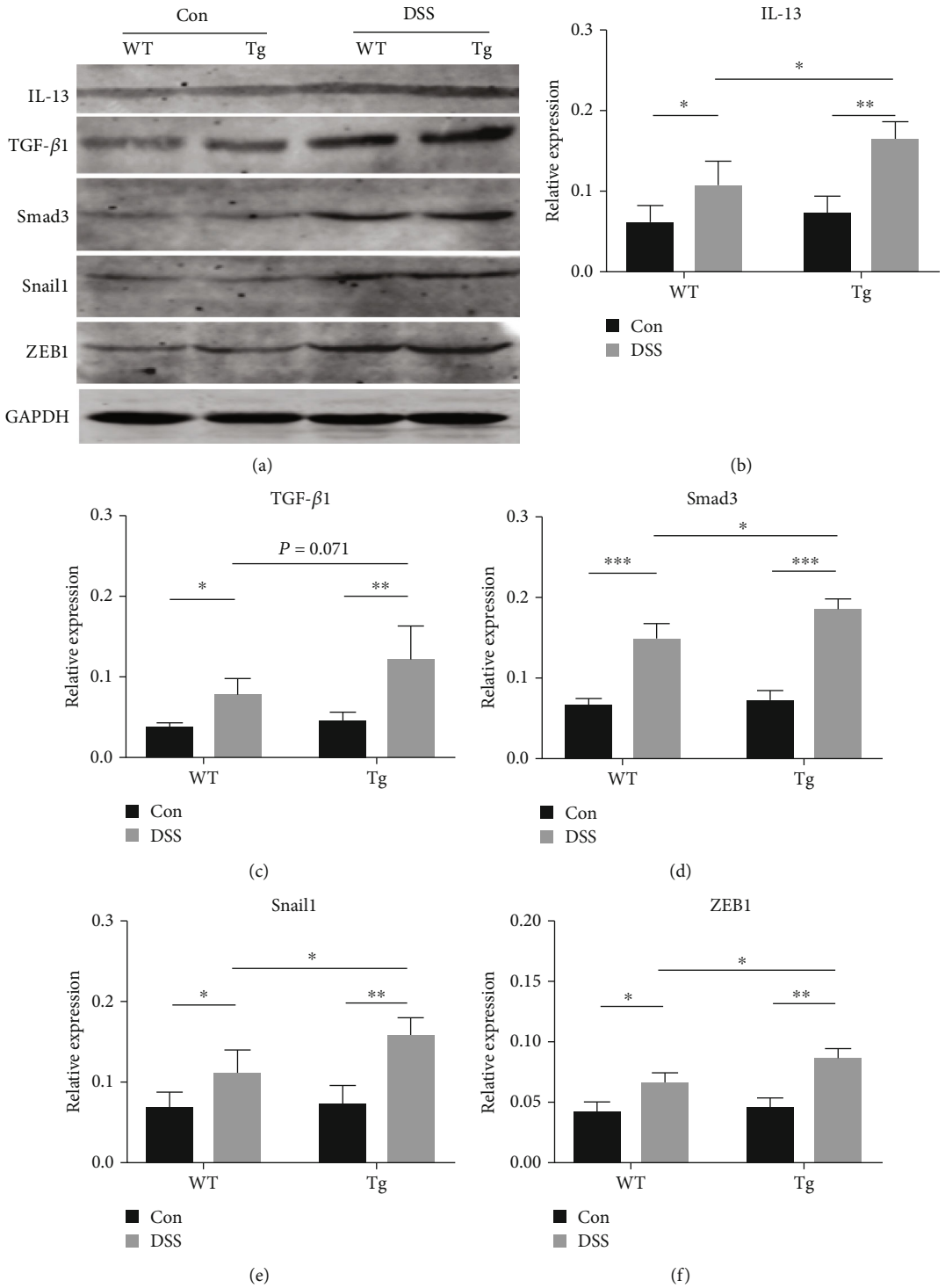

Figure 6: Continued.

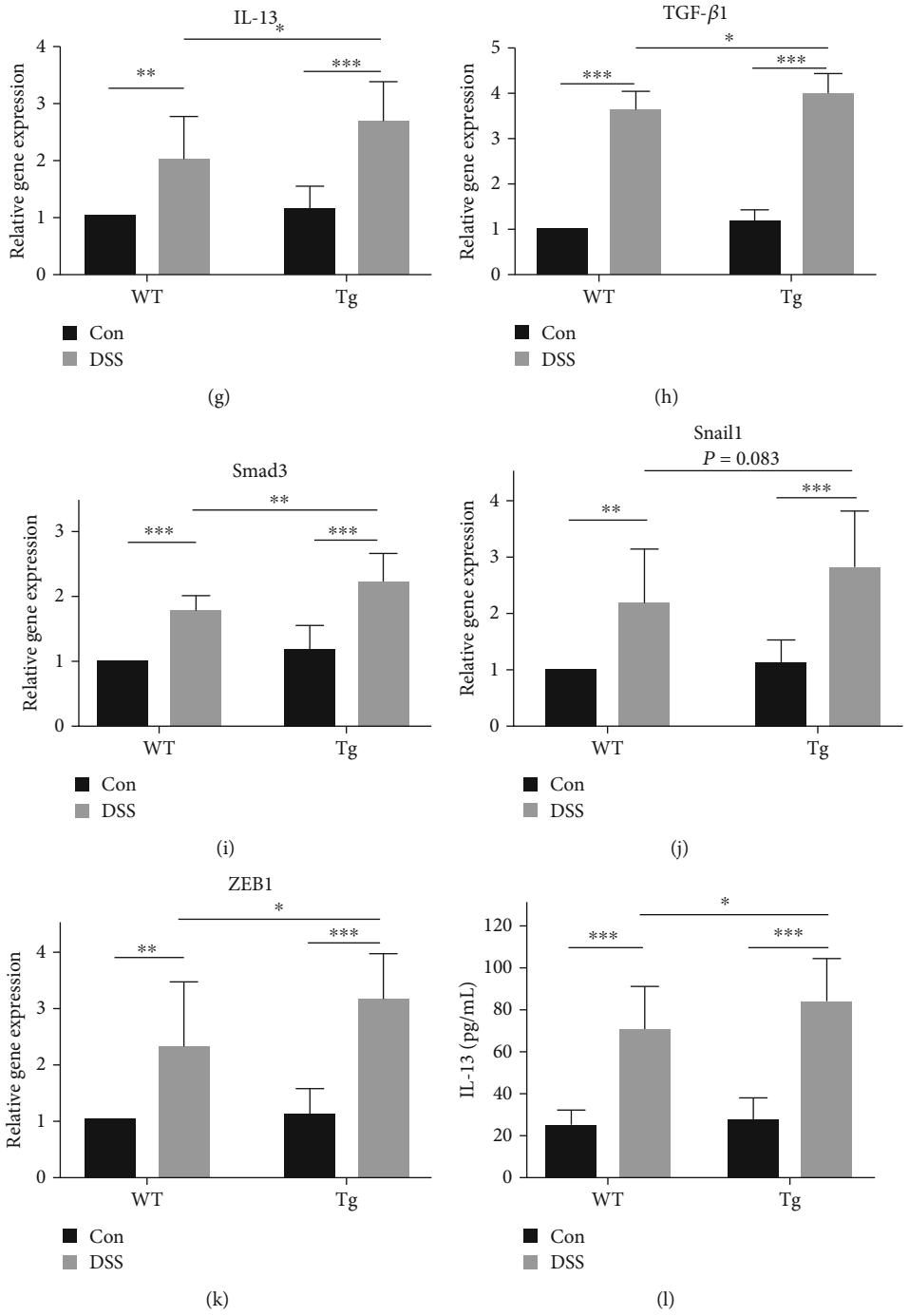

Figure 6: Continued.

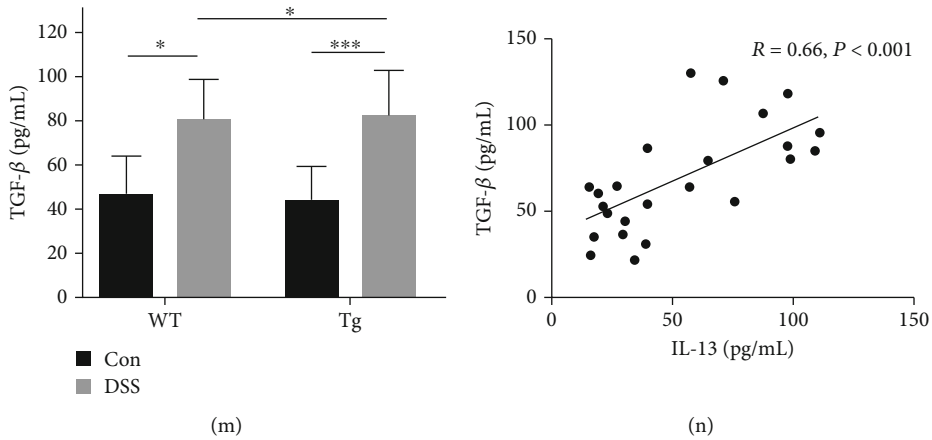

Figure 6: TL1A promotes epithelial to mesenchymal transition (EMT) via IL-13 and the TGF-β1/Smad3 pathway in DSS-induced colitis-related intestinal fibrosis mouse model. (a–f) Western blot analysis of IL-13, TGF-β1, Smad3, ZEB1, and Snail1 in intestinal tissues from previously described groups. (g–k) RT-PCR analysis of IL-13, TGF-β1, Smad3, ZEB1, and Snail1 mRNA levels in mice treated as described above. (l, m) ELISA showed expressions of IL-13 and TGF-β1. (n) Serum TGF-β1 was associated with IL-13 expression. As compared to the control group: $^{*}P < 0.05$, $^{**}P \leq 0.01$, and $^{***}P \leq 0.001$.

while there was no statistically significant difference in mRNA levels of Snail1 between DSS/Tg mice and DSS/WT mice (Figure 6(j)). The presence of IL-13 and TGF-β1 in serum from the DSS-induced intestinal fibrosis mouse model was detected by ELISA. The levels of IL-13 and TGF-β1 in circulating serum of DSS/Tg mice were increased compared with that of DSS/WT mice (Figures 6(l) and 6(m)). Furthermore, a positive correlation between IL-13 and TGF-β1 in the serum was observed (Figure 6(n)).

3.8. Inhibition of Intestinal Fibrosis by BMP-7 or Anti-TL1A Antibody In Vitro. EMT was induced in human HT-29 cells under the stimulation of TL1A. HT-29 cells in control medium without TL1A had intense E-cadherin expression and FSP1 labeling (Figures 7(a) and 7(b)). In contrast, upon incubation with TL1A, HT-29 cells lost E-cadherin expression, and FSP1 expression increased. The addition of BMP-7 or anti-TL1A antibody to the medium prevented EMT induced by TL1A. Additionally, the inhibitory effects of BMP-7 and anti-TL1A antibody *in vitro* were highly similar. The expression levels of β-catenin, E-cadherin, FSP1, and α-SMA were compared using Western blot analysis (Figures 7(c) and 7(d)). Compared with the control group, the expression of E-cadherin was decreased in TL1A group but was upregulated when BMP-7 or anti-TL1A antibodies were added. In contrast, the expression of β-catenin, FSP1, and α-SMA was decreased after the addition of BMP-7 or anti-TL1A antibodies.

4. Discussion

Intestinal stenosis and obstruction caused by intestinal fibrosis are still intractable problems in the treatment of IBD. Myofibroblasts are key effector cells in the formation of intestinal fibrosis [27]. Multiple studies have stressed that EMT is one of the important sources of intestinal myofibroblasts [12, 28, 29]. However, there are still many unknowns that need to be investigated. This study provides strong evidence for the involvement of TL1A in intestinal fibrosis both *in vitro* and *in vivo*. The abnormal accumulation of TL1A in intestinal mucosa of patients with IBD is related to the degree of fibrosis and EMT-related markers. In addition, TL1A participates in intestinal fibrosis by promoting the secretion of inflammatory factors such as IL-13 and TGF-β1, and by activating the expression of EMT-related transcription factors via the TGF-β1/Smad3 pathway. TL1A can also directly induce EMT *in vitro*, and the process can be effectively inhibited by anti-TL1A antibodies or BMP-7. These findings underline the potential role of TL1A in EMT and provide evidence for anti-fibrosis treatment in the future.

A growing body of evidence suggests that TL1A is closely linked to the process of inflammation and fibrosis diseases [30–32]. TL1A is a member of the TNF family, which can bind to death receptor 3 (DR3) [33], and can enhance T cell proliferation and cytokine production [34]. A previous study demonstrated that overexpression of TL1A in myeloid cells can aggravate liver fibrosis by macrophage recruitment and cytokine secretion [35]. Moreover, TL1A can promote intestinal fibrosis by disrupting immune responses [22] or intestinal flora [18]. It has been reported that transgenic mice with TL1A overexpression develop spontaneous ileitis and inflammation and fibrosis of proximal colitis [19]. GWAS support a role for TL1A in the process of IBD. In this study, serum inflammation indicators and intestinal mucosal inflammation were more severe in patients with IBD, and large amounts of collagen fibers were deposited in the intestinal mucosa of these patients. Immunohistochemical staining showed that TL1A expression in the UC and CD groups was significantly increased compared with the control group. The expression of TL1A was positively associated with fibrosis area and with the expression of β-catenin, FSP1, and α-SMA, but was negatively associated with expression of E-cadherin. These results confirm that TL1A may participate in the process of intestinal fibrosis through EMT.

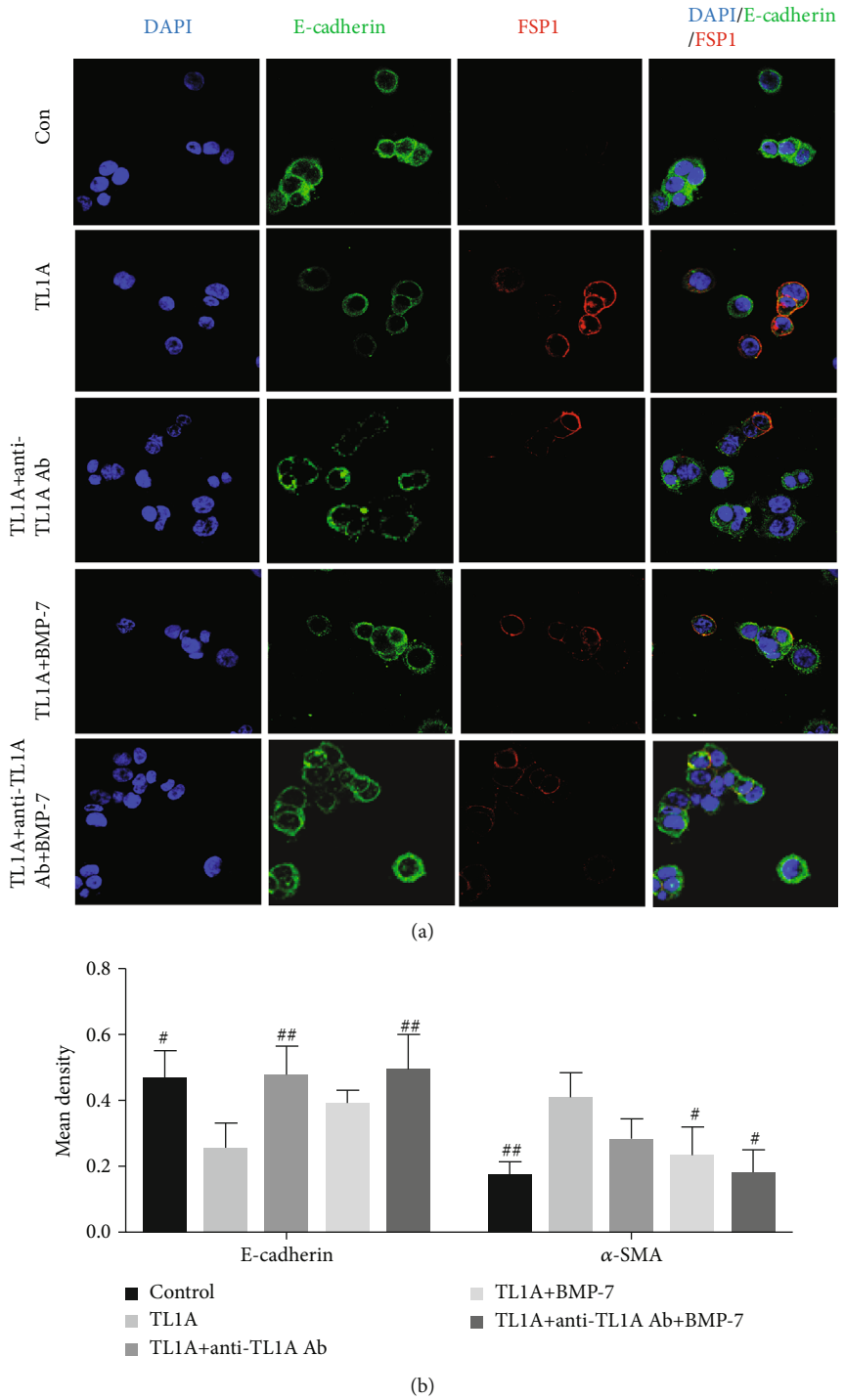

Figure 7: Continued.

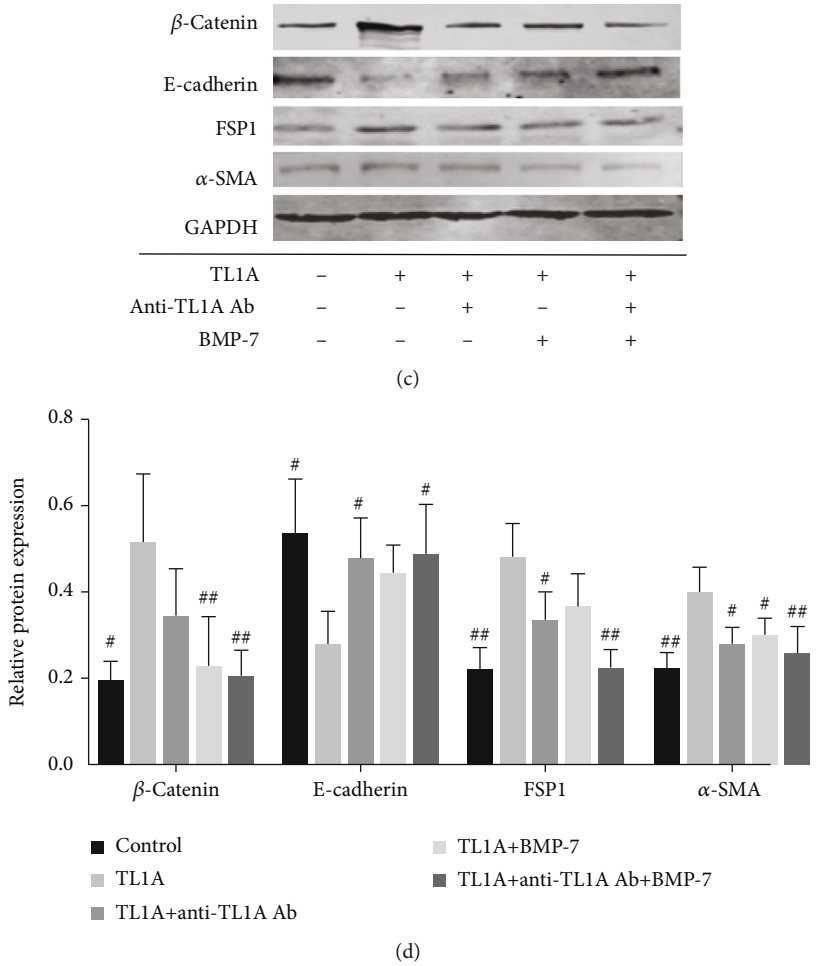

Figure 7: Inhibition of TL1A in intestinal epithelial cells *in vitro* using anti-TL1A antibodies and BMP-7. HT-29 cells were exposed to TL1A, anti-TL1A antibodies, and/or BMP-7, respectively. (a, b) The cells were probed with fluorescently labeled antibodies against E-cadherin (red) and FSP1 (green); E-cadherin and FSP1 colocalization (yellow) (1000x) and the mean density of E-cadherin and FSP1 were detected by IPP software. (c, d) Western blot analysis of β-catenin, E-cadherin, α-SMA, and FSP1 in different groups of HT-29 cells. $^{*}P < 0.05$, $^{**}P < 0.01$, and $^{***}P < 0.001$ versus TL1A-treated cells. Data were given as mean ± standard deviation (SD). $^{\#}P < 0.05$, $^{\#\#}P < 0.01$, and $^{\#\#\#}P < 0.001$ versus TL1A-treated cells.

Furthermore, similar results were obtained in animal experiments. Wild-type mice and transgenic mice with high TL1A expression were given DSS to construct a chronic colitis-related fibrosis model. The DSS groups exhibited more severe intestinal inflammation and collagen deposition, and the protein and mRNA expressions of collagen I and collagen III were increased. These findings were more pronounced in the DSS/Tg group, indicating that the high expression of TL1A increased susceptibility to intestinal inflammation and fibrosis.

EMT is the process of tissue repair and healing, in which epithelial cells lose polarity and intercellular adhesions to obtain interstitial markers and transform into mesenchymal stem cells [36]. Flier et al. [11] used immunofluorescence staining to evaluate the colocalization of FSP1 and E-cadherin, and found that E-cadherin^{+}FSP1^{+} cells were detected in mice treated with 2,4,6-trinitrobenzene sulfonic acid (TNBS). The same conclusion can be obtained in our research. The epithelial marker E-cadherin was significantly decreased in DSS/Tg mice compared with DSS/WT mice, and the interstitial marker FSP1 was significantly increased in DSS/Tg mice compared with DSS/WT mice, confirming that EMT is involved in DSS-induced intestinal fibrosis.

Many studies suggest that TL1A promotes the development of inflammation by inducing Th2/IL-13 mucosal responses, which are currently considered a main cause of colitis. Mice with constitutive expression of TL1A in lymphoid or myeloid cells exhibit spontaneous ileitis [19, 32, 37]. The upregulation of activated T cells and regulatory Foxp3^{+}CD4^{+} T cells exacerbates intestinal inflammation related to the mucosal response of Th2 cells [38]. Expression of IL-13 was increased in TL1A transgenic mice, and blocking IL-13 release alleviates the severity of ileitis [19, 32, 37]. In our study, the protein and mRNA expression levels of IL-13 were significantly higher in DSS/Tg mice than in DSS/WT mice. Therefore, we concluded that TL1A affects the intestinal fibrosis process by promoting the secretion of the fibrotic factor IL-13.

The fourth ECCO guidelines state that IL-13 activates the TGF-β1/Smad3 pathway as the central process in intestinal fibrosis formation [21]. It is reported that IL-4 and IL-13 can synergize with high glucose to promote the expression of TGF-β1, FN, and collagen I in cultured HK-2 cells, indicating that the secretion of Th2 cytokines (IL-4 and IL-13) and the upregulated expression of TGF-β1 are key factors in the development of renal fibrosis [39]. Another study showed that IL-13 induces fibrosis through the activation of TGF-β1, and the synergistic effect of IL-13 and TGF-β1 may increase the expression of eotaxin in human fibroblast [40]. It has also been reported that IL-13 expression could lead to the proliferation of bronchial epithelial cells via the production of TGF-α and activation of the epidermal growth factor receptor (EGFR) [41]. In the current study, IL-13 and TGF-β1 levels were significantly upregulated in the serum of DSS mice (most dramatically in DSS/Tg mice) compared with those of control mice. This positive correlation indicates that IL-13 and TGF-β1 may be involved in EMT of intestinal fibrosis.

EMT involves a large number of cell signaling pathways and complex gene regulation processes, including classical TGF-β-dependent and TGF-β-independent pathways. TGF-β signals by binding to its receptor to activate the Smad complex, which can translocate to the nucleus and regulate the expression of target genes, such as Snail, ZEB, and bHLH. In clinical studies, the expression of Slug in inflammatory mucosa and fibrotic tissue of UC and CD patients was shown to be increased [42], and the expression of Snail was also increased in relation to fistula formation of IBD [43]. In the current study, the protein and mRNA levels of EMT-related transcription factors Snail1 and ZEB1 were detected by immunohistochemical staining, Western blot analysis, and RT-PCR, respectively. It was found that Snail1 and ZEB1 expression was higher in DSS mice, especially in DSS/Tg mice, than in controls, indicating that EMT is involved in intestinal fibrosis.

As previously reported, the application of anti-TL1A antibodies reduce the expression of α-SMA and vimentin, and are even capable of reversing intestinal fibrosis by suppressing the TGF-β1/Smad3 pathway in adoptively transferred T-cell colitic mice [22]. BMP-7 is a member of the transforming growth factor β (TGF-β) superfamily and has antifibrotic effects in the liver through inhibition of the TGF-β1/Smad pathway [44]. In mice treated with TNBS, colocalization of E-cadherin and FSP1 was significantly decreased when mice received concomitant BMP-7 treatment [11]. In our study, immunofluorescence staining of HT-29 cells stimulated with TL1A showed that the expression of E-cadherin decreased, while the expression of FSP1 increased. This process was blocked by the application of either anti-TL1A antibody or BMP-7, and the inhibitory effect was maximized by using both *in vitro*. This could offer as a novel strategy for the cure or reversal of intestinal fibrosis.

In summary, we conclude that increased TL1A levels correlate with IBD-associated intestinal fibrosis. Accumulation of TL1A induces EMT and collagen fiber production in intestinal epithelial cells through an IL-13- and TGF-β1/Smad3 signaling pathway-mediated process. Inhibition of TL1A expression, therefore, may provide an effective strategy for relieving intestinal fibrosis.

Data Availability

The data used to support the findings of this study are available from the author upon request.

Consent

All patients or their relatives provided informed consent to participate.

Conflicts of Interest

All authors declare that they have no potential conflicts of interest.

Supplementary Materials

Supplementary Table 1 Criteria for Histologic Fibrosis Score of Intestine. Supplementary Table 2 Primers used for qRT-PCR analysis. Supplementary Figure 1 The identification of the LCK-CD2-TL1A-GFP transgenic mouse. Supplementary Figure 2 Effect of TL1A on HT-29 cell viability. *(Supplementary Materials)*

References

[1] P. Pakshir and B. Hinz, "The big five in fibrosis: macrophages, myofibroblasts, matrix, mechanics, and miscommunication," *Matrix Biology*, vol. 68-69, pp. 81–93, 2018.

[2] M. V. Lenti and S. A. Di, "Intestinal fibrosis," *Molecular Aspects of Medicine*, vol. 65, pp. 100–109, 2019.

[3] K. T. Thia, W. J. Sandborn, W. S. Harmsen, A. R. Zinsmeister, and E. V. Loftus, "Risk Factors Associated With Progression to Intestinal Complications of Crohn's Disease in a Population-Based Cohort," *Gastroenterology*, vol. 139, no. 4, pp. 1147–1155, 2010.

[4] F. Rieder, E. M. Zimmermann, F. H. Remzi, and W. J. Sandborn, "Crohn's disease complicated by strictures: a systematic review," *Gut*, vol. 62, no. 7, pp. 1072–1084, 2013.

[5] F. Rieder, C. Fiocchi, and G. Rogler, "Mechanisms, management, and treatment of fibrosis in patients with inflammatory bowel diseases," *Gastroenterology*, vol. 152, no. 2, pp. 340–350.e6, 2017.

[6] I. O. Gordon, N. Agrawal, J. R. Goldblum, C. Fiocchi, and F. Rieder, "Fibrosis in ulcerative colitis: mechanisms, features, and consequences of a neglected problem," *Inflammatory Bowel Diseases*, vol. 20, no. 11, pp. 2198–2206, 2014.

[7] I. O. Gordon, N. Agrawal, E. Willis et al., "Fibrosis in ulcerative colitis is directly linked to severity and chronicity of mucosal inflammation," *Alimentary Pharmacology & Therapeutics*, vol. 47, no. 7, pp. 922–939, 2018.

[8] F. Wu, Q. Shao, M. Hu et al., "Wu-Mei-Wan ameliorates chronic colitis-associated intestinal fibrosis through inhibiting fibroblast activation," *Journal of Ethnopharmacology*, vol. 252, p. 112580, 2020.

[9] D. Ortiz-Masià, P. Salvador, D. C. Macias-Ceja et al., "WNT2b activates epithelial-mesenchymal transition through FZD4:

relevance in penetrating Crohn's disease," *Journal of Crohn's & Colitis*, vol. 14, no. 2, pp. 230–239, 2020.

[10] M. A. Nieto, R. Y. Huang, R. A. Jackson, and J. P. Thiery, "EMT: 2016," *Cell*, vol. 166, no. 1, pp. 21–45, 2016.

[11] S. N. Flier, H. Tanjore, E. G. Kokkotou, H. Sugimoto, M. Zeisberg, and R. Kalluri, "Identification of epithelial to mesenchymal transition as a novel source of fibroblasts in intestinal fibrosis," *The Journal of Biological Chemistry*, vol. 285, no. 26, pp. 20202–20212, 2010.

[12] S. He, M. Xue, C. Liu, F. Xie, and L. Bai, "Parathyroid hormone-like hormone induces epithelial-to-mesenchymal transition of intestinal epithelial cells by activating the runt-related transcription factor 2," *The American Journal of Pathology*, vol. 188, no. 6, pp. 1374–1388, 2018.

[13] M. Scharl, N. Huber, S. Lang, A. Fürst, E. Jehle, and G. Rogler, "Hallmarks of epithelial to mesenchymal transition are detectable in Crohn's disease associated intestinal fibrosis," *Clinical and Translational Medicine*, vol. 4, no. 1, 2015.

[14] S. K. Yang, M. Hong, W. Zhao et al., "Genome-wide association study of Crohn's disease in Koreans revealed three new susceptibility loci and common attributes of genetic susceptibility across ethnic populations," *Gut*, vol. 63, no. 1, pp. 80–87, 2014.

[15] Y. Arimura, H. Isshiki, K. Onodera et al., "Characteristics of Japanese inflammatory bowel disease susceptibility loci," *Journal of Gastroenterology*, vol. 49, no. 8, pp. 1217–1230, 2014.

[16] S. N. Hong, C. Park, S. J. Park et al., "Deep resequencing of 131 Crohn's disease associated genes in pooled DNA confirmed three reported variants and identified eight novel variants," *Gut*, vol. 65, no. 5, pp. 788–796, 2016.

[17] M. Yang, W. Jia, D. Wang et al., "Effects and mechanism of constitutive TL1A expression on intestinal mucosal barrier in DSS-induced colitis," *Digestive Diseases and Sciences*, vol. 64, no. 7, pp. 1844–1856, 2019.

[18] N. Jacob, J. P. Jacobs, K. Kumagai et al., "Inflammation-independent TL1A-mediated intestinal fibrosis is dependent on the gut microbiome," *Mucosal Immunology*, vol. 11, no. 5, pp. 1466–1476, 2018.

[19] F. Meylan, Y. J. Song, I. Fuss et al., "The TNF-family cytokine TL1A drives IL-13-dependent small intestinal inflammation," *Mucosal Immunology*, vol. 4, no. 2, pp. 172–185, 2011.

[20] P. Giuffrida, F. Caprioli, F. Facciotti, and A. di Sabatino, "The role of interleukin-13 in chronic inflammatory intestinal disorders," *Autoimmunity Reviews*, vol. 18, no. 5, pp. 549–555, 2019.

[21] G. Latella, G. Rogler, G. Bamias et al., "Results of the 4th scientific workshop of the ECCO (I): pathophysiology of intestinal fibrosis in IBD," *Journal of Crohn's & Colitis*, vol. 8, no. 10, pp. 1147–1165, 2014.

[22] H. Li, J. Song, G. Niu et al., "TL1A blocking ameliorates intestinal fibrosis in the T cell transfer model of chronic colitis in mice," *Pathology, Research and Practice*, vol. 214, no. 2, pp. 217–227, 2018.

[23] R. Barrett, X. Zhang, H. W. Koon et al., "Constitutive TL1A expression under colitogenic conditions modulates the severity and location of gut mucosal inflammation and induces fibrostenosis," *The American Journal of Pathology*, vol. 180, no. 2, pp. 636–649, 2012.

[24] R. Aranda, B. C. Sydora, M. A. PL et al., "Analysis of intestinal lymphocytes in mouse colitis mediated by transfer of CD4+, CD45RBhigh T cells to SCID recipients," *Journal of Immunology*, vol. 158, no. 7, pp. 3464–3473, 1997.

[25] A. L. Theiss, C. R. Fuller, J. G. Simmons, B. Liu, R. B. Sartor, and P. K. Lund, "Growth hormone reduces the severity of fibrosis associated with chronic intestinal inflammation," *Gastroenterology*, vol. 129, no. 1, pp. 204–219, 2005.

[26] K. Scheibe, C. Kersten, A. Schmied et al., "Inhibiting interleukin 36 receptor signaling reduces fibrosis in mice with chronic intestinal inflammation," *Gastroenterology*, vol. 156, no. 4, pp. 1082–1097.e11, 2019.

[27] C. Li and J. F. Kuemmerle, "The fate of myofibroblasts during the development of fibrosis in Crohn's disease," *Journal of Digestive Diseases*, vol. 21, no. 6, pp. 326–331, 2020.

[28] M. Pierdomenico, F. Palone, V. Cesi et al., "Transcription factor ZNF281: a novel player in intestinal inflammation and fibrosis," *Frontiers in Immunology*, vol. 9, p. 2907, 2018.

[29] X. Xu, S. Sun, F. Xie et al., "Advanced oxidation protein products induce epithelial-mesenchymal transition of intestinal epithelial cells via a PKC δ-mediated, redox-dependent signaling pathway," *Antioxidants & Redox Signaling*, vol. 27, no. 1, pp. 37–56, 2017.

[30] P. Tougaard, L. O. Martinsen, L. F. Zachariassen et al., "TL1A aggravates cytokine-induced acute gut inflammation and potentiates infiltration of intraepithelial natural killer cells in mice," *Inflammatory Bowel Diseases*, vol. 25, no. 3, pp. 510–523, 2019.

[31] Z. C. Yuan, J. M. Wang, L. C. Su, W. D. Xu, and A. F. Huang, "Gene polymorphisms and serum levels of TL1A in patients with rheumatoid arthritis," *Journal of Cellular Physiology*, vol. 234, no. 7, pp. 11760–11767, 2019.

[32] D. Q. Shih, R. Barrett, X. Zhang et al., "Constitutive TL1A (TNFSF15) expression on lymphoid or myeloid cells leads to mild intestinal inflammation and fibrosis," *PLoS One*, vol. 6, no. 1, article e16090, 2011.

[33] T. S. Migone, J. Zhang, X. Luo et al., "TL1A is a TNF-like ligand for DR3 and TR6/DcR3 and functions as a T cell costimulator," *Immunity*, vol. 16, no. 3, pp. 479–492, 2002.

[34] F. Meylan, A. C. Richard, and R. M. Siegel, "TL1A and DR3, a TNF family ligand-receptor pair that promotes lymphocyte costimulation, mucosal hyperplasia, and autoimmune inflammation," *Immunological Reviews*, vol. 244, no. 1, pp. 188–196, 2011.

[35] J. Guo, Y. Luo, F. Yin et al., "Overexpression of Tumor Necrosis Factor-Like Ligand 1 A in Myeloid Cells Aggravates Liver Fibrosis in Mice," *Journal of Immunology Research*, vol. 2019, Article ID 7657294, 15 pages, 2019.

[36] Z. Yang, Q. Xie, Z. Chen et al., "Resveratrol suppresses the invasion and migration of human gastric cancer cells via inhibition of MALAT1-mediated epithelial-to-mesenchymal transition," *Experimental and Therapeutic Medicine*, vol. 17, no. 3, pp. 1569–1578, 2019.

[37] V. Y. Taraban, T. J. Slebioda, J. E. Willoughby et al., "Sustained TL1A expression modulates effector and regulatory T-cell responses and drives intestinal goblet cell hyperplasia," *Mucosal Immunology*, vol. 4, no. 2, pp. 186–196, 2011.

[38] V. Valatas, G. Kolios, and G. Bamias, "TL1A (TNFSF15) and DR3 (TNFRSF25): a co-stimulatory system of cytokines with diverse functions in gut mucosal immunity," *Frontiers in Immunology*, vol. 10, p. 583, 2019.

[39] C. Liu, L. Qin, J. Ding et al., "Group 2 innate lymphoid cells participate in renal fibrosis in diabetic kidney disease partly via TGF-β1 signal pathway," *Journal Diabetes Research*, vol. 2019, article 8512028, 12 pages, 2019.

[40] H. Koga, N. Miyahara, Y. Fuchimoto et al., "Inhibition of neutrophil elastase attenuates airway hyperresponsiveness and inflammation in a mouse model of secondary allergen challenge: neutrophil elastase inhibition attenuates allergic airway responses," *Respiratory Research*, vol. 14, no. 1, p. 8, 2013.

[41] S. Allahverdian, N. Harada, G. K. Singhera, D. A. Knight, and D. R. Dorscheid, "Secretion of IL-13 by airway epithelial cells enhances epithelial repair via HB-EGF," *American Journal of Respiratory Cell and Molecular Biology*, vol. 38, no. 2, pp. 153–160, 2008.

[42] N. Zidar, E. Boštjančič, M. Jerala et al., "Down-regulation of microRNAs of the miR-200 family and up-regulation of Snail and Slug in inflammatory bowel diseases—hallmark of epithelial-mesenchymal transition," *Journal of Cellular and Molecular Medicine*, vol. 20, no. 10, pp. 1813–1820, 2016.

[43] M. Scharl, A. Weber, A. Fürst et al., "Potential role for SNAIL family transcription factors in the etiology of Crohn's disease-associated fistulae," *Inflammatory Bowel Diseases*, vol. 17, no. 9, pp. 1907–1916, 2011.

[44] G. L. Zou, S. Zuo, S. Lu et al., "Bone morphogenetic protein-7 represses hepatic stellate cell activation and liver fibrosis via regulation of TGF-β/Smad signaling pathway," *World Journal of Gastroenterology*, vol. 25, no. 30, pp. 4222–4234, 2019.

Hindawi
Mediators of Inflammation
Volume 2021, Article ID 1610251, 12 pages
https://doi.org/10.1155/2021/1610251

Research Article

Xi Lei San Attenuates Dextran Sulfate Sodium-Induced Colitis in Rats and TNF-α-Stimulated Colitis in CACO2 Cells: Involvement of the NLRP3 Inflammasome and Autophagy

Zhang Tao,[1,2] Xiaoqing Zhou,[1] Yan Zhang,[1] Wenfeng Pu,[1] Yi Yang,[3] Fuxia Wei,[1] Qian Zhou,[1] Lin Zhang,[2] Zhonghan Du,[1] and Ji Wu[4]

[1]*Department of Gastroenterology, Nanchong Central Hospital, The Second Clinical Medical College, North Sichuan Medical College, Nanchong, Sichuan Province, China*
[2]*Department of Gastroenterology, Jing Men No. 2 People's Hospital, Jing Men City, Hubei Province, China*
[3]*Department of Gastroenterology, People's Hospital of Nanjiang, Bazhong City, Sichuan Province, China*
[4]*Department of Urology, Nanchong Central Hospital, The Second Clinical Medical College, North Sichuan Medical College, Nanchong, Sichuan Province, China*

Correspondence should be addressed to Ji Wu; wuji2168@sina.com

Received 1 June 2020; Revised 4 March 2021; Accepted 21 March 2021; Published 22 April 2021

Academic Editor: Francesco Giudici

Objective. Inflammatory bowel disease (IBD) is a chronic nonspecific inflammatory bowel disease with an unclear etiology. The active ingredients of traditional Chinese medicines (TCMs) exert anti-inflammatory, antitumor, and immunomodulatory effects, and their multitarget characteristics provide them with a unique advantage for treating IBD. However, the therapeutic effects and underlying mechanisms of Xi Lei San in treatment of IBD remain unknown. This study was designed to investigate whether Xi Lei San exerted an anti-inflammatory effect in IBD via a mechanism involving NLRP3 inflammasomes and autophagy. *Methods*. We successfully established a rat model of dextran sulfate sodium- (DSS-) induced colitis as well as a cellular model of TNF-α-induced colitis. Xi Lei San and indirubin were identified by HPLC analysis. Rats were treated with Xi Lei San or alum crystals, and their body weights and morphology of intestinal tissues were examined. A western blot analysis was performed to determine the expression levels of inflammasome-related proteins and autophagy-related proteins, ELISA was performed to analyze IL-1β, IL-18, and IL-33 concentrations, and flow cytometry was used to monitor cell apoptosis and ROS levels. *Results*. Xi Lei San and indirubin were identified by HPLC analysis. We found that Xi Lei San could significantly increase the weights of rats and improve the structure of the intestinal tissues in DSS-induced colitis model rats. We also found that Xi Lei San significantly inhibited NLRP3 inflammasome activity, reduced the levels of inflammatory cytokines, and suppressed autophagy in DSS-induced colitis model rats. *In vitro* experiments revealed that Xi Lei San could repress apoptosis as well as ROS and inflammatory cytokine production in TNF-α-induced CACO2 cells by reducing the activity of NLRP3 inflammasomes and autophagy. *Conclusions*. Our findings showed that Xi Lei San significantly ameliorated IBD by inhibiting NLRP3 inflammasome, autophagy, and oxidative stress.

1. Introduction

Inflammatory bowel disease (IBD) is a persistent, chronic, recurrent, and nonspecific inflammatory disease [1]. IBD is characterized by the development of intestinal inflammation caused by polymorphonuclear neutrophils, macrophages, lymphocytes, and mastocytes and can result in mucosal damage and ulcers [2]. The incidence of IBD has gradually increased in recent years. While the current affected population is mainly young adults, the incidence of IBD is also increasing among children [3]. IBD includes two types of intestinal idiopathic inflammatory diseases: ulcerative colitis

(UC) and Crohn's disease (CD) [4]. Currently, it is generally believed that the pathogenic factors associated with IBD include intestinal mucosa damage, persistent inflammatory factors, genetic susceptibility, intestinal microecological damage, and environmental factors [5–7]. However, the etiology and specific pathogenesis of IBD remain unclear. The current treatment for IBD consists of general treatment (rest and nutrition), medications (anti-inflammatory drugs and immune regulators), and surgical treatment (total colon resection) [8, 9]. Conventional Western medicines have drawbacks that include side effects, a high financial cost, and a high rate of disease recurrence [10, 11]. Therefore, it is important to explore the pathogenic mechanism of IBD and develop new therapeutic drugs and methods for its treatment.

Numerous clinicians have achieved good results in treating diseases by using combined methods of syndrome differentiation, internal administration, external irrigation, and acupuncture [12, 13]. Previous research revealed that traditional Chinese medicines (TCMs) produce obvious effects in treating colitis and have the important advantages of low cost, fewer side effects, and ease of use for an extended time period [14, 15]. Some domestic literature has reported that Xi Lei San, a class of Chinese patent medicine, is highly effective for treating IBD and shows unique advantages in terms of symptom control and producing fewer side effects [16]. Xi Lei San consists of seven TCMs, including indigo naturalis, calculus bovis factitius, pearl, borneol, human fingernails, ivory crumbs, and uroctea, and has been shown to be effective in detoxifying saprophytes [17]. Xi Lei San was recently shown to facilitate the healing of peptic ulcers and exert broad-spectrum antibacterial, anti-inflammatory, and astringent myogenesis effects [17]. However, the efficacy of Xi Lei San and its mechanism of action in treatment of IBD are not fully understood.

The NLRP3 inflammasome is a multiprotein complex [18] that not only plays a central role in the innate immune response but also plays an important role in the pathogenesis of autoimmune diseases by regulating the differentiation and function of immune cells [19, 20]. The activation of NLRP3 inflammasomes can activate caspase-1, further induce the maturation of interleukin 1β (IL-1β), and thereby regulate an inflammatory response [21]. Some studies have shown that NLRP3 inflammasome is closely related to IBD remission [22, 23]. Additionally, autophagy has been widely recognized being participated in IBD. For example, Pott et al. suggest that autophagy in intestinal epithelial cell protects cells from chronic inflammatory injury (Pott, 2018 #52). However, the relationship between autophagy and NLRP3 inflammasomes remains uncertain whether Xi Lei San alleviates IBD by regulating NLRP3 inflammasome activity and autophagy.

In the current study, we successfully established both a DSS-induced rat model of colitis and a TNF-α-induced cellular model of colitis. We then explored the influence of Xi Lei San on body weight, morphological changes in intestinal tissues, NLRP3 inflammasome, autophagy, and apoptosis. Our studies revealed that Xi Lei San exerts a regulatory effect on NLRP3 inflammasomes, suggesting those inflammasomes as targets for treating IBD.

2. Materials and Methods

2.1. Animals. A total of 20 healthy SPF-grade SD female rats (180-220 g) were purchased from Sun Yat-sen University (No. 44008500019433; License no.: SYXK (Guangdong) 2016-0112) and housed at the North Sichuan Medical College. The rats were housed in a room with a 12 h light/dark cycle, a temperature of 20-24°C, and a humidity of 50-60%; food and water were available *ad libitum*. The study protocol was approved by the Ethical Review Committee of SLAS.

2.2. Colitis Rat Model. After 1 week of adaptive feeding, SD rats were fed 4.5% dextran sulfate sodium (DSS; MP Biomedicals) in water for 7 days along with their normal diet. In brief, the rats were randomly assigned to a control group (conventional diet), model group (regular diet followed by drinking 4.5% DSS in water for 7 days), low-dose Xi Lei San group (DSS model rats were treated with 100 mg/kg/day of Xi Lei San for 7 days), and high-dose Xi Lei San group (DSS model rats were treated with 200 mg/kg/d of Xi Lei San for 7 days). The body weights of the SD rats in each group were examined at 1, 3, 5, 7, 9, 11, and 14 days. The SD rats received a daily Disease Activity Index (DAI) score. The stool properties of the rats were observed, and any fecal occult blood was detected and recorded. After the dietary intervention, a 10 cm segment of distal colon was collected from each rat. The colon segments were quick-frozen in iquid nitrogen and subsequently stored at -80°C for use in western blot assays. A portion of each distal colon was fixed in 4% paraformaldehyde for H&E staining and immunohistochemistry analysis. Samples of blood serum were collected and stored in a -80°C refrigerator for use in ELISA.

2.3. Cell Culture and Treatment. Frozen CACO2 cells were warmed to 37°C and then pelleted by centrifugation (1000g for 5 min). After being resuspended, the cells were cultured in Dulbecco's modified Eagle's medium (DMEM, Invitrogen, Carlsbad, CA, USA) containing 10% fetal bovine serum (FBS; Gibco, cat. no. 10099-141) and 10 g/mL penicillin/streptomycin (Gibco, cat. no. 15140122) in a 37°C incubator containing 5% CO_2. A cellular model of colitis was constructed by adding TNF-α to the CACO cells. Other groups of CACO2 were also treated with Xi Lei San and/or alum crystals in addition to TNF-α.

2.4. High-Performance Liquid Chromatography (HPLC). As in previous studies [24, 25], the chromatograms of Xi Lei San and indirubin were confirmed by HPLC. Xi Lei San and indirubin solutions were prepared and analyzed by HPLC performed using a Hypersil NH2 column (250 mm × 4.6 mm, 5 mm). The column temperature, flow rate, and injection volume were 30°C, 1 mL/min, and 2.0 μL, respectively. The detection wavelength was 289 nm. The mobile phase consisted of water (A) and acetonitrile (B), and the samples were eluted using the following gradient: 0~5.5 min, 97% (B); 5.5-6 min, 97-90% (B); 6~20 min, 90% (B); and 20~21 min, 90%~97% (B). MS/MS was conducted using ionized electrospray ionization (ESI+). The atomization temperature of the ion source was 500°C; the flow rates were 8, 6, and 14 mL/min, respectively; and the focusing voltage, suction voltage, and suction voltage of

collision charge were 82 V, 10 V, and 13 V, respectively. Results were determined using a multireaction monitoring model. The Xi Lei San used for this study was provided by Zhejiang Dongtan Pharmaceutical., Ltd., Taiji Group (Batch No. 18010003).

2.5. Hematoxylin and Eosin Staining (H&E Staining). Tissues were fixed by 4% paraformaldehyde and embedded by paraffin. Serial sections were obtained, and then, dehydration and dewaxing were performed. Sections were placed in distilled water for 2 min and then stained with hematoxylin for 5 min. After washing, the sections were dehydrated with 95% ethanol for 5 s and then stained with eosin for 30 s. After staining, the sections were dehydrated two times in 95% ethanol and then made transparent by two 5 min immersions in xylene. Finally, the tissue sections were sealed with neutral gum.

2.6. Western Blotting. The colonic tissues from each group were ground, and the CACO2 cells from each group were collected. Next, the cells were lysed in RIPA lysate buffer (Beyotime, China) containing a protease inhibitor and then centrifuged. The total protein content in each supernatant was determined using a Bradford protein assay kit (Bio-Rad, Hercules, CA, USA). A 40 μg sample of total protein from each sample was separated by SDS-PAGE electrophoresis (separation gel: 80 V, spacer gel: 100 V), and the protein bands were transferred onto PVDF membranes (30 mA, 90 min). After being blocked, the membranes were incubated with primary antibodies overnight at 4°C, followed by incubation with an HRP-labeled secondary antibody for 60 min at 37°C. The immunostained protein bands were visualized using an ECL kit (Thermo Fisher Scientific, Waltham, MA, USA), and their staining intensities were determined. The primary antibodies used were obtained from Abcam (Cambridge, UK) and included antibodies against NLRP3 (1 : 1000, ab263899), IL-1β (1 : 1000, ab9722), caspase-1 (1 : 1000, ab62698), ASC (1 : 1000, ab175449), IL-18 (1 : 1000, ab71495), LC3B (1 : 800, Boster), p62 (1 : 1500, Boster), and GAPDH (1 : 2000, ab9485).

2.7. ELISA. The levels of IL-1β, IL-18, and IL-33 were determined by using the appropriate ELISA kits according to instructions provided by the supplier. The optical density (OD) of each well at 450 nm was determined by using an automatic enzyme marker (RT-2100C).

2.8. Flow Cytometry Analysis for Apoptosis. The CACO2 cells from each group were suspended in PBS and then diluted to a concentration of 1×10^6 cells/mL. After the cells were washed, 5 μL of PI and 5 μL of Annexin V-FITC (Abnova, cat. no. KA3805) were added to each tube of cells, and the tubes were placed in the dark for 10 min. Next, 200 μL of binding buffer was added to each tube, and the cells were analyzed by flow cytometry (BD Biosciences, Franklin Lakes, NJ, USA). The data were analyzed using ModFit software.

2.9. Immunohistochemistry. Serial sections have undergone antigen retrieval and blocking after dehydration and dewaxing. Subsequently, sections were incubated with primary antibody (caspase-3, Boster Bio, cat. no. PB9188, 1 : 100). Afterward, sections were incubated with secondary antibody (Dako, cat. no. K5007, ready-to-use) followed by color development using DAB reagent (Beyotime, cat. no. P0202) and redyed by hematoxylin. Finally, sections were sealed by neutral resins for observation under a microscope.

2.10. Flow Cytometry Analysis for ROS. Treated CACO2 cells were placed into the wells of 6-well plates with ~80% surface coverage. After 48 h of culture, the cells in each well were washed 3 times and then treated with 40 μmol/L DCFH-DA staining solution for 30 min. After washing, the ROS levels were determined by flow cytometry (BD Biosciences) performed with an excitation wavelength of 488 nm and an emission wavelength of 525 nm.

2.11. Statistical Analysis. All data were analyzed using IBM SPSS Statistics for Windows, Version 20.0 software (IBM Corp., Armonk, NY, USA), and results are expressed as the mean value obtained from three replicate experiments. Differences between groups were analyzed by one-tailed ANOVA followed by Tukey's post hoc test. P values < 0.05 were considered to be statistically significant.

3. Results

3.1. Xi Lei San and Indirubin Were Identified by HPLC. To examine the potential effects of Xi Lei San in colitis, we first analyzed the structure and molecular weight of Xi Lei San and indirubin. The molecular structure of indirubin is shown in Figure 1(a), and its molecular formula is $C_{16}H_{10}N_2O_2$. We used HPLC to confirm the chemical structures and relative molecular weights of Xi Lei San and indirubin used in this study. A chromatographic peak for indirubin was detected, as shown in Figure 1(b). The same method was used to detect the chromatographic peak for Xi Lei San (Figure 1(c)). These findings showed that indirubin was the main active component.

3.2. Xi Lei San Relieved DSS-Induced Colitis in Rats. In order to assess the therapeutic effect of Xi Lei San in colitis, we established a DSS-induced model of enteric colitis in rats. We found that administration of 4.5% DSS for 7 days resulted in a significant weight loss in rats, and the weight loss could be attenuated by the addition of Xi Lei San and especially high doses of Xi Lei San to the diet of the model rats ($P < 0.05$ and $P < 0.01$, Figure 2(a)). We also found that the DAI values for the DSS model rats were significantly reduced after treatment with Xi Lei San, due to increases in body weight reduced defecation ($P < 0.05$, Figure 2(b)). H&E staining results showed that the intestinal mucosa of rats in the normal group was intact and no obvious abnormalities were observed. In the DSS model group, most of the intestinal glands had disappeared, the structure of epithelial cells was destroyed, and the intestinal tissues showed severe inflammatory changes and evidence of neutrophil infiltration. However, Xi Lei San notably ameliorated all those changes in the DSS model group (Figure 2(c)). Besides, caspase-3 expression was higher in the DSS model group compared with that in rats in the control group, while Xi Lei San administration reversed caspase-3 expression (Figure 2(d)). These results indicated that Xi Lei San could significantly ameliorate the histological features of colitis in rats induced with DSS.

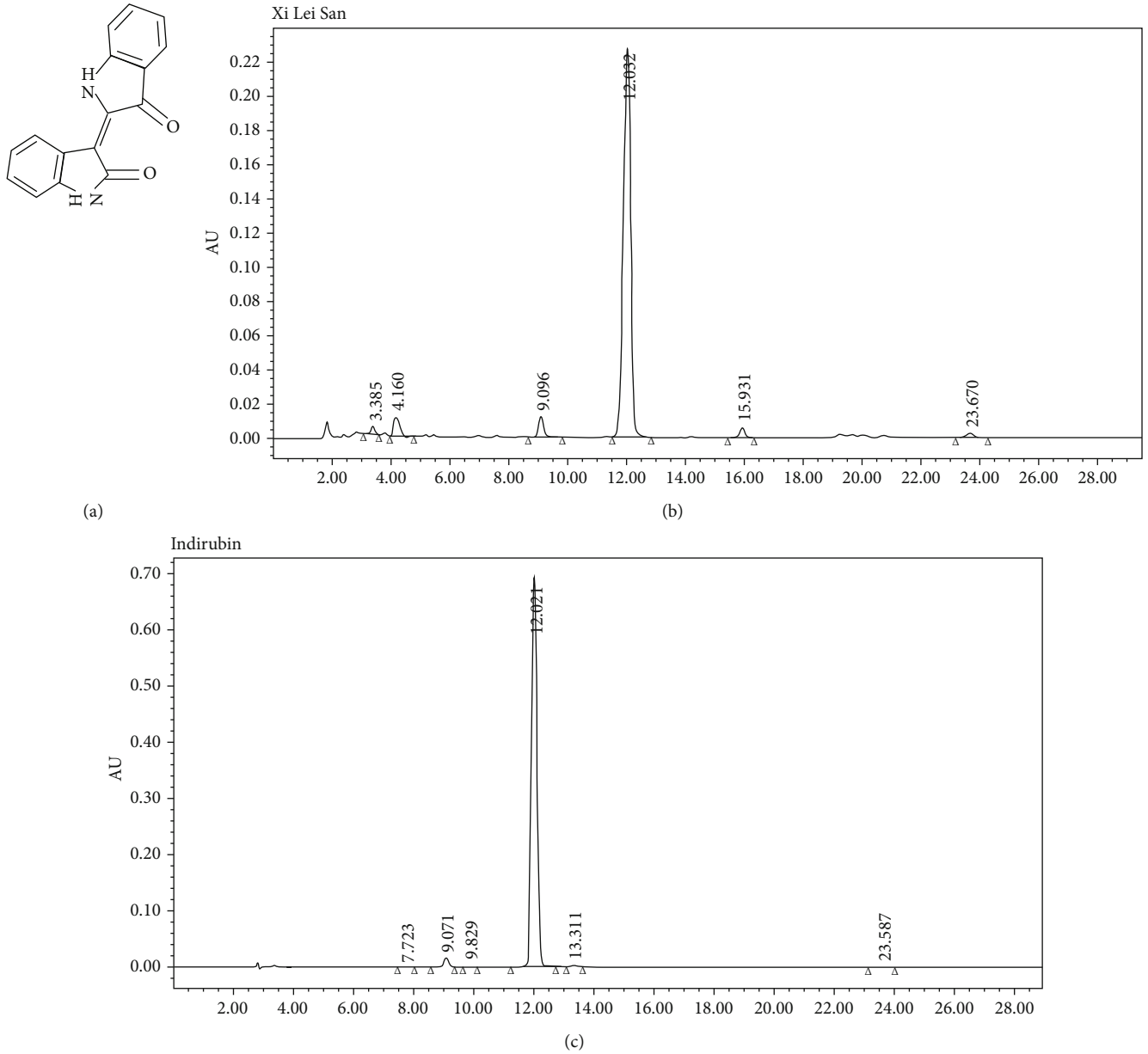

Figure 1: Xi Lei San and indirubin were identified by HPLC. (a) The molecular structure of indirubin. The chromatograms of (b) Xi Lei San and (c) indirubin as obtained by HPLC.

3.3. Xi Lei San Prevented the Activation of NLRP3 Inflammasomes and Autophagy in Rats with DSS-Induced Colitis. We next sought to examine how Xi Lei San affected inflammation in rats with colitis induced by DSS. First, the expression levels of NLRP3 inflammasome-related proteins were determined by western blotting. Our results showed that the levels of NLRP3, IL-1β, and caspase-1 expression were significantly increased in the DSS-induced model group when compared with those in the control group, and those elevated expression levels could be significantly reduced by Xi Lei San treatment and particularly by treatment with high doses of Xi Lei San. In contrast, there was little change in the levels of ASC in each group (Figure 3(a)). ELISA data showed that the DSS model rats had significantly higher levels of IL-1β, IL-18, and IL-33 in their serum, and those increases could be reversed by Xi Lei San, with the high-dose Xi Lei San group showing the more significant reversal effect ($P < 0.05$ and $P < 0.01$, Figure 3(b)). As shown in Figure 3(c), activation of autophagy in DSS model rats was presented as characterized by higher value of LC3B II/I and weaker expression of p62, while the LC3B II/I ratio was reversed by Xi Lei San delivery, together with elevated p62 expression (Figure 3(c)). When taken together, these findings showed that Xi Lei San significantly inhibited the activity of NLRP3 inflammasomes and autophagy in the DSS-induced colitis model rats.

3.4. Xi Lei San Inhibited NLRP3 Inflammasomes and Apoptosis and Reduced ROS and Inflammatory Cytokine Production in TNF-α-Stimulated CACO2 Cells. Similarly,

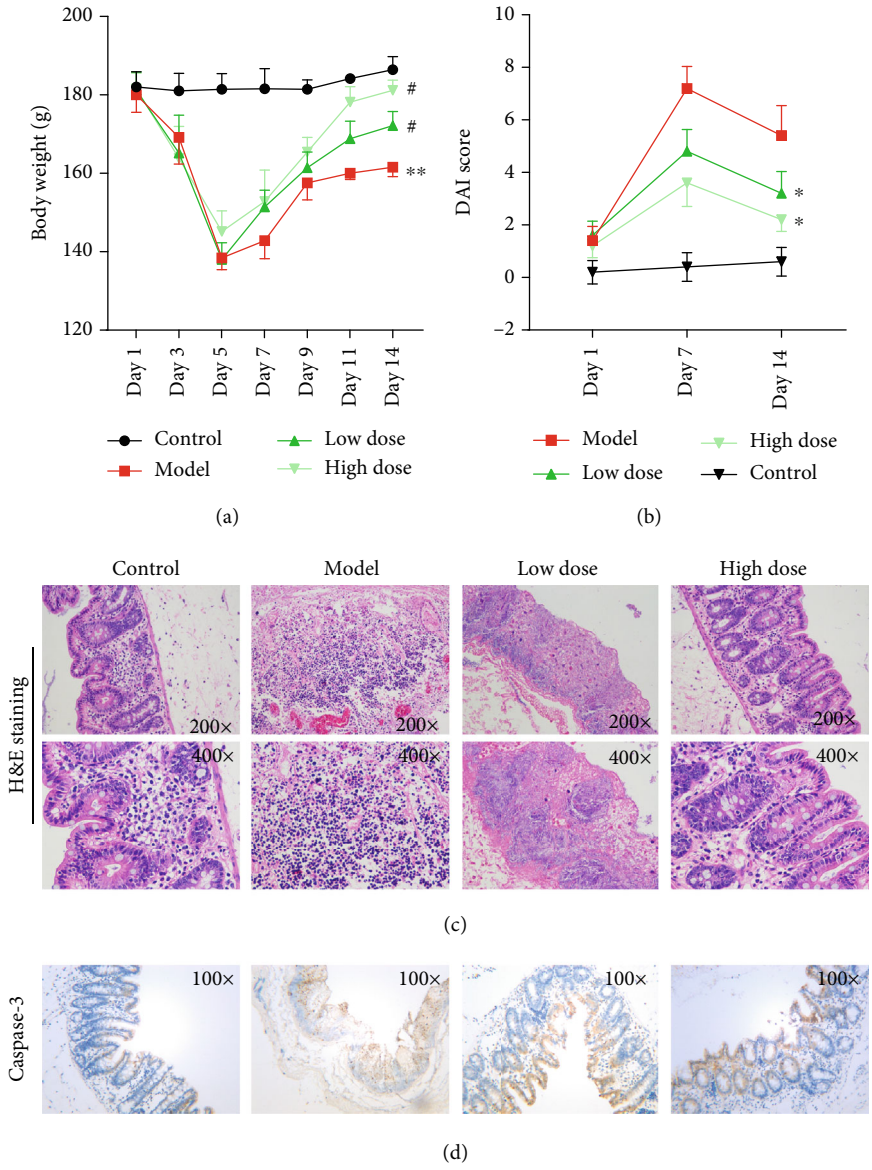

Figure 2: Xi Lei San relieved DSS-induced colitis in rats. (a) A DSS-induced rat model of colitis was constructed, and the model rats were treated with low or high doses of Xi Lei San. The body weights of the rats in each group were measured. (b) After treatment with Xi Lei San, a DAI score was calculated for each group of rats. (c) The pathological examination for rat intestinal tissues was observed after H&E staining. (d) Caspase-3 expression was detected by using immunohistochemistry. $^{*}P < 0.05$ and $^{**}P < 0.01$ vs. the control group; $^{\#}P < 0.05$ vs. the model group.

in vitro experiments further verified the effects of Xi Lei San on NLRP3 inflammasomes, apoptosis, ROS, and inflammatory factors. For conducting these studies, we established a cellular model of colitis by stimulating CACO2 cells with TNF-α. Our results showed that the levels of NLRP3, IL-18, IL-33, and IL-1β expression in the TNF-α-induced model cells were significantly higher than those in blank cells. Furthermore, administration of Xi Lei San could partially reverse the increases in those three proteins in TNF-α-stimulated CACO2 cells ($P < 0.05$ and $P < 0.01$, Figures 4(a) and 4(b)). We also found that the apoptosis rate of CACO2 cells in the TNF-α induction group was higher than that of cells in the blank group, and the enhancement in apoptosis could be attenuated by Xi Lei San (Figure 4(c)). Furthermore, we found that TNF-α could increase the levels of ROS in CACO cells, while Xi Lei San attenuated those increases (Figure 4(d)). Finally, the levels of IL-1β, IL-18, and IL-33 were significantly higher in the TNF-α model cells than those in the control cells, while those levels were significantly lower in the Xi Lei San-treated cells than in the TNF-α-treated cells ($P < 0.05$ and $P < 0.01$, Figure 4(e)). These data further confirmed that Xi Lei San could exert a regulatory effect in an *in vitro* CACO2 cell model of colitis.

3.5. Xi Lei San Suppressed Apoptosis, ROS Production, and Autophagy in TNF-α-Stimulated CACO2 Cells by NLRP3 Inflammasomes. After considering the relationships found among NLRP3 inflammasomes, apoptosis, ROS, and

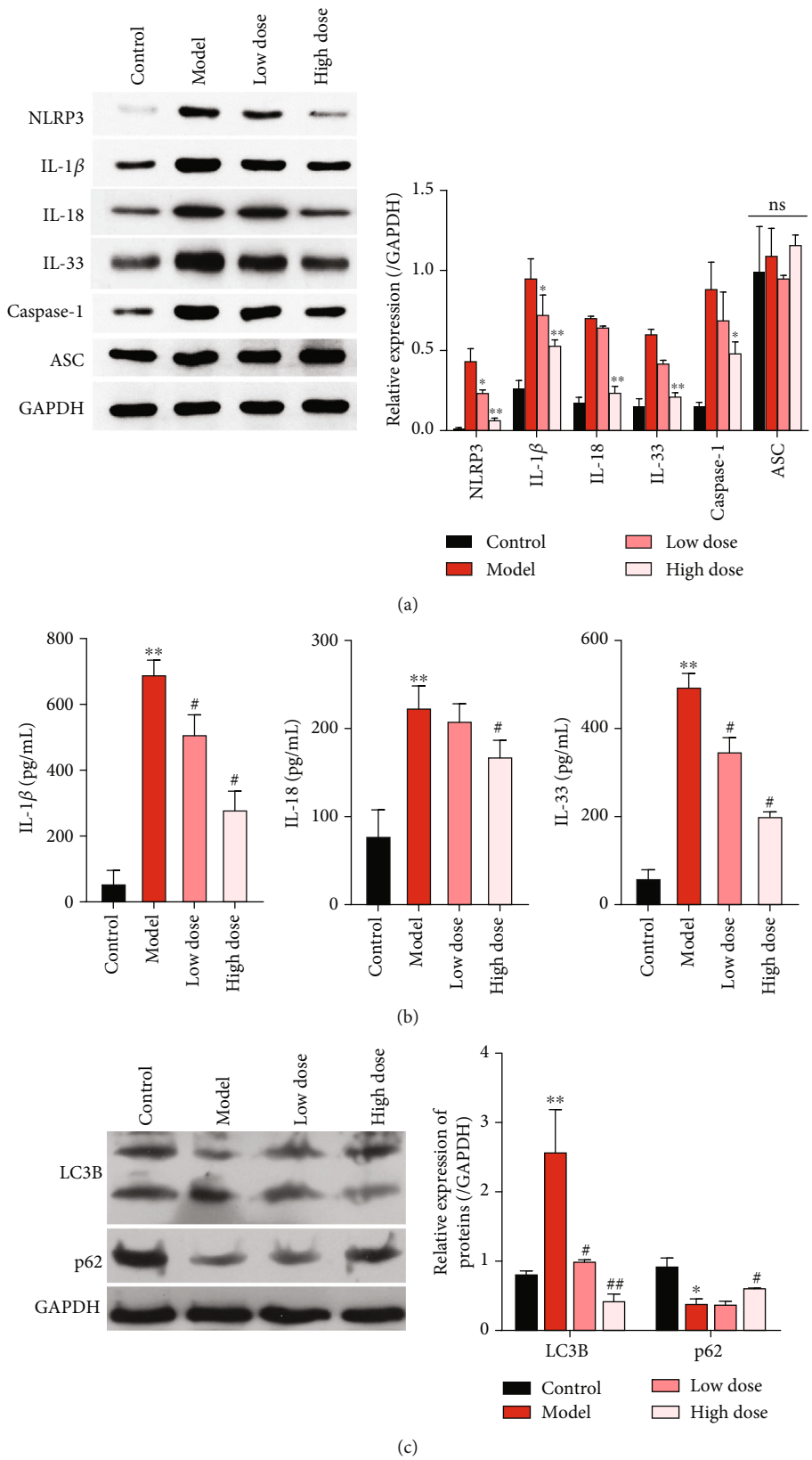

Figure 3: Xi Lei San prevented the activation of NLRP3 inflammasomes and autophagy in rats with DSS-induced colitis. (a) The DSS model rats with ulcerative colitis were treated with low or high doses of Xi Lei San. NLRP3, IL-1β, caspase-1, and ASC expression determined by western blotting. GAPDH served an internal reference protein. (b) ELISA kits were used to analyze the concentrations of IL-1β, IL-18, and IL-33 in each group. (c) Autophagy-related proteins, LC3B and p62, were measured by western blotting. $^{*}P < 0.05$ and $^{**}P < 0.01$ vs. the control group; $^{\#}P < 0.05$ and $^{\#\#}P < 0.01$ vs. the model group.

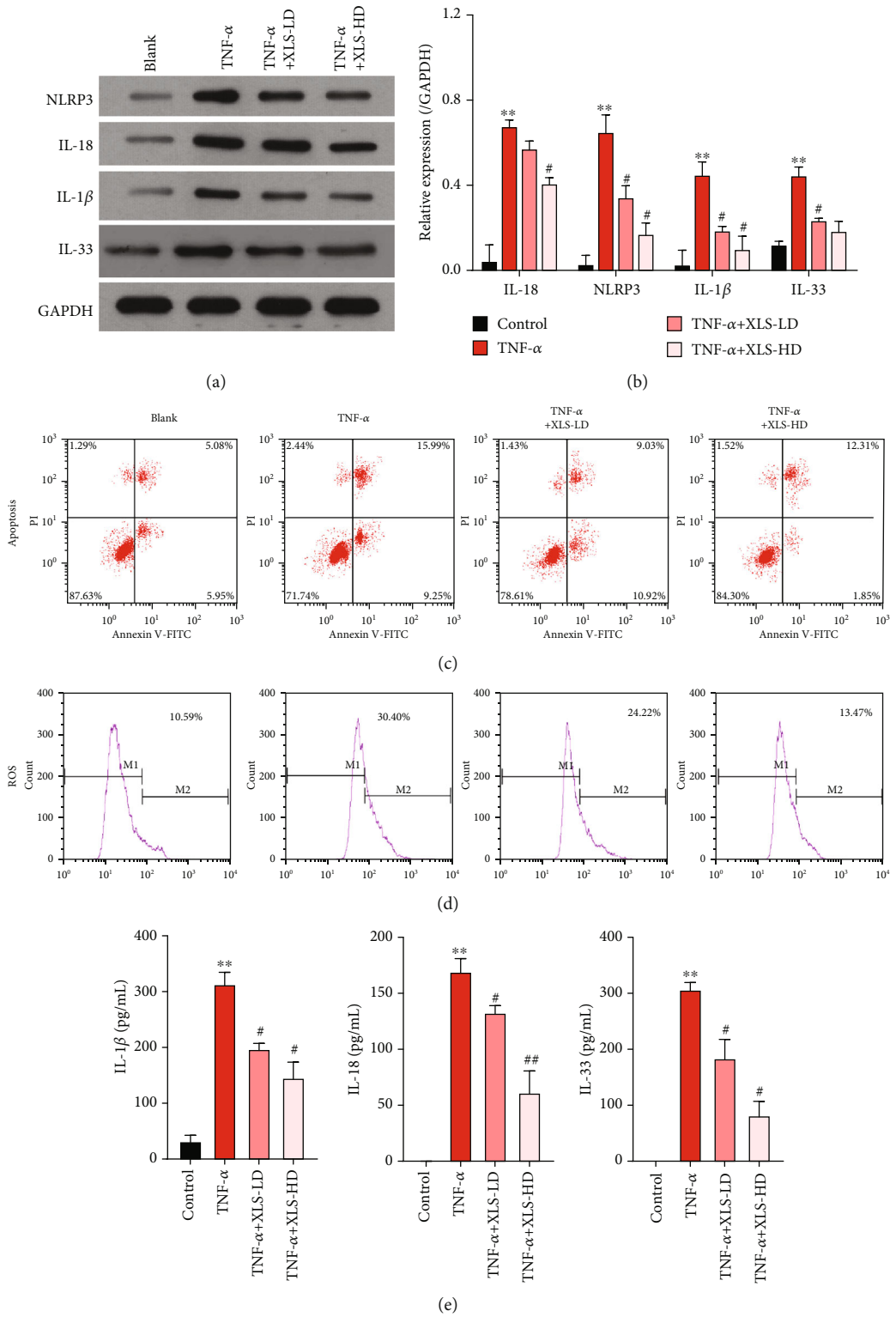

Figure 4: Xi Lei San inhibited NLRP3 inflammasome activity and apoptosis and reduced the levels of ROS and inflammatory cytokines in TNF-α-stimulated CACO2 cells. A cellular model of colitis was constructed by inducing CACO2 cells with TNF-α, and groups of colitis model cells were then treated with low or high doses of Xi Lei San, respectively. (a) NLRP3, IL-18, IL-33, and IL-1β levels in the CACO2 cells were examined by western blotting. (b) A statistical analysis of western blotting results was performed based on grayscales. (c) The effect of Xi Lei San on the apoptosis of TNF-α-induced CACO2 cells was examined by flow cytometry. (d) The ROS levels in each group of CACO2 cells were also examined by flow cytometry. (e) ELISA was performed to monitor IL-1β, IL-18, and IL-33 levels. $^{**}P < 0.01$ vs. the control group; $^{\#}P < 0.05$ and $^{\#\#}P < 0.01$ vs. the TNF-α group.

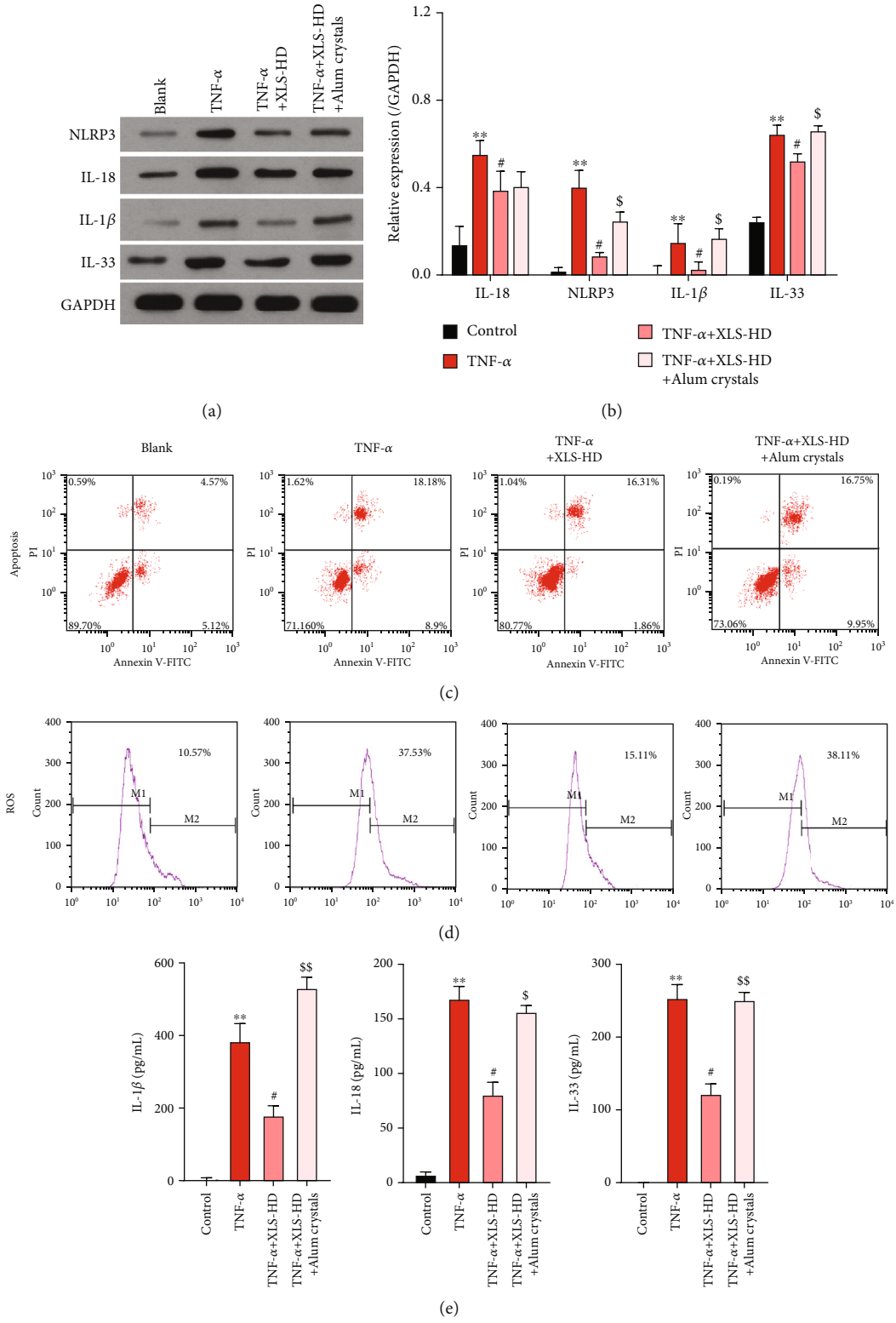

Figure 5: Xi Lei San suppressed apoptosis and reduced ROS levels and inflammation in TNF-α-stimulated CACO2 cells by inhibiting NLRP3 inflammasomes. TNF-α-induced CACO2 cells were treated with Xi Lei San and alum crystals. (a) A western blotting analysis was performed to examine the levels of NLRP3, IL-18, IL-33, and IL-1β expression in the CACO2 cells following their treatment with Xi Lei San and alum crystals. (b) A quantitative analysis of western blotting results was performed. (c) A flow cytometry analysis showed the apoptosis rate of CACO2 cells after treatment. (d) ROS production was determined by flow cytometry. (e) ELISA assay was used to detect the concentrations of IL-1β, IL-18, and IL-33 in the treated CACO2 cells. $^{**}P < 0.01$ vs. the control group; $^{\#}P < 0.05$ vs. the TNF-α group; $^{\$}P < 0.05$ and $^{\$\$}P < 0.01$ vs. the TNF-α+Xi Lei San group.

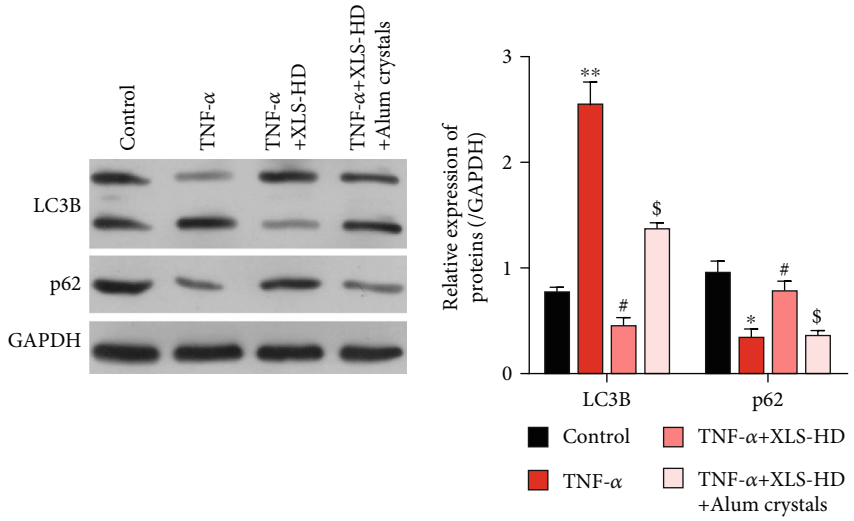

Figure 6: Xi Lei San reversed autophagy in rats with DSS-induced colitis. $^{*}P < 0.05$ and $^{**}P < 0.01$ vs. the control group; $^{\#}P < 0.05$ vs. the TNF-α group; $^{\$}P < 0.05$ vs. the TNF-α+Xi Lei San group.

inflammation in previous studies [26, 27], we decided to further examine whether NLRP3 inflammasomes played a dominant role in the regulatory effects of Xi Lei San on apoptosis, ROS production, and inflammation in our cellular model of colitis. The colitis model cells were induced with TNF-α and then treated with Xi Lei San and alum crystals. As expected, the alum crystals further reversed the downregulation of NLRP3, IL-18, IL-33, and IL-1β expression that was mediated by Xi Lei San in TNF-α-stimulated CACO2 cells ($P < 0.05$ and $P < 0.01$, Figures 5(a) and 5(b)). Similarly, the inhibitory effect of Xi Lei San on apoptosis in TNF-α-induced CACO2 cells was noticeably reversed by the alum crystals (Figure 5(c)). We also found that alum crystals could significantly attenuate the reduction in ROS levels that was caused by Xi Lei San in TNF-α-stimulated CACO2 cells (Figure 5(d)). Moreover, ELISA results showed that the Xi Lei San-mediated reductions in IL-1β, IL-18, and IL-33 concentrations could be largely recovered by treatment with alum crystals ($P < 0.05$ and $P < 0.01$, Figure 5(e)). As shown in Figure 6, the LC3B II/I ratio was increased by TNF-α, along with decreased p62 expression. Xi Lei San suppressed autophagy significantly by attenuating LC3B II/I. However, LC3B II/I was reversed by alum crystal treatment, with a decreased p62 expression. When taken together, these results showed that the attenuating effects of Xi Lei San on cell apoptosis, ROS production, and inflammation could be achieved by regulating NLRP3 inflammasomes.

4. Discussion

The incidence of IBD has been increasing on a yearly basis, and IBD has become a universal disease of the digestive system [28]. IBD has been reported to be associated with a variety of factors, including genetic factors, the autoimmune system, gut microbes, environmental factors, and mental factors [29, 30]. Because there is no safe and effective clinical treatment for IBD, it is important to further study its pathogenesis. DSS is a water-soluble sulfated polysaccharide that has been widely used to create rat models of colitis [31]. It was found that DSS-induced colitis was particularly similar to human IBD in terms of its clinical manifestations and histopathology [32]. In our study, we used DSS to establish a rat model of colitis. We found that rats in the DSS-induced colitis group lost significantly more weight and their colon tissues showed signs of structural damage and severe inflammation when compared to colon tissues in control rats. TNF-α, as the initiating molecule in the cytokine network, is mainly produced by activated mononuclear macrophages [33, 34]. Research has shown that TNF-α can induce the production of inflammatory cytokines, amplify inflammatory chain reactions, and cause intestinal mucosal damage when participating in the inflammatory and immune responses of IBD [35, 36]. In our study, TNF-α-induced CACO2 cells were used as an *in vitro* model of colitis. We found that apoptosis, ROS levels, and inflammation were all significantly enhanced in the TNF-α-induced colitis model cells.

From the perspective of traditional medicine, IBD belongs in the category of "intestinal apnea" and "dysentery" and should be treated with drugs that clear heat, cool blood, and promote granulation [37]. Xi Lei San is composed of seven TCMs, which have the effects of detoxification, resolving stagnation, and promoting granulation [17]. Xi Lei San was originally used to treat mouth ulcers, throat erosion, and swelling [16]. The intestinal mucosa of IBD lesions show signs of ulceration, erosion, and bleeding, and the pathogenesis and manifestations of IBD lesions are similar to those of oral ulcers and laryngeal erosion. The indigo naturalis contained in Xi Lei San can cool blood detoxification, sterilize tissues, and diminish inflammation [38]. Calculus bovis factitius functions as a sedative, acesodyne, sterilizing agent, anti-inflammatory agent, and vasoconstrictor and also increases blood hemoglobin levels [39]. Borneol can relieve swelling and pain, enhance antisepsis activity, and promote tissue regeneration [40]. Pearl and ivory crumb have heat

clearing and detoxification effects; they also promote granulation, the healing of mucosal ulcers, and the removal of toxins [41]. Studies have shown that Xi Lei San can relieve symptoms such as diarrhea, pus and blood in stools, and bellyache as well as promote the healing of ulcers, improve the clinical symptoms of patients, and reduce the recurrence rate of IBD [16]. In our study, we further verified that Xi Lei San could dramatically increase the body weight of rats and improve the structure and inflammation of colonic tissues in DSS-induced colitis model rats. Inflammasomes comprise a class of protein complexes that can recognize different damage signals [42]. The NLRP3 inflammasome is the main type of NLRP inflammasome and consists of NLRP3, ASC, and caspase-1 [20]. The NLRP inflammasome is an intracellular receptor that can regulate an inflammatory response [43]. NLRP3 inflammasomes, as complexes of multiple proteins, mainly regulate caspase-1 activity to promote the maturation and secretion of IL-1β and IL-18 and thus help to regulate the innate immune response. NLRP3 inflammasomes are also known to be associated with IBD pathogenesis [22, 44]. In our study, we found that Xi Lei San could significantly inhibit NLRP3 inflammasome activity in rats with DSS-induced colitis and also in TNF-α-induced CACO2 cells. We also showed that Xi Lei San could reduce apoptosis, ROS production, and inflammatory cytokine production in TNF-α-induced model cells by regulating NLRP3 inflammasomes. However, ASC expression was not altered by Xi Lei San administration. Apoptosis-related speck protein (ASC) is an adaptor protein that connects intracytoplasmic receptors and caspase-1 in inflammasomes. The dimer formed by ASC aggregation during inflammasome activation is referred to as ASC speck and usually exists in a soluble form. ASC is located in the cytoplasm and nucleus of cells undergoing a stress response. ASC was gathered forming dimer, as a caspase-1 activation platform [45]. The previous results reported by Samir et al. [46] are similar to ours [46]. Besides, we know that an interaction between NLRP3 inflammasome and autophagy has been widely studied. Autophagy inhibits NLRP3 inflammasome by cleaning infection pathogenic microorganism (Shao, 2019 #44) and thus enhances the innate immunity response (Jin, 2020 #50). However, evidence indicates that autophagy is positively regulated by NLRP3 inflammasomes (Dupont, 2011 #51). In this study, we found that NLRP3 inflammasomes were activated in DSS-induced rat and TNF-α-treated cells in vitro, along with activated autophagy. Results of this in vitro experiment hinted that NLRP3 activation by alum crystals also enhanced autophagy. This might be due to the fact that autophagy was also alum crystal treatment in vitro and this should be further focused on.

In summary, our *in vivo* and *in vitro* studies showed that Xi Lei San could significantly relieve the symptoms of colitis in DSS-induced colitis model rats by suppressing the activity of NLRP3 inflammasomes and reducing autophagy. These findings suggest Xi Lei San as a Chinese medicine that is capable of attenuating inflammation in IBD via a mechanism that involves NLRP3 inflammasomes. However, the interaction between autophagy and NLRP3 inflammasomes should be further investigated in the future.

Data Availability

The original contributions presented in the study are included in the article; further inquiries can be directed to the corresponding author.

Conflicts of Interest

The authors declare no conflict of interest.

Authors' Contributions

Corresponding author Ji Wu and first author Zhang Tao had contributed to design and organized the experiments. Authors Zhang Tao, Xiaoqing Zhou, Yan Zhang, and Wenfeng Pu had contributed to carry out the animal experiments. Authors Yi Yang, Fuxia Wei, Lin Zhang, and Qian Zhou had contributed to the cell experiments. Author Zhonghan Du had contributed to the statistical analysis. All authors approved the paper before submission.

Acknowledgments

This work was funded by the Science & Technology Department of Sichuan Province (No. 2018JY0417), the Science & Technology Department of Hubei Province (No. 2017CFB175), the Education Department of Sichuan Province (No. 18ZB0211), and the Bureau of Science & Technology Nanchong City (No. 18SXHZ0466).

References

[1] J. M. Shapiro, S. Subedi, and N. S. LeLeiko, "Inflammatory bowel disease," *Pediatrics in Review*, vol. 37, no. 8, pp. 337–347, 2016.

[2] T. Sairenji, K. L. Collins, and D. V. Evans, "An update on inflammatory bowel disease," *Primary Care*, vol. 44, no. 4, pp. 673–692, 2017.

[3] M. J. Rosen, A. Dhawan, and S. A. Saeed, "Inflammatory bowel disease in children and adolescents," *JAMA Pediatrics*, vol. 169, no. 11, pp. 1053–1060, 2015.

[4] J. F. Colombel and U. Mahadevan, "Inflammatory bowel disease 2017: innovations and changing paradigms," *Gastroenterology*, vol. 152, no. 2, pp. 309–312, 2017.

[5] T. A. Malik, "Inflammatory bowel disease," *The Surgical Clinics of North America*, vol. 95, no. 6, pp. 1105–1122, 2015.

[6] A. V. Vila, F. Imhann, V. Collij et al., "Gut microbiota composition and functional changes in inflammatory bowel disease and irritable bowel syndrome," *Science translational medicine*, vol. 10, no. 472, 2018.

[7] L. S. Celiberto, F. A. Graef, G. R. Healey et al., "Inflammatory bowel disease and immunonutrition: novel therapeutic approaches through modulation of diet and the gut microbiome," *Immunology*, vol. 155, no. 1, pp. 36–52, 2018.

[8] B. P. Abraham, T. Ahmed, and T. Ali, "Inflammatory bowel disease: pathophysiology and current therapeutic approaches," *Handbook of Experimental Pharmacology*, vol. 239, pp. 115–146, 2017.

[9] S. S. Seyedian, F. Nokhostin, and M. D. Malamir, "A review of the diagnosis, prevention, and treatment methods of

inflammatory bowel disease," *Journal of Medicine and Life*, vol. 12, no. 2, pp. 113–122, 2019.

[10] L. Peyrin-Biroulet, W. Sandborn, B. E. Sands et al., "Selecting therapeutic targets in inflammatory bowel disease (STRIDE): determining therapeutic goals for treat-to-target," *The American Journal of Gastroenterology*, vol. 110, no. 9, pp. 1324–1338, 2015.

[11] S. C. Ng, H. Y. Shi, N. Hamidi et al., "Worldwide incidence and prevalence of inflammatory bowel disease in the 21st century: a systematic review of population-based studies," *The Lancet*, vol. 390, no. 10114, pp. 2769–2778, 2018.

[12] M. J. Zhang, "Disease-syndrome combination in integrated traditional Chinese and Western medicine in andrology: confusions and countermeasures in studies," *National Journal of Andrology*, vol. 23, no. 7, pp. 579–582, 2017.

[13] S. Eisenhardt and J. Fleckenstein, "Traditional Chinese medicine valuably augments therapeutic options in the treatment of climacteric syndrome," *Archives of Gynecology and Obstetrics*, vol. 294, no. 1, pp. 193–200, 2016.

[14] Y. L. Zhang, L. T. Cai, J. Y. Qi et al., "Gut microbiota contributes to the distinction between two traditional Chinese medicine syndromes of ulcerative colitis," *World Journal of Gastroenterology*, vol. 25, no. 25, pp. 3242–3255, 2019.

[15] K. Zheng, H. Shen, J. Jia et al., "Traditional Chinese medicine combination therapy for patients with steroid-dependent ulcerative colitis: study protocol for a randomized controlled trial," *Trials*, vol. 18, no. 1, p. 8, 2017.

[16] G. Holleran, F. Scaldaferri, A. Gasbarrini, and D. Currò, "Herbal medicinal products for inflammatory bowel disease: a focus on those assessed in double-blind randomised controlled trials," *Phytotherapy Research*, vol. 34, no. 1, pp. 77–93, 2020.

[17] J. Wen, B. Teng, P. Yang et al., "The potential mechanism of Bawei Xileisan in the treatment of dextran sulfate sodium-induced ulcerative colitis in mice," *Journal of Ethnopharmacology*, vol. 188, pp. 31–38, 2016.

[18] N. Song and T. Li, "Regulation of NLRP3 Inflammasome by phosphorylation," *Frontiers in Immunology*, vol. 9, p. 2305, 2018.

[19] Z. Zhong, E. Sanchez-Lopez, and M. Karin, "Autophagy, NLRP3 inflammasome and auto-inflammatory/immune diseases," *Clinical and Experimental Rheumatology*, vol. 34, no. 4, 98, pp. 12–16, 2016.

[20] D. Liu, X. Zeng, X. Li, J. L. Mehta, and X. Wang, "Role of NLRP3 inflammasome in the pathogenesis of cardiovascular diseases," *Basic Research in Cardiology*, vol. 113, no. 1, 2018.

[21] H. Yin, Q. Guo, X. Li et al., "Curcumin suppresses IL-1β secretion and prevents inflammation through inhibition of the NLRP3 inflammasome," *Journal of Immunology*, vol. 200, no. 8, pp. 2835–2846, 2018.

[22] T. D. Kanneganti, "Inflammatory bowel disease and the NLRP3 inflammasome," *The New England Journal of Medicine*, vol. 377, no. 7, pp. 694–696, 2017.

[23] Y. Zhen and H. Zhang, "NLRP3 inflammasome and inflammatory bowel disease," *Frontiers in Immunology*, vol. 10, p. 276, 2019.

[24] A. Hussain, M. F. AlAjmi, I. Hussain, and I. Ali, "Future of ionic liquids for chiral separations in high-performance liquid chromatography and capillary electrophoresis," *Critical Reviews in Analytical Chemistry*, vol. 49, no. 4, pp. 289–305, 2019.

[25] Z. Pan, J. Peng, X. Zang et al., "High-performance liquid chromatography study of gatifloxacin and sparfloxacin using erythrosine as post-column resonance Rayleigh scattering reagent and mechanism study," *Luminescence*, vol. 33, no. 2, pp. 417–424, 2018.

[26] N. Li, H. Zhou, H. Wu et al., "STING-IRF3 contributes to lipopolysaccharide-induced cardiac dysfunction, inflammation, apoptosis and pyroptosis by activating NLRP3," *Redox Biology*, vol. 24, p. 101215, 2019.

[27] X. Wu, H. Zhang, W. Qi et al., "Nicotine promotes atherosclerosis via ROS-NLRP3-mediated endothelial cell pyroptosis," *Cell Death & Disease*, vol. 9, no. 2, p. 171, 2018.

[28] J. S. Moon, "Clinical aspects and treatments for pediatric inflammatory bowel disease," *Intest Res*, vol. 17, no. 1, pp. 17–23, 2019.

[29] C. Norton, W. Czuber-Dochan, M. Artom, L. Sweeney, and A. Hart, "Systematic review: interventions for abdominal pain management in inflammatory bowel disease," *Alimentary Pharmacology & Therapeutics*, vol. 46, no. 2, pp. 115–125, 2017.

[30] Y. Uno, "Hypothesis: mechanism of irritable bowel syndrome in inflammatory bowel disease," *Medical Hypotheses*, vol. 132, p. 109324, 2019.

[31] J. C. Martin, G. Bériou, and R. Josien, "Dextran sulfate sodium (DSS)-induced acute colitis in the rat," *Methods in Molecular Biology*, vol. 1371, pp. 197–203, 2016.

[32] Z. Gong, S. Zhao, J. Zhou et al., "Curcumin alleviates DSS-induced colitis via inhibiting NLRP3 inflammsome activation and IL-1β production," *Molecular Immunology*, vol. 104, pp. 11–19, 2018.

[33] R. Batra, M. K. Suh, J. S. Carson et al., "IL-1β (interleukin-1β) and TNF-α (tumor necrosis factor-α) impact abdominal aortic aneurysm formation by differential effects on macrophage polarization," *Arteriosclerosis, Thrombosis, and Vascular Biology*, vol. 38, no. 2, pp. 457–463, 2018.

[34] K. Chmaj-Wierzchowska, K. Małgorzata, S. Sajdak, and M. Wilczak, "Serum MCP-1 (CCL2), MCP-2 (CCL8), RANTES (CCL5), KI67, TNF-beta levels in patients with benign and borderline," *European Journal of Gynaecological Oncology*, vol. 40, no. 2, pp. 278–283, 2019.

[35] D. Pugliese, C. Felice, A. Papa et al., "Anti TNF-α therapy for ulcerative colitis: current status and prospects for the future," *Expert Review of Clinical Immunology*, vol. 13, no. 3, pp. 223–233, 2017.

[36] Y. L. Jones-Hall and C. H. Nakatsu, "The intersection of TNF, IBD and the microbiome," *Gut microbes*, vol. 7, no. 1, pp. 58–62, 2016.

[37] X. L. Chen, L. H. Zhong, Y. Wen et al., "Inflammatory bowel disease-specific health-related quality of life instruments: a systematic review of measurement properties," *Health and Quality of Life Outcomes*, vol. 15, no. 1, p. 177, 2017.

[38] S. Yanai, S. Nakamura, and T. Matsumoto, "Indigo naturalis-induced colitis," *Digestive Endoscopy*, vol. 30, no. 6, p. 791, 2018.

[39] Z. J. Yu, Y. Xu, W. Peng et al., "Calculus bovis: a review of the traditional usages, origin, chemistry, pharmacological activities and toxicology," *Journal of Ethnopharmacology*, vol. 254, p. 112649, 2020.

[40] Z. X. Chen, Q. Q. Xu, C. S. Shan et al., "Borneol for regulating the permeability of the blood-brain barrier in experimental ischemic stroke: preclinical evidence and possible mechanism," *Oxidative Medicine and Cellular Longevity*, vol. 2019, 2019.

[41] D. Ernst, "Ivory, the pearl of the forest," *Scientific American*, vol. 144, no. 1, pp. 9–12.

[42] P. Yerramothu, A. K. Vijay, and M. D. P. Willcox, "Inflammasomes, the eye and anti-inflammasome therapy," *Eye (London, England)*, vol. 32, no. 3, pp. 491–505, 2018.

[43] M. M. Gaidt and V. Hornung, "The NLRP3 inflammasome renders cell death pro-inflammatory," *Journal of Molecular Biology*, vol. 430, no. 2, pp. 133–141, 2018.

[44] B. Z. Shao, S. L. Wang, P. Pan et al., "Targeting NLRP3 inflammasome in inflammatory bowel disease: putting out the fire of inflammation," *Inflammation*, vol. 42, no. 4, pp. 1147–1159, 2019.

[45] J. Cheng, A. L. Waite, E. R. Tkaczyk et al., "Kinetic properties of ASC protein aggregation in epithelial cells," *Journal of Cellular Physiology*, vol. 222, no. 3, pp. 738–747, 2010.

[46] P. Samir, S. Kesavardhana, D. M. Patmore et al., "DDX3X acts as a live-or-die checkpoint in stressed cells by regulating NLRP3 inflammasome," *Nature*, vol. 573, no. 7775, pp. 590–594, 2019.

Hindawi
Mediators of Inflammation
Volume 2021, Article ID 8854916, 11 pages
https://doi.org/10.1155/2021/8854916

Research Article

Long-Term Follow-Up, Association between CARD15/NOD2 Polymorphisms, and Clinical Disease Behavior in Crohn's Disease Surgical Patients

Francesco Giudici,[1] **Tiziana Cavalli**,[1] **Cristina Luceri**,[2] **Edda Russo**,[1] **Daniela Zambonin**,[1] **Stefano Scaringi**,[1] **Ferdinando Ficari**,[1] **Marilena Fazi**,[1] **Amedeo Amedei**,[1] **Francesco Tonelli**,[1] **and Cecilia Malentacchi**[3]

[1]*Department of Clinical and Experimental Medicine, Surgical Unit, University of Florence, Italy*
[2]*Department of Neuroscience, Psychology, Pharmacology and Child Health (NEUROFARBA), Italy*
[3]*Department of Biomedical Experimental and Clinical Sciences, "Mario Serio", Italy*

Correspondence should be addressed to Edda Russo; edda.russo@unifi.it

Received 18 September 2020; Revised 4 February 2021; Accepted 8 February 2021; Published 25 February 2021

Academic Editor: Elena Dozio

Background. CARD15/NOD2 is the most significant genetic susceptibility in Crohn's disease (CD) even though a relationship between the different polymorphisms and clinical phenotype has not been described yet. The study is aimed at analyzing, in a group of CD patients undergoing surgery, the relationship between CARD15/NOD2 polymorphisms and the clinical CD behavior after a long-term follow-up, in order to identify potential clinical biomarkers of prognosis. *Methods*. 191 surgical CD patients were prospectively characterized both for the main single nucleotide polymorphisms of CARD15/NOD2 and for many other environmental risk factors connected with the severe disease form. After a mean follow-up of 7.3 years, the correlations between clinical features and CD natural history were analyzed. *Results*. CARD15/NOD2 polymorphisms were significantly associated with younger age at diagnosis compared to wild type cases ($p < 0.05$). Moreover, patients carrying a 3020insC polymorphism presented a larger Δ between diagnosis and surgery ($p = 0.0344$). Patients carrying an hz881 and a 3020insC exhibited, respectively, a lower rate of responsiveness to azathioprine ($p = 0.012$), but no difference was found in biologic therapy. Finally, the risk of surgical recurrence was significantly associated, respectively, to age at diagnosis, to familial CD history, to diagnostic delay, to arthritis, and to the presence of perioperative complications. *Conclusions*. 3020insC CARD15 polymorphism is associated with an earlier CD onset, and age at CD diagnosis < 27 years was confirmed to have a detrimental effect on its clinical course. In addition, the familiarity seems to be connected with a more aggressive postoperative course. Finally, for the first time, we have observed a lower rate of responsiveness to azathioprine in patients carrying an hz881 and a 3020insC.

1. Introduction

Crohn's disease (CD (MIM 266600)) is classified as an idiopathic inflammatory bowel disease (IBD) with a multifactorial pathogenesis [1–3]. The role of genetics in the development of CD began to be outlined in the 1980s, based on studies showing an increased number of cases among patients' family members [4]. Genome-wide association studies (GWAS) provided the identification of up to 163 loci in the human genome associated with IBD, significantly more than that in any other complex diseases [5, 6–13].

In addition, several risk factors for CD development have been reported, but it is still unknown if their pathogenic mechanism could be mediated by genetics: smoking habit is probably the most studied one [14, 15–23], and medical and surgical recurrence rates are significantly higher in smoking CD patients [24–28, 29, 30]. Previous appendectomy seems another risk factor [31–33, 34, 35]; also, the use

of antibiotics during the first years of life seems to be associated with early CD development [36–38], and similar experiences in adults who underwent long-lasting prior antibiotic or NSAID use are reported too [39–44]; breastfeeding seems protective for CD [45–48].

Little experiences reported that patients carrying NOD2/CARD15 polymorphisms could develop a more aggressive form of Crohn's disease showing a trend for an early surgery followed by multiple surgical interventions [13]. However, a real clinical definition of aggressiveness is still lacking, and the role of genetic factors in the clinical CD history is still undefined.

In this monocentric study, we have enrolled a cohort of patients characterized by a severe CD disease requiring surgery and analyzed the relationship between the different polymorphisms and the postoperative clinical disease behavior after a long-term follow-up in order to detect potential biomarkers of Crohn's disease course.

2. Materials and Methods

2.1. Patients. After Ethical Committee approval and informed consent signature, prospectively, peripheral blood samples were collected from 191 Caucasian CD patients consecutively admitted for abdominal surgical operation to the IBD surgical unit of the Department of Surgery and Translational Medicine of the University of Florence, during the period January 2010-December 2014. No other exclusion criteria were adopted in our prospective observational study, characterized by a mean follow-up of 7.3 years (range 5.1-9.2). Examined clinical data included gender, age at diagnosis, family history of IBD, presence of extraintestinal or perianal disease, number of IBD-associated surgeries and intersurgical interval, recurrence of disease, surgical complications, and status of disease. Demographic and clinical features of patients are reported in Table 1.

2.2. Genomic DNA Extraction. Genomic DNA of patients was extracted from peripheral blood leukocytes with a Wizard Genomic DNA Purification Kit (Promega, Madison, WI, USA) according to the manufacturer's instructions and quantified by a NanoDrop-1000 Spectrophotometer (NanoDrop Technologies, Wilmington, DE, USA).

2.3. CARD15/NOD2 Gene Polymorphism Analysis. Exons 4, 8, and 11 of the NOD2 gene were amplified by PCR for the detection of R702W, G881R, and 3020insC polymorphisms (representing 32%, 18%, and 31%, respectively, of the total CD polymorphisms). They were sequenced using specific couples of primers and PCR condition as reported in Table 2. The distribution of detected genotypes of our surgical patients is shown in Figure 1 and Table 3.

R702W and 3020insC polymorphism were screened by PCR-based sequencing reaction, using a BigDye Terminator Purification Kit (Applied Biosystems, Foster City, CA, USA) and the ABI Prism 310 Genetic Analyzer (Applied Biosystems). G881R polymorphism has been screened by PCR-based enzymatic digestion using HhaI restriction endonuclease (Fermentas, Burlington, Canada).

Through sequencing reaction and microcapillary electrophoresis in a ABI Prism 310 automated sequencer (Applied Biosystems®, Foster City, Calif., USA), electropherogram by fluorescence detection was obtained. Clinical and anamnestic data collected for the CD patients—including age of disease onset, disease location and severity, and smoking habit—were analyzed and correlated with the genetic profile.

2.4. Statistical Analysis. Statistical analyses were performed using the STATGRAPHICS Centurion XVI.II (Statpoint Technologies Inc., Warrenton, VA) and GraphPad Prism 7.00 (GraphPad Software, San Diego, CA). Normality was verified with the Kolmogorov-Smirnov test. Normally distributed and continuous variables were expressed as the mean ± standard error (SE). Nonnormally distributed variables were expressed as the median and interquartile range. Differences among proportions were evaluated using the χ^2 test or t-test, as appropriate. Comparison of continuous variables between two groups was performed using Student's t-test (normally distributed) or Mann–Whitney test (nonnormally distributed); differences among groups were analyzed by ANOVA or Kruskal-Wallis test if nonnormally distributed.

Logistic regression analysis was used to determine the predictors of recurrence, perianal disease, surgical complications, and disease behavior. The independent variables tested include patient factors (age at diagnosis, gender, genotype, smoking habits, cigarettes/years, family history of IBD, allergies, breastfeeding, and antibiotic use in childhood), disease factors (first clinical presentation, diagnostic delay (calculated as the time between the first symptom/s due to CD and the clinical diagnosis), number of previous surgeries, presence of fistulae and/or abscesses, and disease location), pharmacological therapy factors, and other preoperative factors: presence of anaemia, appendectomy before surgery, tonsillectomy, arthritis, skin extension, neoplasia, and autoimmune disease.

All the independent variables were forced in the Cox proportional hazard model with backward elimination and applied to select the most promising subset of predictors by multiple regression.

Results of regression analysis are reported as odds ratios (ORs) with the respective 95% CI while statistical significance was set at $p < 0.05$.

3. Results

3.1. Patient's Characteristics. CARD15/NOD2 polymorphisms were found in 66 out of 191 CD patients analyzed: 53 patients were heterozygotes, carrying both a normal and a mutated sequence, and 13 individuals were found to be homozygotes.

The mean age at diagnosis was shown to be significantly different between wt (wild type) patients (33.25 ± 1.2, range 10-71) and the mutated (etero+omo) group (27.28 ± 1.28, range 11-57).

Additionally, data regarding the residence country of the patients was collected: 55.28% of wt patients live in central Italy, 41.46% in southern Italy, and 3.25% in northern Italy.

Table 1: Demographic and clinical features of CD patients.

	All cases	Wild type (WT)	Polymorphism carriers (etero+omo)
Number of patients	191	125	66
Age of onset (yrs)	27 (21.5-38.5)	28 (23-43.5)	25 (19.25-34)*
Δ diagnosis-surgery (months)	12 (6-36)	12 (5-40)	12 (6-36)
Gender			
Male	110 (58%)	68 (54%)	42 (64%)
Female	81 (42%)	57 (46%)	24 (36%)
Smoking habit			
No	57 (33%)	31 (28%)	26 (44%)*
Yes	54 (32%)	35 (31%)	19 (32%)
Former	60 (35%)	46 (41%)	14 (24%)
Pack years	15 (6-27)	18 (10-35)	9 (5-18)**
Disease location			
Ileo	112 (59%)	74 (59%)	38 (57%)
Colon	20 (10%)	15 (12%)	5 (8%)
Ileocolon	59 (31%)	36 (29%)	23 (35%)
Disease behavior			
Inflammatory	20 (11%)	13 (10%)	7 (11%)
Stricturing	84 (44%)	57 (46%)	27 (41%)
Fistulising	18 (9%)	10 (8%)	8 (12%)
Stricturing and fistulising	69 (36%)	45 (36%)	24 (36%)
Extraintestinal disease			
Skin	27 (14%)	19 (15%)	8 (12%)
Arthritis	60 (31%)	41 (33%)	19 (29%)
Perianal fistulae	65 (34%)	39 (31%)	26 (39%)
Medication responsiveness			
Mesalazine	140 (92%)	94 (93%)	46 (88%)
Steroids	126 (81%)	80 (81%)	46 (82%)
Azathioprine	73 (72%)	44 (72%)	29 (73%)
Infliximab	33 (57%)	20 (54%)	13 (62%)
Adalimumab	46 (75%)	24 (75%)	22 (76%)
Type of surgery			
Resection	157 (82%)	100 (80%)	55 (83%)
Resection+SXPL	34 (18%)	25 (20%)	11 (17%)
Recurrence	99 (52%)	64 (51%)	35 (53%)
Multiple operations (≥2)	99 (52%)	63 (50%)	36 (55%)
History of urgent surgery	47 (25%)	32 (26%)	15 (23%)
Minimum surgery-free interval (yrs)	3 (0.5-9)	3 (0.5-8)	3 (0.2-13.5)
Mean surgery-free interval (yrs)	5 (2-9)	5 (2-8)	5 (2-13.5)
Digestive cancer	5 (3%)	3 (2%)	2 (3%)
Extraintestinal cancer	9 (5%)	7 (6%)	2 (3%)
Immunological comorbidity			
Autoimmunity	26 (14%)	17 (14%)	9 (14%)
Asthma	8 (4%)	4 (3%)	4 (6%)
Allergies	49 (26%)	28 (22%)	21 (32%)
Familial IBD	42 (26%)	29 (27%)	13 (24%)
Disease status			
Quiescent	95 (66%)	56 (62%)	39 (74%)
Active	49 (34%)	35 (38%)	14 (26%)

Data are median (interquartile range 25–75) for continuous variables and number (percentage) for categorical variable. $^{*}p < 0.05$, $^{**}p < 0.01$ WT vs. etero+omo, by χ^2 or Mann–Whitney test.

Table 2: Primers and PCR condition used for the detection of R702W, G881R, and 3020insC polymorphisms in NOD2 gene.

Exon	Polymorphism	Primers	Annealing temperature
4	Arg702Trp (R702W)	5′-AGATCACAGCAGGCCTTCCTG-3′ 5′-GCCAATGTCACCCACAGAGT-3′	59°C
8	Gly881Arg (G881R)	5′-AAGTCTGTAATGTAAAGCCAC-3′ 5′-CCCAGCTCCTCCCTCTTC-3′	55°C
11	3020insC	5′-CTCACCATTGTATCTTCTTTTC-3′ 5′-GAATGTCAGAATCAGAAGGG-3′	55°C

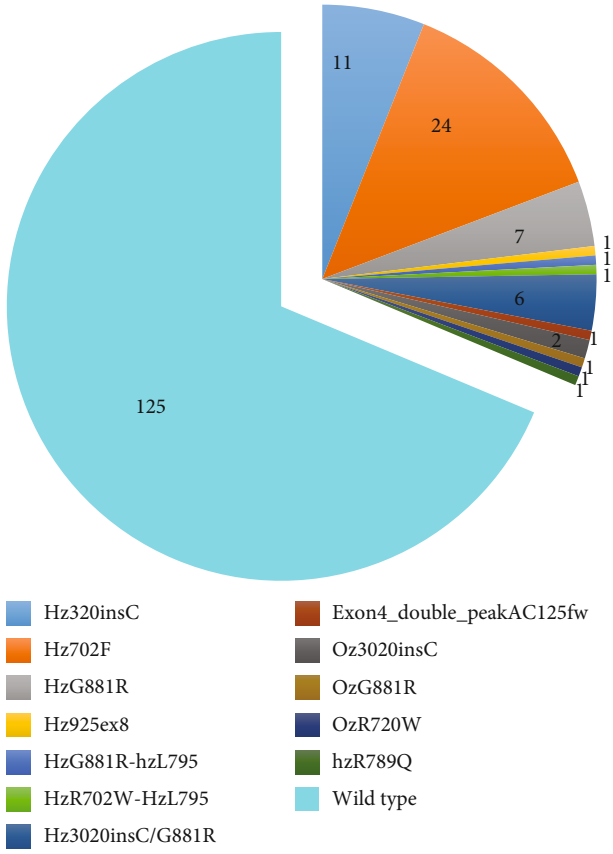

Figure 1: Genotype distribution of the clinical sample population. The figure shows the distribution of *CARD15*/*NOD2* genotypes detected in the examined cohort of surgical patients (number of patients).

The etero+omo group had a slightly higher but not significant percentage of individuals coming from central Italy (60.32%).

The distribution of never smoker, current smoker, and former smoker patients was significantly different in the two genetic groups ($p = 0.04$): compared to wt, etero+omo patients presented a higher percentage of nonsmokers (44.07% vs. 27.68%) and fewer former smokers (23.73% vs. 41.10%). Moreover, the mean smoked pack-years in smokers (number of cigarettes smoked per day/20 × number of years smoked) were 20.70 ± 3.62 for wt and 13.24 ± 2.78 in the etero+omo group ($p = 0.0017$).

About childbirth, 48 patients did not clearly remember their delivery and early-life period, and so, we consider for this analysis only the other 143 patients (7.69% reported birth by caesarean delivery, and 1.40% referred obstetrical complications); wt and etero+omo did not differ significantly. In addition, 23.78% did not receive maternal breastfeeding, with a similar frequency in the genotype groups; 34.96% have received long-lasting or repeated antibiotic treatment in childhood, more frequently in the etero+omo group (38.46% vs. 31.87%). Family IBD history documented through specialist medical genetic counselling was reported in 25.61% of the cases. Up to 20.12% declared to have one or more relatives affected by CD, 3.05% by UC, and 2.44% referred family history positive for both IBDs. The percentages of familial and sporadic cases were similar in the wt and etero+omo groups.

3.2. Association with Clinical Features. No differences were found between wt and etero+omo regarding the median delay (12 months for both groups), although the mean value was higher in the wt group (50.21 ± 9.23 vs. 28.67 ± 5.49 months, $p = 0.13$). However, when divided according to the type of polymorphism, an etero+omo patient presented a diagnostic delay significantly different ($p = 0.0344$); in particular, patients carrying a 3020insC polymorphism presented a larger Δ between diagnosis and surgery.

No evidence of different clinical presentation was found between the wt and etero+omo patients. The majority of them in both groups declared that the first symptom was alteration of the alvus (intestinal obstruction 29.71% or diarrhoea 18.86%); 3.43% presented with perianal fistulae, while 34.29% referred a wider spectrum of symptoms (diarrhoea, abdominal pain, weight loss, asthenia, and anaemia).

The distribution of disease location was not significantly related to the genotype: isolated ileal location was present in 57.57% of etero+omo and in 59.20% of wt patients; similar frequency in the two groups was found for colic disease (7.57 vs. 12.00%, respectively), while 34.85% of etero+omo and 28.80% of wt had ileocolic disease.

Moreover, arthritis was reported in 31.41% of the population, and skin manifestations such as erythema nodosum or pyoderma gangrenosum were present in 14.14% of the patients. The frequency of arthropathy did not show a difference between etero+omo and wt (28.69% and 32.80%, respectively, $p = 0.32$), as well as skin extension (12.12% and 15.20%, respectively, $p = 0.33$).

We documented a perianal disease in 34.03% of cases, affecting 31.20% of wt and 39.39% of etero+omo patients (Table 4). Further, 3 etero+omo and 1 wt patients referred

Table 3: Demographic and clinical features of polymorphism carriers.

Type of polymorphism	R702W	G881R	3020insC	Double variant
Number of patients	25	15	13	10
Age of onset (yrs)	24.5 (19-31.25)	29 (20-38)	22.5 (19.25-26.5)	28 (16-42.5)
Δ diagnosis-surgery (months)	12 (4-12)	10 (6-43)	36 (12-84)	24 (12-55)*
Gender				
Male	15 (60%)	10 (67%)	6 (46%)	9 (90%)
Female	10 (40%)	5 (33%)	7 (54%)	1 (10%)
Smoking habit				
No	6 (27%)	10 (72%)	7 (58%)	3 (33%)
Yes	9 (41%)	2 (14%)	3 (25%)	4 (45%)
Former	7 (32%)	2 (14%)	2 (17%)	2 (22%)
Disease status				
Quiescent	17 (85%)	8 (61%)	9 (82%)	3 (43%)
Active	3 (15%)	5 (39%)	2 (18%)	4 (57%)
Disease location				$p = 0.0527$
Ileo	15 (60%)	8 (53%)	11 (84%)	2 (20%)
Colon	2 (8%)	0	1 (8%)	2 (20%)
Ileocolon	8 (32%)	7 (47%)	1 (8%)	6 (60%)
Disease behavior				
Inflammatory	1 (4%)	1 (7%)	1 (8%)	1 (12%)
Stricturing	11 (46%)	7 (46%)	3 (25%)	4 (44%)
Fistulising	2 (8%)	1 (7%)	3 (25%)	2 (22%)
Stricturing and fistulising	10 (42%)	6 (40%)	5 (42%)	2 (22%)
Extraintestinal disease				
Skin	4 (19%)	2 (14%)	1 (9%)	1 (14%)
Arthritis	7 (33%)	4 (28%)	5 (45%)	2 (28%)
Perianal fistulae	10 (40%)	4 (27%)	4 (33%)	6 (60%)
Medication responsiveness				
Mesalazine	18 (95%)	9 (75%)	11 (100%)	6 (86%)
Steroids	16 (84%)	9 (64%)	11 (100%)	8 (89%)
Azathioprine	15 (100%)	5 (55%)	4 (44%)	4 (80%)*
Infliximab	4 (50%)	1 (25%)	5 (100%)	3 (75%)
Adalimumab	9 (82%)	4 (67%)	7 (78%)	1 (50%)
Type of surgery				
Resection	18 (86%)	12 (80%)	10 (83%)	9 (90%)
Resection+SXPL	3 (14%)	3 (20%)	2 (17%)	1 (10%)
Recurrence	9 (43%)	8 (53%)	8 (67%)	6 (67%)
Multiple operations (≥2)	9 (41%)	9 (60%)	8 (67%)	8 (80%)
History of urgent surgery	2 (9%)	5 (33%)	3 (25%)	$p = 0.673$ 5 (50%)
Minimum surgery-free interval (yrs)	5.058 ± 2.02	7.796 ± 2.8	7.886 ± 2.6	4.157 ± 2.7
Mean surgery-free interval (yrs)	5.81 ± 1.9	8.133 ± 2.7	9.438 ± 2.2	5.957 ± 2.5
Digestive and/or extraintestinal cancer	1 (4%)	1 (7%)	2 (14%)	0
Immunological comorbidity				
Autoimmunity	3 (15%)	1 (8%)	3 (27%)	1 (14%)
Asthma	1 (5%)	0	2 (18%)	1 (14%)
Allergies	9 (45%)	5 (36%)	6 (54%)	1 (12%)
Familial IBD	6 (33%)	5 (36%)	1 (10%)	1 (11%)

Data are mean ± SE or median (interquartile range 25–75) for continuous variables and number (percentage) for categorical variable. $^*p < 0.05$, $^{**}p < 0.01$ WT vs. etero+omo, by χ^2 or Kruskal-Wallis test.

anal fissure without fistulae; one patient reported both. The risk of perianal disease was significantly lower in patients with disease localized in the upper part of the intestine, ileum, or ileum-colon and, borderline, in those with a median of pack/year less than 6 ($p = 0.0538$) and higher in the presence of CARD15 polymorphisms ($p = 0.0886$) (Table 5). Perianal disease was correlated to both ileostomy (8.02% of our patients) and colostomy (2.14%). Smoking habits seemed to be associated with increased risk of faecal derivation: 9.43% of current smokers and 13.33% of former smokers underwent ileostomy, vs. 4.88% of never smokers ($p = 0.12$). The percentage of definitive stoma did not differ significantly between etero+omo and wt patients (12.50 and 9.68%, respectively).

Disease behavior was analyzed and correlated to genetic profile. Stricturing disease was observed in 43.98% of cases, 9.42% had fistulising behavior, and 36.13% presented both types of disease, while 10.47% had an inflammatory pattern. The etero+omo and wt groups presented similar behavior distribution ($p = 0.75$).

Drug response was analyzed in terms of reported clinical improvement (reduction of diarrhoea and/or abdominal pain). The majority of the patient population (88.43%) had assumed mesalamine with initial good clinical results; 6.94% reported resistance to the therapy, 0.58% intolerance, and etero+omo and wt did not differ for such distribution. Regarding steroid therapy, 81.29% was responsive, 10.79% showed resistance, and 5.68% showed dependence on cortisone. No statistical difference was seen related to genotype. A similar distribution was evidenced for azathioprine, with 72.28% of responsiveness, 11.44% of resistance, and 5.42% of intolerance. In this case, we noted significant differences among etero+omo patients, according to the type of polymorphism ($p = 0.012$); those carrying an hz881 and a 3020insC allelic variant exhibited in fact a lower rate of responsiveness to azathioprine (Figure 2).

A little number of wt patients (4.71%) received methotrexate with partial benefit, while one etero+omo patient reported unresponsiveness. Similarly, 56.90% of patients assumed infliximab with good clinical results; 10.84% declared resistance, and 4.22% showed intolerance. Genotype did not correlate to particular responsiveness to infliximab. 75.41% of cases treated with adalimumab received benefit, 8.43% was resistant, and only one case resulted intolerant. History of previous emergency surgery was evaluated as a marker of disease aggressiveness: 22.73% of etero+omo and 25.60% of wt underwent at least once urgent bowel operation.

About the surgery, 92 patients (48.17%) underwent primary surgery for CD, while 99 patients (51.83%) were operated on for a surgical recurrence. Interestingly, surgical recurrence risk was significantly higher in younger patients (less than 27 years old) and those with familial IBD; on the contrary, it was significantly lower in patients with a short diagnostic delay (less than 1 year), with quiescent disease, or with no associated arthritis or surgical complications (Table 3). The presence of CARD15 variants did not change that frequency nor influenced the site of disease recurrence, which was, respectively, perianastomotic in 91.21% of cases, located elsewhere in 7.69%, and both in the site of previous resection and distally in 1.10% of recurrent patients. Regarding the number of surgical recurrence, 48.17% of patients were operated once, 27.75% twice, and 24.08% 3 or more times, with no difference related to genotype, despite the higher frequency of multiple surgeries among polymorphic patients (54.54%). Active smokers presented a higher percentage of multiple surgeries (37.78%) than never smokers (33.33%) or former smokers (28.89%). As a parameter of disease aggressiveness, for patients operated at least twice, the minimum and mean interval of time between two consecutive operations were also considered. The former presented a mean value of 5.36 years (range 0.005-23 years) without significant difference based on genotype. Similarly, the medium interval had a mean value of 6.47 years (range 0-24).

Table 4: Independent variables associated to the perianal disease risk.

Perianal disease risk	Odds ratio	95.0% confidence intervals		p value
		Lower limit	Upper limit	
Site				0.0007
Ileum	0.15	-2.94017	-0.802703	
Ileocolon	0.36	-2.12092	0.0871799	
Pack/years < 6 (yrs)	0.50	-1.38701	0.0248437	0.0538
Genotype	1.87	-0.103337	1.36101	0.0886

Evaluating globally primary and recurrent surgery, the type of surgical treatment in wt and etero+omo did not differ significantly: overall, 82.20% of the patients underwent resective surgery and 17.80% received resection and conservative operation (one or more strictureplasty/ies).

Furthermore, postoperative complications were reported in 30.77% of patients (48/156): anastomotic leakage occurred in 29.17% cases, anaemia-requiring blood transfusion in 14.58%, incisional hernia in 20.83%, wound infection in 12.5%, anastomotic strictures in 4.17%, and mechanical ileus in 1 case (2.08%) as short bowel syndrome, while 14.58% experienced a combination of complications.

Postoperative follow-up of the patients was performed assessing the disease status (quiescent or active inflammation) or exitus: only a wt 78-year-old woman died, because of a multiorgan failure 2 years after colic resection for Crohn colitis. At follow-up, 34.03% of patients had symptomatic active disease and 65.97% had no sign of inflammation at both clinical and instrumental follow-up (endoscopy and MRI). No statistical significance resulted from the comparison of the outcome in the etero+omo and wt groups.

History of malignancies was observed in 7.3% of patients, with no significant difference by genetic profile: cancer of the gastrointestinal tract was observed in five patients, and 9 extraintestinal sites of tumours were observed. Among wt patients, one woman presented a rectal adenocarcinoma associated with hereditary nonpolyposis colorectal cancer syndrome, 1 woman was operated on for breast cancer at the age of 20, a heavy smoker man had larynx cancer, two men were operated on for prostate tumour, two men had

Table 5: Independent variables associated with the surgical recurrence risk.

Recurrence risk	Odds ratio	95.0% confidence intervals		p value
		Lower limit	Upper limit	
Age at diagnosis < 27 yrs	3.00	0.251699	1.94821	0.0086
Diagnostic delay < 12 months	0.35	-1.93322	-0.180071	0.0139
No arthritis	0.394	-1.77804	-0.0821999	0.0276
No surgical complications	0.292	-2.14659	-0.314302	0.0062
Follow-up (quiescent disease)	0.231	-2.35501	-0.576888	0.0007
Familial IBD	2.14	0.171336	2.25389	0.0160

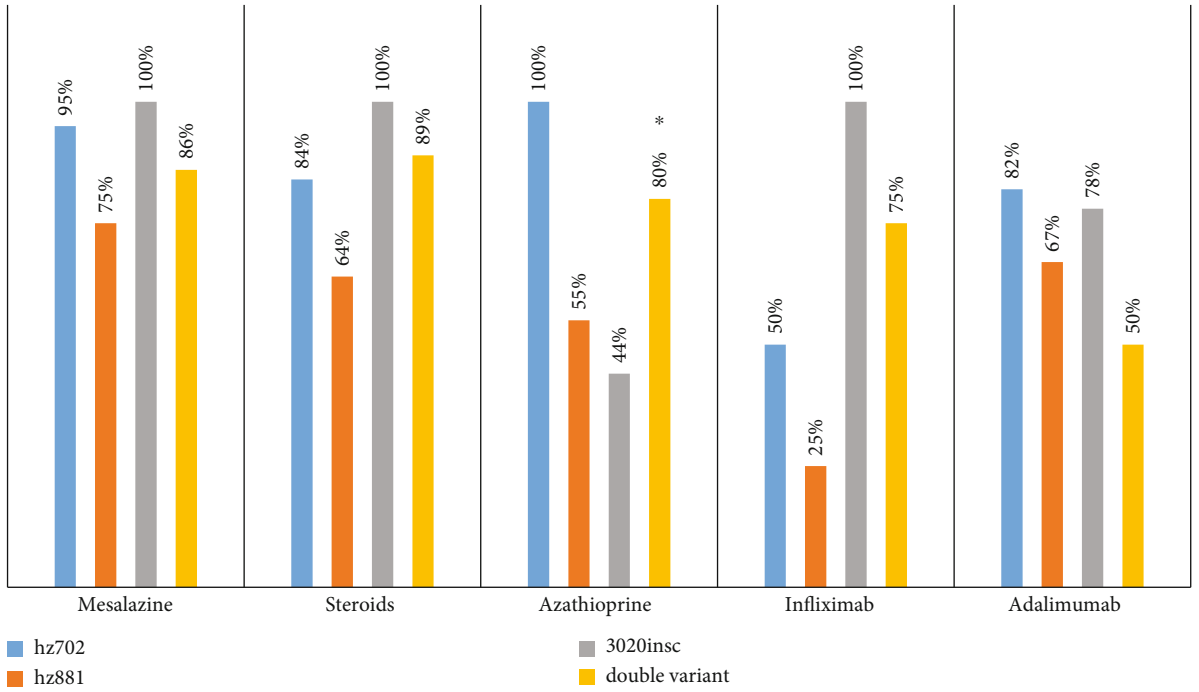

Figure 2: Medication responsiveness of polymorphism carriers. The figure shows the medication responsiveness of polymorphism carrier CD patients. Data are expressed as percentage. $^{*}p < 0.05$.

papillary kidney carcinoma, and one man had papillary thyroid carcinoma. Among etero+omo patients, a male patient heterozygote for 3020insC polymorphism underwent surgery for colloid colon carcinoma which developed on an ulcerated stenosis after 24 years of Crohn colitis. Breast cancer occurred at a young age for a woman with heterozygotes for 3020insC. A never smoker man carrier of G881R heterozygosis and affected by ileocolic CD since the age of 29 had bladder cancer at the age of 53. A woman hzR702W suffering from colic CD since the age of 36, when she underwent vulvectomy for a rare cancer of the clitoris, and at the age of 68 was operated for rectal adenocarcinoma ex tubulevillous adenoma.

The presence of autoimmune disease (Hashimoto thyroiditis, psoriasis, and vitiligo) showed identical frequency in both etero+omo and wt groups, 13.6%. Allergies were reported in 25.65% of the study population, with a higher but not significantly different frequency among etero+omo patients (31.82 vs. 22.4% of wt). Even asthma, occurring in 4.19% of the cases, showed no association with genotype.

History of appendectomy performed at a young age was recorded and correlated to genotype. In the etero+omo group, 33.93% of cases underwent surgery for acute appendicitis, as well as 24.52% of wt ($p = 0.20$). Moreover, history of tonsillectomy was investigated as a condition indicating a possible childhood immune alteration associated with oral microbiota modification. Etero+omo patients declared to have undergone tonsillectomy in 22.64% of cases, which is fewer than wt (32.65%). This finding, though not significant ($p = 0.19$), suggest a potential contribution of the removal of tonsils in the patient immunological alterations.

4. Discussion

IBD-associated loci account for only 13.60% of disease variance in CD, the rest resulting from the environment or "hidden heritability" caused by genetic interactions or epigenetics [5, 10, 49]. In our series, polymorphisms of CARD15/NOD2 were detected in 66 patients (34.55% of the study population). We did not find a phenotypic difference between CD

patients who were either homozygous for one or compound heterozygous for any of the R702W, G908R, and L1007fs variants, suggesting that the respective roles of these variants are comparable.

According to a systematic review performed by Loftus et al. among North American IBD patients, the mean age for CD diagnosis ranged from 33 to 45 years [50]. Moreover, a recent study investigating all known 163 IBD risk gene loci has found that increased genetic burden was associated with early CD diagnosis [51].

In our cohort, the mean age at the time of diagnosis was 31.09 years, but mutant CARD15 subjects were significantly younger compared to wild type patients: 27.28 years versus 33.25, respectively ($p = 0.004$). As previously reported, the risk for CD is 13-fold higher in first-degree relatives of individuals affected by CD [52]. In our cohort, familial history of IBD was observed in 25.61% of cases, with similar frequency in the two genotype groups, and remarkable phenotypic concordance among affected relatives was reported, except for 3.05% of cases who referred familial history positive for UC. In agreement with published studies, we observed that familial IBD history increased recurrence risk (OR = 2.14; $p = 0.016$) together with a younger age at diagnosis (OR = 3; $p = 0.0086$).

Several authors reported a less frequent involvement of the colon in patients carrying CARD15 polymorphisms, and ileal location was predicted by higher genetic burden in CD [53, 54]. Accordingly, ileal CD is allegedly determined in part by genetic factors, while CD with colonic localization could be explained more by environmental factors [55]. However, in our series, the genotype is not associated with a particular disease location.

Ileal CD patients have been demonstrated to present reduced levels of the antimicrobial peptide alpha-defensin originating from Paneth-cells [56]. This decrease was more evident in patients with a 1007 fs variant, suggesting an altered intestinal microbiota and dysregulated innate immunity. Studies conducted on a murine model suggest that NOD2 polymorphisms may predispose to CD by decreasing tolerance to the resident microbial flora [57]. Indeed, CD in patients carrying at least one variant of CARD15 tends to show a more aggressive clinical course [58]. In our study, a retrospective assessment of a possible early-life dysbiosis was obtained through a multi-item questionnaire investigating common childhood conditions associated with microbial impairment, such as caesarean delivery, artificial breastfeeding, and long-term use of antibiotics [59]. In our cohort, several patients claimed one or more of these factors, independently of the genotype, in particular one-third of them, the antibiotic use in childhood, thus suggesting the dysbiosis as a pathogenic factor. However, the evidence supporting a causative role of *in utero* or perinatal measles in CD development is still insufficient. Our enrolled patients are Caucasian subjects living in urban areas, mostly in central and southern Italy, with medium to high social status and hygiene conditions. A recent study has identified higher social status, higher educational level of parents, and living in urban areas as important risk factors for CD and complications [60, 61].

We included surgical patients, which are complicated CD cases refractory to medical treatments or with severe organic complications (fistula-abscess, severe stricture) characterized according to the parameters indicated by the Montreal classification. In this cohort, we further analyzed the presence of possible risk factors that could influence the postoperative course, promoting recurrence.

An extensive survey investigating genetic and clinical factors predisposing to perianal manifestations of CD identified colic CD location as the only significant predictor of perianal disease [62]. In agreement, our data showed that perianal disease risk was lower in patients with ileo and ileocolon CD location ($p < 0.001$). Genetic variations within the CARD15/-NOD2 resulted in a higher but not significant risk factor for perianal CD (OR = 1.87; $p = 0.0886$). Studies on perianal disease in CD contrast regarding gender as a risk factor for perianal fistulae. In our cohort, the female/male ratio in patients affected by perianal disease was 0.80 and not significantly different from the gender ratio of the whole cohort (0.74). On the contrary, we noted a borderline significant association between perianal disease risk and the smoke habit ($p = 0.0538$), suggesting an increased risk for heavy smokers.

Evaluating our results, we observed several clinical factors associated with a more aggressive natural CD history, such as (i) the development of early-onset disease leading to complications requiring surgery a few years after diagnosis, (ii) the presence of extraintestinal disease and perianal fistula, and (iii) the necessity of a permanent stoma. The latter are factors related to the development of single or multiple surgical recurrences during follow-up. Even if we did not find significant association between CARD15 polymorphisms and disease location, disease behavior, perianal fistulae, risk of permanent stoma, number of reoperations, and extraintestinal manifestations, analyzing the diagnostic delay of etero +omo patients, according to the type of polymorphism, we found that patients carrying a 3020insC polymorphism presented a larger Δ between diagnosis and surgery ($p = 0.0344$). This data indicate that their CD course could be characterized by a lower rate of complications that usually bring patients to surgery. On the contrary, the study of Bhullar et al. performed in a cohort of only 30 CD patients reported that patients with 3020insC polymorphism had a significantly reduced time between their diagnosis and first surgical resection, suggesting that the polymorphism leads to a more aggressive disease form, which rapidly progresses requiring early surgical intervention [13]. On the other hand, another study reported that children with the 3020insC polymorphism have a 6.6-fold increased risk for developing a stricturing phenotype requiring surgery [63].

Interestingly, we also noted, for the first time, that patients carrying an hz881 and a 3020insC exhibited a lower rate of responsiveness to azathioprine ($p = 0.012$), but no difference was found in biologic therapy (Figure 2). About azathioprine, we observed a decrease in responsiveness of 20%, statistically significant in double polymorphism carriers (Table 3). This evidence is clinically relevant as azathioprine is commonly used in CD patients. Therefore, a preventive screening of the double polymorphism carriers could avoid both delays in starting postoperative therapy with biological

drugs and the development of adverse events due to azathioprine administration, thus maximizing the cost-effectiveness of medical therapy and tailoring the efficacy on the patients' characteristics.

Currently, many studies have reduced the importance of the genetic component in the pathogenesis of Crohn's disease, but this study underlines the importance of considering not only the single mutation but also the associations between them in the various susceptibility genes known.

The detection of particular combinations of variants related to the clinical course or treatment responsiveness could allow the design of new genetic biomarkers, prognostic or theranostic, leading to a more personalized approach in CD.

In conclusion, the present study confirms that in Caucasian patients, CD natural history seems not strictly related to genetic factors; however, CARD15 polymorphisms are associated with an earlier CD onset, and both age at diagnosis < 27 years and familiarity for CD were confirmed to have a detrimental effect on the postoperative natural history of the patients. Differences in relation to the three polymorphisms have been also detected in our cohort, but essentially, we documented for the first time that patients carrying an hzG881R and a 3020insC exhibited a lower rate of responsiveness to azathioprine with relevant clinical-correlated impact.

Data Availability

The underlying data supporting our study will be shown after a via email request.

Ethical Approval

This study was approved by the Ethical Committee of Azienda Ospedaliero-Universitaria Careggi, Firenze, on May 2, 2011, protocol no. 2011/0016888, ref. 95/10, authorization Gen Dir 17/572011, protocol no. 2011/0018055.

Consent

Written informed consent was obtained from all study subjects.

Conflicts of Interest

The authors declare that they have no competing interests.

Authors' Contributions

F. Giudici and T. Cavalli contributed equally to this work. F. Giudici, T. Cavalli, D. Zambonin, S. Scaringi, and F. Ficari revised the literature on this topic; F. Giudici, T. Cavalli, E. Russo, D. Zambonin, S. Scaringi, F. Ficari, and F. Tonelli collected the data; C. Luceri, F. Giudici, T. Cavalli, D. Zambonin, Russo E, and S. Scaringi analyzed the data; F. Giudici, T. Cavalli, C. Luceri, D. Zambonin, and C. Malentacchi wrote the manuscript; E. Russo edited the manuscript, F. Giudici, S. Scaringi, F. Ficari, and C. Malentacchi supervised and revised the manuscript. A. Amedei revised critically for important intellectual content; F. Giudici, E Russo, and C Malentacchi provided funding acquisition. Malentacchi is legally responsible for the data collected and reported in this work. Francesco Giudici and Tiziana Cavalli equally contributed to this work.

Acknowledgments

The authors are grateful to Dr. Goti Emanuele for DNA sequencing service, Dr. Michele Tanturli for the statistical contribution, Prof. Maria Gabriella Torcia for English revision, Dr. Loredana Cavalli for supporting data collection of patients, and Dr. Francesca Gensini for the genetic consulting. This research was supported by Fondazione Cassa di Risparmio di Firenze N 13472-(2016.0842), No. 2008.1581, and No. 2009.1301.

References

[1] R. J. Xavier and D. K. Podolsky, "Unravelling the pathogenesis of inflammatory bowel disease," *Nature*, vol. 448, no. 7152, pp. 427–434, 2007.

[2] J. Burisch, N. Pedersen, S. Cukovic-Cavka et al., "Environmental factors in a population-based inception cohort of inflammatory bowel disease patients in Europe–an ECCO-EpiCom study," *Journal of Crohn's & Colitis*, vol. 8, no. 7, pp. 607–616, 2014.

[3] Y. Ko, R. Butcher, and R. W. Leong, "Epidemiological studies of migration and environmental risk factors in the inflammatory bowel diseases," *World Journal of Gastroenterology*, vol. 20, no. 5, pp. 1238–1247, 2014.

[4] B. A. Lashner, A. A. Evans, J. B. Kirsner, and S. B. Hanauer, "Prevalence and incidence of inflammatory bowel disease in family members," *Gastroenterology*, vol. 91, no. 6, pp. 1396–1400, 1986.

[5] The International IBD Genetics Consortium (IIBDGC), L. Jostins, S. Ripke et al., "Host-microbe interactions have shaped the genetic architecture of inflammatory bowel disease," *Nature*, vol. 491, no. 7422, pp. 119–124, 2012.

[6] J. P. Hugot, M. Chamaillard, H. Zouali et al., "Association of NOD2 leucine-rich repeat variants with susceptibility to Crohn's disease," *Nature*, vol. 411, no. 6837, pp. 599–603, 2001.

[7] Y. Ogura, D. K. Bonen, N. Inohara et al., "A frameshift mutation in _NOD2_ associated with susceptibility to Crohn's disease," *Nature*, vol. 411, no. 6837, pp. 603–606, 2001.

[8] G. Muzes, Z. Tulassay, and F. Sipos, "Interplay of autophagy and innate immunity in Crohn's disease: a key immunobiologic feature," *World Journal of Gastroenterology*, vol. 19, no. 28, pp. 4447–4454, 2013.

[9] C. R. Homer, A. L. Richmond, N. A. Rebert, J.–. P. Achkar, and C. McDonald, "_ATG16L1_ and _NOD2_ Interact in an Autophagy-Dependent Antibacterial Pathway Implicated in Crohn's Disease Pathogenesis," *Gastroenterology*, vol. 139, no. 5, pp. 1630–1641.e2, 2010.

[10] N. T. Ventham, N. A. Kennedy, E. R. Nimmo, and J. Satsangi, "Beyond gene discovery in inflammatory bowel disease: the emerging role of epigenetics," *Gastroenterology*, vol. 145, no. 2, pp. 293–308, 2013.

[11] R. Kellermayer, "Epigenetics and the developmental origins of inflammatory bowel diseases," *Canadian Journal of Gastroenterology*, vol. 26, no. 12, pp. 909–915, 2012.

[12] E. R. Nimmo, J. G. Prendergast, M. C. Aldhous et al., "Genome-wide methylation profiling in Crohn's disease identifies altered epigenetic regulation of key host defense mechanisms including the Th17 pathway," *Inflammatory Bowel Diseases*, vol. 18, no. 5, pp. 889–899, 2012.

[13] M. Bhullar, F. Macrae, G. Brown, M. Smith, and K. Sharpe, "Prediction of Crohn's disease aggression through NOD2/-CARD15 gene sequencing in an Australian cohort," *World Journal of Gastroenterology*, vol. 20, no. 17, pp. 5008–5016, 2014.

[14] O. Höie, F. Wolters, L. Riis et al., "Ulcerative colitis: patient characteristics may predict 10-yr disease recurrence in a European-wide population-based cohort," *The American Journal of Gastroenterology*, vol. 102, no. 8, pp. 1692–1701, 2007.

[15] P. L. Lakatos, Z. Vegh, B. D. Lovasz et al., "Is current smoking still an important environmental factor in inflammatory bowel diseases? Results from a population-based incident cohort," *Inflammatory Bowel Diseases*, vol. 19, no. 5, pp. 1010–1017, 2013.

[16] H. S. Odes, A. Fich, S. Reif et al., "Effects of current cigarette smoking on clinical course of Crohn's disease and ulcerative colitis," *Digestive Diseases and Sciences*, vol. 46, no. 8, pp. 1717–1721, 2001.

[17] G. Bastida and B. Beltran, "Ulcerative colitis in smokers, non-smokers and ex-smokers," *World Journal of Gastroenterology*, vol. 17, no. 22, pp. 2740–2747, 2011.

[18] I. A. Finnie, B. J. Campbell, B. A. Taylor et al., "Stimulation of colonic mucin synthesis by corticosteroids and nicotine," *Clinical Science (London, England)*, vol. 91, no. 3, pp. 359–364, 1996.

[19] J. T. Green, C. Richardson, R. W. Marshall et al., "Nitric oxide mediates a therapeutic effect of nicotine in ulcerative colitis," *Alimentary Pharmacology & Therapeutics*, vol. 14, no. 11, pp. 1429–1434, 2000.

[20] S. D. AlSharari, H. I. Akbarali, R. A. Abdullah et al., "Novel insights on the effect of nicotine in a murine colitis model," *The Journal of Pharmacology and Experimental Therapeutics*, vol. 344, no. 1, pp. 207–217, 2012.

[21] E. D. Srivastava, J. R. Barton, S. O'Mahony et al., "Smoking, humoral immunity, and ulcerative colitis," *Gut*, vol. 32, no. 9, pp. 1016–1019, 1991.

[22] S. S. Mahid, K. S. Minor, A. J. Stromberg, and S. Galandiuk, "Active and passive smoking in childhood is related to the development of inflammatory bowel disease," *Inflammatory Bowel Diseases*, vol. 13, no. 4, pp. 431–438, 2007.

[23] G. Corrao, A. Tragnone, R. Caprilli et al., "Risk of inflammatory bowel disease attributable to smoking, oral contraception and breastfeeding in Italy: a nationwide case-control study. Cooperative Investigators of the Italian Group for the Study of the Colon and the Rectum (GISC)," *International Journal of Epidemiology*, vol. 27, no. 3, pp. 397–404, 1998.

[24] J. Cosnes, L. Beaugerie, F. Carbonnel, and J.–. P. Gendre, "Smoking cessation and the course of Crohn's disease: an intervention study," *Gastroenterology*, vol. 120, no. 5, pp. 1093–1099, 2001.

[25] B. D. Breuer-Katschinski, N. Hollander, and H. Goebell, "Effect of cigarette smoking on the course of Crohn's disease," *European Journal of Gastroenterology & Hepatology*, vol. 8, no. 3, pp. 225–228, 1996.

[26] J. Cosnes, F. Carbonnel, L. Beaugerie, Y. le Quintrec, and J. P. Gendre, "Effects of cigarette smoking on the long-term course of Crohn's disease," *Gastroenterology*, vol. 110, no. 2, pp. 424–431, 1996.

[27] Y. Zabana, E. Garcia-Planella, M. van Domselaar et al., "Does active smoking really influence the course of Crohn's disease? A retrospective observational study," *Journal of Crohn's & Colitis*, vol. 7, no. 4, pp. 280–285, 2013.

[28] J. Kalra, A. K. Chaudhary, and K. Prasad, "Increased production of oxygen free radicals in cigarette smokers," *International Journal of Experimental Pathology*, vol. 72, no. 1, pp. 1–7, 1991.

[29] V. Bergeron, V. Grondin, S. Rajca et al., "Current smoking differentially affects blood mononuclear cells from patients with Crohn's disease and ulcerative colitis: relevance to its adverse role in the disease," *Inflammatory Bowel Diseases*, vol. 18, no. 6, pp. 1101–1111, 2012.

[30] M. C. Aldhous, K. Soo, L. A. Stark et al., "Cigarette smoke extract (CSE) delays NOD2 expression and affects NOD2/RIPK2 interactions in intestinal epithelial cells," *PLoS One*, vol. 6, no. 9, article e24715, 2011.

[31] F. Scaldaferri, V. Gerardi, L. R. Lopetuso et al., "Gut microbial flora, prebiotics, and probiotics in IBD: their current usage and utility," *BioMed Research International*, vol. 2013, 9 pages, 2013.

[32] S. C. Ng, C. N. Bernstein, M. H. Vatn et al., "Geographical variability and environmental risk factors in inflammatory bowel disease," *Gut*, vol. 62, no. 4, pp. 630–649, 2013.

[33] G. L. Radford-Smith, J. E. Edwards, D. M. Purdie et al., "Protective role of appendicectomy on onset and severity of ulcerative colitis and Crohn's disease," *Gut*, vol. 51, no. 6, pp. 808–813, 2002.

[34] G. G. Kaplan, B. V. Pedersen, R. E. Andersson, B. E. Sands, J. Korzenik, and M. Frisch, "The risk of developing Crohn's disease after an appendectomy: a population-based cohort study in Sweden and Denmark," *Gut*, vol. 56, no. 10, pp. 1387–1392, 2007.

[35] P. B. Eckburg, E. M. Bik, C. N. Bernstein et al., "Diversity of the human intestinal microbial flora," *Science*, vol. 308, no. 5728, pp. 1635–1638, 2005.

[36] M. F. Dubeau, M. Iacucci, P. L. Beck et al., "Drug-induced inflammatory bowel disease and IBD-like conditions," *Inflammatory Bowel Diseases*, vol. 19, no. 2, pp. 445–456, 2013.

[37] S. Y. Shaw, J. F. Blanchard, and C. N. Bernstein, "Association between the use of antibiotics in the first year of life and pediatric inflammatory bowel disease," *The American Journal of Gastroenterology*, vol. 105, no. 12, pp. 2687–2692, 2010.

[38] M. P. Kronman, T. E. Zaoutis, K. Haynes, R. Feng, and S. E. Coffin, "Antibiotic exposure and IBD development among children: a population-based cohort study," *Pediatrics*, vol. 130, no. 4, pp. e794–e803, 2012.

[39] T. Card, R. F. Logan, L. C. Rodrigues, and J. G. Wheeler, "Antibiotic use and the development of Crohn's disease," *Gut*, vol. 53, no. 2, pp. 246–250, 2004.

[40] D. J. Margolis, M. Fanelli, O. Hoffstad, and J. D. Lewis, "Potential association between the oral tetracycline class of antimicrobials used to treat acne and inflammatory bowel disease," *The American Journal of Gastroenterology*, vol. 105, no. 12, pp. 2610–2616, 2010.

[41] M. H. Gleeson and A. J. Davis, "Non-steroidal anti-inflammatory drugs, aspirin and newly diagnosed colitis: a case-control study," *Alimentary Pharmacology & Therapeutics*, vol. 17, no. 6, pp. 817–825, 2003.

[42] S. S. Chan and A. R. Hart, "Aspirin use and development of inflammatory bowel disease: confounding or causation? Authors' reply," *Alimentary Pharmacology & Therapeutics*, vol. 34, no. 11-12, p. 1351, 2011.

[43] A. N. Ananthakrishnan, L. M. Higuchi, E. S. Huang et al., "Aspirin, nonsteroidal anti-inflammatory drug use, and risk for Crohn disease and ulcerative colitis: a cohort study," *Annals of Internal Medicine*, vol. 156, no. 5, pp. 350–359, 2012.

[44] J. B. Felder, B. I. Korelitz, R. Rajapakse, S. Schwarz, A. P. Horatagis, and G. Gleim, "Effects of nonsteroidal antiinflammatory drugs on inflammatory bowel disease: a case-control study," *The American Journal of Gastroenterology*, vol. 95, no. 8, pp. 1949–1954, 2000.

[45] E. Klement, R. V. Cohen, J. Boxman, A. Joseph, and S. Reif, "Breastfeeding and risk of inflammatory bowel disease: a systematic review with meta-analysis," *The American Journal of Clinical Nutrition*, vol. 80, no. 5, pp. 1342–1352, 2004.

[46] A. Hörnell, H. Lagström, B. Lande, and I. Thorsdottir, "Breastfeeding, introduction of other foods and effects on health: a systematic literature review for the 5th Nordic Nutrition Recommendations," *Food & Nutrition Research*, vol. 57, no. 1, p. 20823, 2017.

[47] K. L. Madsen, R. N. Fedorak, M. M. Tavernini, and J. S. Doyle, "Normal breast milk limits the development of colitis in IL-10-deficient mice," *Inflammatory Bowel Diseases*, vol. 8, no. 6, pp. 390–398, 2002.

[48] P. L. Ogra and R. C. Welliver Sr., "Effects of early environment on mucosal immunologic homeostasis, subsequent immune responses and disease outcome," *Nestlé Nutrition Workshop Series. Paediatric Programme*, vol. 61, pp. 145–181, 2008.

[49] N. N. Salkic, G. Adler, I. Zawada et al., "NOD2/CARD15 mutations in Polish and Bosnian populations with and without Crohn's disease: prevalence and genotype-phenotype analysis," *Bosnian Journal of Basic Medical Sciences*, vol. 15, no. 2, pp. 67–72, 2015.

[50] E. V. Loftus Jr., P. Schoenfeld, and W. J. Sandborn, "The epidemiology and natural history of Crohn's disease in population-based patient cohorts from North America: a systematic review," *Alimentary Pharmacology & Therapeutics*, vol. 16, no. 1, pp. 51–60, 2002.

[51] A. N. Ananthakrishnan, H. Huang, D. D. Nguyen, J. Sauk, V. Yajnik, and R. J. Xavier, "Differential effect of genetic burden on disease phenotypes in Crohn's disease and ulcerative colitis: analysis of a North American cohort," *The American Journal of Gastroenterology*, vol. 109, no. 3, pp. 395–400, 2014.

[52] M. Peeters, H. Nevens, F. Baert et al., "Familial aggregation in Crohn's disease: increased age-adjusted risk and concordance in clinical characteristics," *Gastroenterology*, vol. 111, no. 3, pp. 597–603, 1996.

[53] S. Lesage, H. Zouali, J. P. Cézard et al., "_CARD15/NOD2_ mutational analysis and genotype-phenotype correlation in 612 patients with inflammatory bowel disease," *American Journal of Human Genetics*, vol. 70, no. 4, pp. 845–857, 2002.

[54] C. M. Onnie, S. A. Fisher, N. J. Prescott et al., "Diverse effects of the CARD15 and IBD5 loci on clinical phenotype in 630 patients with Crohn's disease," *European Journal of Gastroenterology & Hepatology*, vol. 20, no. 1, pp. 37–45, 2008.

[55] J. Halfvarson, "Genetics in twins with Crohn's disease: less pronounced than previously believed?," *Inflammatory Bowel Diseases*, vol. 17, no. 1, pp. 6–12, 2011.

[56] J. Wehkamp, N. H. Salzman, E. Porter et al., "Reduced Paneth cell alpha-defensins in ileal Crohn's disease," *Proceedings of the National Academy of Sciences of the United States of America*, vol. 102, no. 50, pp. 18129–18134, 2005.

[57] T. Watanabe, A. Kitani, P. J. Murray, and W. Strober, "NOD2 is a negative regulator of Toll-like receptor 2-mediated T helper type 1 responses," *Nature Immunology*, vol. 5, no. 8, pp. 800–808, 2004.

[58] V. Annese, G. Lombardi, F. Perri et al., "Variants of CARD15 are associated with an aggressive clinical course of Crohn's disease–an IG-IBD study," *The American Journal of Gastroenterology*, vol. 100, no. 1, pp. 84–92, 2005.

[59] E. Russo and A. Amedei, "The role of the microbiota in the genesis of gastrointestinal cancers," in *Frontiers in Anti-Infective Drug Discovery*, pp. 1–44, Bentham Science Publishers, 2018.

[60] K. Radon, D. Windstetter, A. L. Poluda et al., "Contact with farm animals in early life and juvenile inflammatory bowel disease: a case-control study," *Pediatrics*, vol. 120, no. 2, pp. 354–361, 2007.

[61] P. López-Serrano, J. L. Pérez-Calle, M. T. Pérez-Fernández, J. M. Fernández-Font, D. Boixeda de Miguel, and C. M. Fernández-Rodríguez, "Environmental risk factors in inflammatory bowel diseases. Investigating the hygiene hypothesis: a Spanish case-control study," *Scandinavian Journal of Gastroenterology*, vol. 45, no. 12, pp. 1464–1471, 2010.

[62] Z. Kanaan, S. Ahmad, N. Bilchuk, C. Vahrenhold, J. Pan, and S. Galandiuk, "Perianal Crohn's disease: predictive factors and genotype-phenotype correlations," *Digestive Surgery*, vol. 29, no. 2, pp. 107–114, 2012.

[63] S. Kugathasan, N. Collins, K. Maresso et al., "CARD15 gene mutations and risk for early surgery in pediatric-onset Crohn's disease," *Clinical Gastroenterology and Hepatology*, vol. 2, no. 11, pp. 1003–1009, 2004.

Hindawi
Mediators of Inflammation
Volume 2020, Article ID 3070345, 8 pages
https://doi.org/10.1155/2020/3070345

Research Article

Mica Can Alleviate TNBS-Induced Colitis in Mice by Reducing Angiotensin II and IL-17A and Increasing Angiotensin-Converting Enzyme 2, Angiotensin 1-7, and IL-10

Mengdie Shen,[1] Bibi Zhang,[2] Mengyao Wang,[2] Li'na Meng ,[2,3,4] and Bin Lv[2,3,4]

[1]*Department of Internal Medicine, Women's Hospital, Zhejiang University School of Medicine, Hangzhou, 310006 Zhejiang Province, China*
[2]*Department of Gastroenterology, First Affiliated Hospital of Zhejiang Chinese Medical University, Hangzhou City, Zhejiang Province 310006, China*
[3]*Key Laboratory of Digestive Pathophysiology of Zhejiang Province, China*
[4]*Institute of Digestive Pathophysiology, Zhejiang Chinese Medical University, China*

Correspondence should be addressed to Li'na Meng; mln6713@163.com

Received 11 May 2020; Revised 18 August 2020; Accepted 1 October 2020; Published 10 October 2020

Academic Editor: Edda Russo

Aim. To explore the treatment effect of mica on 2,4,6-trinitrobenzenesulfonic acid solution- (TNBS-) induced colitis in mice. *Materials and Methods*. Thirty male BALB/C mice were randomly divided into the control group, the TNBS group, and the mica group. Control mice were treated with saline solution. Experimental colitis was induced by TNBS (250 mg/kg/d) in the TNBS group and the mica group. After modeling, the mica group was treated with mica (180 mg/kg/d) for 3 days, while the TNBS group continued the treatment with TNBS. All solutions were injected intrarectally. During treatment, body weight and mice activity were monitored daily. After treatment, the colon tissues of mice were collected; angiotensin II (Ang II), angiotensin-converting enzyme 2 (ACE2), angiotensin 1-7 (Ang (1-7)), IL-17A, and IL-10 expression was analyzed by ELISA and immunohistochemistry. *Results*. Food intake, activity, and body weight gradually decreased in the TNBS group compared to the control group and the mica group (all $P < 0.05$). Also, black stool adhesion in the anus and thin and bloody stool were observed in the TNBS group, but not in the other two groups. Moreover, the expression of Ang II, ACE2, Ang (1-7), IL-17A, and IL-10 in the TNBS group increased compared to that in the control group. Compared to the TNBS group, ACE2, Ang (1-7), and IL-10 in the mica group increased, while Ang II and IL-17A decreased (all $P < 0.05$). *Conclusion*. Mica can alleviate TNBS-induced colitis in mice by regulating the inflammation process; it reduces Ang II and IL-17A and increases ACE2, IL-10, and Ang (1-7).

1. Introduction

Inflammatory bowel disease (IBD) is a chronic nonspecific inflammatory disease that affects the gastrointestinal tract. Over the past 20 years, the incidence of IBD in Asian countries, especially China, has shown a rapid increase [1]. In 2018, the standardized incidence of IBD in Daqing, a city in the west of Heilongjiang province, was 177/100,000, while it was only 3.14/100,000 in Zhongshan city, Guangdong [2]. IBD is characterized by chronic inflammation of your digestive tract. Early and rapid diagnosis of the disease and improvement of intestinal inflammation are critical steps in preventing further progression and improving prognosis. Yet, the exact etiology and pathogenesis of IBD remain unclear.

Traditional therapeutic drugs can improve symptoms but have no effect on the inflammatory process. The renin-angiotensin system (RAS) is an important regulating system, which participates in multiple inflammatory responses. RAS has a vital role in chronic inflammation and early inflammation. Angiotensin II (Ang II) is an essential active peptide of the RAS system [3]. Previous studies [4, 5] have found that

Ang II is expressed in the colon tissues, where it participates in the process of intestinal inflammatory reaction and tissue damage [6]. Thus, it may have an important role in the occurrence of ulcerative colitis.

Mica is a kind of natural layered mineral crystal, which is used in the clinical treatment of various gastrointestinal diseases. Previous studies have shown that this mineral can promote the regeneration of gastrointestinal mucosal epithelial cells, maintain the mucosal barrier, and have an inhibitory effect on the inflammation [7]. The aim of this study was to explore the treatment effect of mica on TNBS-induced colitis in mice.

2. Materials and Methods

2.1. Animals. Thirty male BALB/C mice, 6-8 weeks old, weighing 20 ± 5 g, were purchased from the animal experimental center of Zhejiang Chinese Medical University (2008001664294). All the animals were housed in an environment with a temperature of 22-26°C, relative humidity of 50-60%, and a light/dark cycle of 12/12 h and fed with standard mouse diet. All animal studies (including the mouse euthanasia procedure) were done in compliance with the regulations and guidelines of Zhejiang Chinese Medical University institutional animal care and conducted according to the AAALAC and the IACUC guidelines.

2.2. Reagents. 2,4,6-Trinitrobenzenesulfonic acid solution (no. P2297) was produced by Sigma Company in the United States. Mica microscopical particles were provided by the Department of Pharmacy, the First Affiliated Hospital of Zhejiang Chinese Medical University. Rabbit polygonal to anti-ACE2 antibody was from Abcam, UK; rabbit polygonal to anti-Ang II antibody from British Biorbyt, UK; rabbit polygonal to anti-Ang (1-7) from Cloud-Clone Corp., USA; and rabbit polygonal to anti-IL-10 from Abcam, UK. A mouse IL-17A ELISA Kit was purchased from Abcam, UK.

2.3. Grouping, Modeling, and Specimen Collection. Thirty male BALB/C mice were randomly divided into three groups (10 mice/group): control group, TNBS group, and mica group. Referring to the modeling method of Inokuchi et al. [8], 5% TNBS solution was mixed with anhydrous ethanol in equal volume, configured into a solution of 50 mg/ml, and enema was given once with the dose of 250 mg/kg.

Before modeling, mice were fasted for 24 h. Then, mice were anesthetized using 1% pentobarbital, and the paraffin oil was adequately lubricated. The silicone tube with a diameter of about 2 mm was then inserted into the anus about 3.5 cm; after which, the TNBS ethanol solution 250 mg/kg (for the TNBS group and the mica group) and saline enema with 1 ml/100 g/d (control group) were slowly injected into the colon. After the silicone tube was pulled out, the anus was pinched, and mice were inverted for another 1 min before being put into the squirrel cage. On days 2, 3, and 4, the control group and the TNBS group were given a normal saline enema, and the mica group received mica enema with 180 mg/kg/d (referring to a previously described approach [9]). On day 5, all the mice were sacrificed, and colon specimens (including the intestinal segment from the anus) were collected.

Table 1: Disease activity index.

Weight loss (%)	Stool consistency*	Occult/gross bleeding	Score
(-)	Normal	Normal	0
1-5			1
5-10	Loose	Guaiac (+)	2
11-15			3
>15	Diarrhea	Gross bleeding	4

The disease activity index = (combined score of weight loss, stool consistency, and bleeding)/3. *Normal stools = well-formed pellets; loose = pasty stools which do not stick to the anus; diarrhea = liquid stools that stick to the anus.

Table 2: Macroscopic damage score.

Macroscopic damage	Score
Normal colonic mucosa	0
Local hyperemia, no ulcer	1
Single ulcer, no obvious inflammation	2
A single ulcer with inflammation	3
Two or more ulcers with inflammation	4
Large ulcer with inflammation	5

Tissue was rinsed with normal saline; the damage of the intestinal mucosa was analyzed using a microscope. In the TNBS group and the mica group, the most apparent lesions were collected; in the control group, colon tissue was collected at a distance of 3-4 cm from the anus. Two segments were taken for each mouse. The first was fixed in 10% formaldehyde and embedded in paraffin, followed by hematoxylin-eosin staining and immunohistochemistry. The other section was placed into a cryopreservation tube and stored in a refrigerator at -80°C for inspection.

2.4. General Condition. The animal weight was analyzed daily. The weight was calculated according to the beginning of the experiment. In addition, fecal characteristics (normal, loose, loose stool), fecal bleeding (occult blood or visual blood stools), activity, and feeding were also monitored on a daily basis. According to the scoring method proposed by Murano et al. [10], the disease activity index was the sum of the three scores of weight loss rate, fecal characteristics, and hematochezia (Table 1). A fecal occult blood test was conducted using tetramethylbenzidine.

2.5. Analysis and Scoring of Intestinal Damage. The degree of colonic mucosal damage and inflammation was observed by the score standard of macroscopic damage, referring to Murano et al. [10]. According to the histological damage score method of Dieleman et al. [11], the histological damage degree was revealed by the sum of inflammation, lesion depth, recess failure score, and lesion range score. The scoring criteria are shown in Tables 2 and 3.

2.6. ELISA Detection of IL-17A in the Colon. The level of IL-17A in the colon tissue was determined by Mouse IL-17A

Table 3: Histological grading of colitis.

Feature graded	Grade	Description
Inflammation	0	None
	1	Slight
	2	Moderate
	3	Severe
Extend	0	None
	1	Mucosa
	2	Mucosa and submucosa
	3	Transmural
Regeneration	4	No tissue repair
	3	Surface epithelium not intact
	2	Regeneration with crypt depletion
	1	Almost complete regeneration
	0	Complete regeneration or normal tissue
Crypt damage	0	None
	1	Basal 1/3 damaged
	2	Basal 2/3 damaged
	3	Only surface epithelium intact
	4	Entire crypt and epithelium lost
Percent involvement	1	1-25%
	2	26-50%
	3	51-75%
	4	76-100%

ELISA Kit (Abcam, UK) and ELISA El 800 readers (BioTek Instruments, USA), following the manufacturer's instruction.

2.7. Immunohistochemical Detection of Ang II, ACE2, Ang (1-7), and IL-10 in Colon Tissue. The colon tissues were fixed with 10% formalin, dehydrated, and cut into 5 μm thickness section. Samples were then subjected to immunohistochemical SP staining. The number of staining-positive cells in more than 200 cells was counted and converted to a positive market index, which was calculated using the following formula: positive index (%) = the number of positive cells in the total field/the number of cells in the field 100%. Staining intensity was analyzed using an immune response score (IRS): 0 for colorless, 1 for light yellow, 2 for brownish yellow, and 3 for brown. The percentage score of positive cells was calculated as follows: 1 was divided into positive cells ≤ 10%, 2 into 11%-50%, 3 into 51-75%, and 4 into >75%. The product of staining intensity and percentage of positive cells was a positive integral. A positive integral greater than 3 was considered to be immunoreactive.

2.8. Statistical Analysis. The measurement data conforming to the normal distribution were expressed as mean ± standard deviation, and the comparison between groups was performed by one-way analysis of variance. Pearson was used for correlation analysis. The statistical significance of all tests was defined as $P < 0.05$. All analysis was performed using IBM SPSS statistical software, version 22.0.

3. Results

3.1. Animal Condition and the Colon Morphology. The mice in the control group showed good activity, a slow weight increase, and a clean anal opening (Figure 1, Table 4). In the TNBS group, the intake, the amount of activity, and body weight gradually decreased (Figure 1, Table 4). In addition, the black stool adhesion in the anus, accompanied by thin stool, positive fecal occult blood, and some blood, was observed in the TNBS group. On the second day after modeling, one mouse died, and the dead mouse was dissected. Colon perforation was found about 4 cm from the anus, and feces were seen in the abdomen.

In the mica group, the weight loss was reduced, and the stool characterization was normal compared to the TNBS group (Figure 1, Table 4). In the mica group, one mouse died on day two. Pathological examination of the dead mice showed that the colon adhered to the surrounding tissues 3-4 cm from the anus.

The disease activity index of mice in the TNBS group significantly increased on the first day after modeling, reaching the highest score on the second day. The disease activity index of mice in the mica group was significantly lower than that in the TNBS group. The weight loss and disease activity index in each group are shown in Figure 1 and Tables 4–5.

3.2. Macroscopic Analysis and Scoring of the Colon Damage. The colonic mucosa of the control group was pale pink,

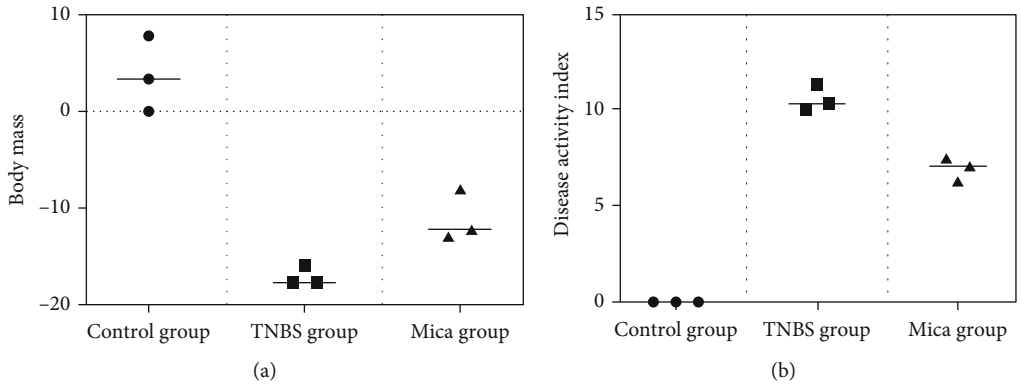

Figure 1: (a) Weight loss in each group and (b) disease activity index in each group.

Table 4: Weight loss (%).

Group	N	D2-1	D3-2	D4-3
Control group	10	1.35 ± 1.00	4.41 ± 3.39	6.31 ± 2.88
TNBS group	9	$-15.19 \pm 4.04^{\blacktriangle}$	$-17.69 \pm 4.97^{\blacktriangle}$	$-17.63 \pm 6.45^{\blacktriangle}$
Mica group	9	$-6.30 \pm 1.84^{\blacktriangle\blacksquare}$	$-12.87 \pm 4.99^{\blacktriangle\blacksquare}$	$-11.29 \pm 5.30^{\blacktriangle\blacksquare}$
F		176.144	155.118	260.946

$^{\blacktriangle}P < 0.01$ vs. control; $^{\blacksquare}P < 0.01$ vs. TNBS.

Table 5: Disease activity index ($\bar{x} \pm s$).

Group	N	D2-1	D3-2	D4-3
Control group	10	0.00 ± 0.00	0.00 ± 0.00	0.00 ± 0.00
TNBS group	9	$10.33 \pm 1.50^{\blacktriangle}$	$11.33 \pm 1.21^{\blacktriangle}$	$10.01 \pm 2.04^{\blacktriangle}$
Mica group	9	$6.33 \pm 1.36^{\blacktriangle\blacksquare}$	$7.5 \pm 1.97^{\blacktriangle\blacksquare}$	$7.1 \pm 2.48^{\blacktriangle\blacksquare}$
F		118.226	111.460	47.532

$^{\blacktriangle}P < 0.01$ vs. control; $^{\blacksquare}P < 0.01$ vs. TNBS.

smooth, and complete, with normal colonic length and uniform thickness. The mice in the TNBS group had hyperemia and edema in the colonic wall, significant erosion; multiple ulcerations of different sizes were observed in the intestinal segment 2-4 cm from the anus, and dark red unformed feces were observed in the intestinal cavity. The colonic damage caused by TNBS was alleviated in the mica group, which showed local hyperemia and scattered erosion.

The TNBS group had a significantly higher colonic macroscopic damage score compared to the control group (4.00 ± 0.89 vs. 0.00 ± 0.00, $P < 0.01$) and the mica group (2.00 ± 1.53 vs. 4.00 ± 0.89, $P < 0.01$). The mica group had higher colonic macroscopic damage score compared to the control group (2.00 ± 1.53 vs. 0.00 ± 0.00, $P < 0.01$).

3.3. Histological Analysis and Scoring of the Colon Damage. In the control group, the colonic mucosa was intact, and the cell structure was normal, and glands were normally arranged. In the TNBS group, the glandular arrangement was disordered, and some of the crypts were deformed or even disappeared, and the mucosa was ulcerated and necrotic. There were a large number of inflammatory cells infiltrated to the mucosa and submucosa. The damage in the mica group was significantly reduced compared with the TNBS group, and the damage degree of the structure of the crypt was alleviated. In addition, only a few inflammatory cells were found to be infiltrated into the mucosal layer. Histological analysis (HE staining) of the colon damage in different groups is shown in Figure 2.

The score of colonic histological damage in the TNBS group and the mica group was significantly higher compared to the control group (8.17 ± 2.99 vs. 1.33 ± 1.03, 3.83 ± 1.47 vs. 1.33 ± 1.03, $P < 0.01$). Yet, the score in the mica group was significantly lower compared to that in the TNBS group (3.83 ± 1.47 vs. 8.17 ± 2.99, $P < 0.01$) (Table 6).

3.4. The Expression of Ang II, ACE2, Ang (1-7), and IL-10 in the Colon. The expression of Ang II, ACE2, Ang (1-7), and IL-10 is shown in Figure 3 and Table 7.

The positive expression of Ang II was observed in the colonic vascular endothelial cytoplasm. It was also partially expressed in the mucosal epithelium and inflammatory cytoplasm. The expression of Ang II in the TNBS group was obviously higher compared to that in the control group (4.83 ± 2.11 vs. 2.16 ± 0.41, $P < 0.01$) and the mica group (2.33 ± 0.52 vs. 4.83 ± 2.11, $P < 0.01$).

The positive expression of ACE2 was mainly expressed in colonic mucosal epithelial cells and inflammatory cytoplasm. The expression of ACE2 in the TNBS group was obviously higher compared to that in the control group (3.50 ± 0.55 vs. 2.04 ± 0.29, $P < 0.05$). The expression of ACE2 further increased in the mica group compared to the TNBS group (5.13 ± 1.84 vs. 3.50 ± 0.55, $P < 0.05$).

The positive expression of Ang (1-7) was mainly found in colonic mucosal epithelial cells and inflammatory

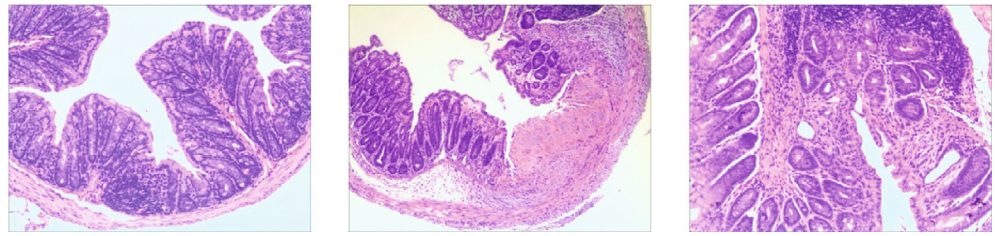

Control group TNBS group Mica group

Figure 2: Histological analysis (HE staining) of the colon damage in different groups, ×200.

Table 6: Macroscopic and histological damage score ($\bar{x} \pm s$).

Group	N	Macroscopic damage score	Histological damage score
Control group	10	0.00 ± 0.00	1.33 ± 1.03
TNBS group	9	$4.00 \pm 0.89^{▲}$	$8.17 \pm 2.99^{▲}$
Mica group	9	$2.00 \pm 1.54^{▲■}$	$3.83 \pm 1.47^{▲■}$
F		22.50	17.64

$^{▲}P < 0.01$ vs. control; $^{■}P < 0.01$ vs. TNBS.

cytoplasm. The expression of Ang (1-7) in the colon tissues of the TNBS group was significantly higher compared to that of the control group (1.04 ± 0.56 vs. 0.13 ± 0.14, $P < 0.05$). The expression of Ang (1-7) further increased in the mica group compared to the TNBS group (2.0 ± 0.63 vs. 1.04 ± 0.56, $P < 0.01$).

The positive expression of IL-10 was mainly expressed in the cytoplasm of the colonic epithelial cells and inflammatory cells. The expression of IL-10 in the colon tissue of the TNBS group was significantly higher compared to that of the control group (4.88 ± 0.83 vs. 2.71 ± 0.78, $P < 0.05$). The expression of IL-10 further increased in the mica group compared to the TNBS group (9.04 ± 2.62 vs. 4.88 ± 0.83, $P < 0.05$).

3.5. ELISA Detection of IL-17A in the Colon. The level of IL-17A in homogenate supernatant of colonic mucosal tissues was determined by ELISA. The results showed that the expression of IL-17A in the TNBS group and the mica group was significantly increased compared to that in the control group (6.93 ± 0.44 vs. 0.65 ± 0.03, 2.63 ± 0.64 vs. 0.65 ± 0.03, $P < 0.01$). However, the expression of IL-17A in the mica group was significantly decreased compared to that in the TNBS group (2.63 ± 0.64 vs. 6.93 ± 0.44, $P < 0.01$) (Table 8).

3.6. Statistical Analysis. The level of Ang II had a positive correlation with the colonic macroscopic damage score ($r = 0.589$, $P < 0.05$), high correlation with the colonic histologic damage score ($r = 0.855$, $P < 0.01$), moderate correlation with the level of IL-17A ($r = 0.647$, $P < 0.05$), and high negative correlation with IL-10 ($r = 0.720$, $P < 0.01$).

The levels of ACE2 and Ang (1-7) were negatively correlated with the colonic macroscopic damage score (ACE2: $r = -0.631$, $P < 0.05$; Ang (1-7): $r = -0.880$, $P < 0.01$), had a moderate negative correlation with the colonic histologic damage score ($r = -0.600$, -0.618, $P < 0.05$) and the level of IL-17A ($r = -0.556$, -0.518, $P < 0.05$), and had a high positive correlation with the level of IL-10 ($r = 0.776$, 0.769, $P < 0.01$).

4. Discussion

Ulcerative colitis is a nonspecific chronic inflammatory disease with unclear pathogenesis. The major causes of ulcerative colitis are genetic, immune, environmental factors, and microorganisms. So far, no effective treatment has been developed.

RAS systems have an important role in a variety of pathophysiological processes. Ang II is the main active substance in the RAS system. Ang II is a proinflammatory substance, which induces the expression of NF-κB, p38MAPK activation, and generates a variety of inflammatory factors, such as IL-6 and IL-17 [12]. Ang II can also have a direct effect on the AT1 receptor on the intestinal cell membrane [13]. It can stimulate the MAPK signaling pathway through the phosphorylation cascade reactions, such as family activate downstream transcription factor that induces the expression of inflammatory factors [14]. Ang II is also part of the ACE-Ang II-AT1R axis, which is mediated through the AT1 receptor. Ang II expression can also lead to blood vessel shrinkage and boot string blood pressure.

Besides the heart, kidney, and brain, RAS is also expressed in the gastrointestinal [15]. Katada et al. [16] found that the expression of Ang II and AT1R in the experimental colitis mice is significantly increased, while the inflammatory response in mice without AT1R is significantly reduced. In the endothermic mice, peroxides significantly increased after Ang II activation, causing endothelial dysfunction and the intestinal tissue ischemia. When mice were treated with Ang II receptor antagonist, the intestinal tissue after ischemia and damage was significantly reduced [17].

Ang (1-7), which has vasodilatation and anti-inflammatory effects, is produced from Ang II. Angiotensin-converting enzyme 2 (ACE2), a new member of the RAS family, is a new ACE homolog. The structures of ACE and ACE2 are similar, but their biological activity is significantly different. ACE2 can increase anti-inflammatory factors such as IL-10 and generate Ang (1-7) of Ang II decomposition. Ang (1-7) is a 7-peptide substance that inhibits inflammation by promoting vasodilation, anti-oxidative stress, and inflammation alleviation [18]. Ang (1-7) is considered to be one of the endogenous Ang II antagonists, which can increase blood flow in the kidney, brain, mesenteric vascular endothelial, and multiple organ tissues, promoting the vasodilation and having a role in the

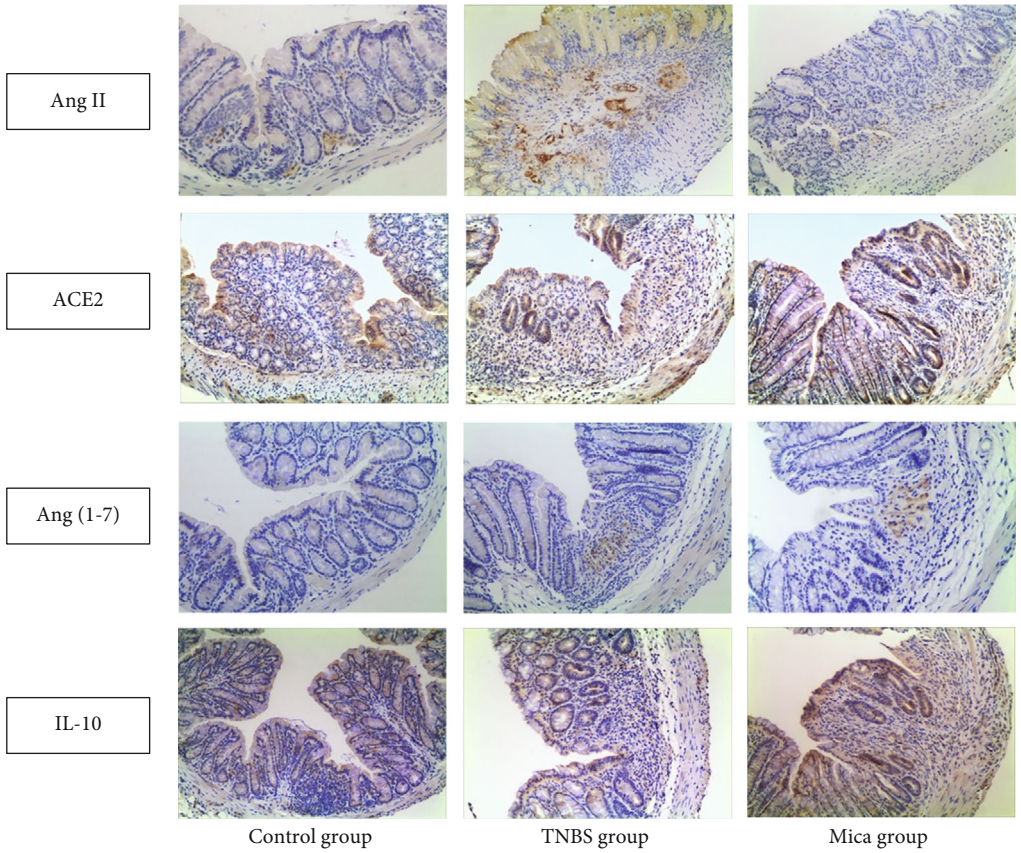

Figure 3: The expression of Ang II, ACE2, Ang (1-7), and IL-10 in different groups, ×200.

Table 7: The expression of Ang II, ACE2, Ang (1-7), and IL-10 in colon tissue.

Group	N	Ang II	ACE2	Ang (1-7)	IL-10
Control group	10	2.16 ± 0.41	2.04 ± 0.29	0.13 ± 0.14	2.71 ± 0.78
TNBS group	9	$4.83 \pm 2.11^{\blacktriangle}$	$3.50 \pm 0.55^{\blacktriangle}$	$1.04 \pm 0.56^{\blacktriangle}$	$4.88 \pm 0.83^{\blacktriangle}$
Mica group	9	$2.33 \pm 0.52^{\blacktriangle\blacksquare}$	$5.13 \pm 1.84^{\blacktriangle\blacksquare}$	$2.00 \pm 0.60^{\blacktriangle\blacksquare}$	$9.04 \pm 2.62^{\blacktriangle\blacksquare}$
F		11.33	8.19	21.7	22.71

$^{\blacktriangle}P < 0.05$ vs. control; $^{\blacksquare}P < 0.05$ vs. TNBS.

Table 8: The level of IL-17A in colon tissue ($\bar{x} \pm s$, pg/ml).

Group	N	IL-17A
Control group	10	0.65 ± 0.03
TNBS group	9	$6.93 \pm 0.44^{\blacktriangle}$
Mica group	9	$2.63 \pm 0.64^{\blacktriangle\blacksquare}$
F		26.39

$^{\blacktriangle}P < 0.01$ vs. control; $^{\blacksquare}P < 0.01$ vs. TNBS.

angiogenesis organization [19]. A previous study [12] showed that inflammation of the intestine increases Ang II and promotes secretion of a variety of proinflammatory factors (TNF-α, IL-17A, TGF-β 1, etc.) from epithelial cells in the focal area. These factors further aggravate the inflammatory response causing damage to the intestinal tissue.

Khajah et al. [20] found that the levels of Ang II, ACE2, and Ang (1-7) were significantly increased in the DSS-induced colitis mice. When the exogenous Ang (1-7) was given, the colonic mucosa damage and ulcer improved. Moreover, Rodrigues et al. [21] showed that colonic mucosa damage in the DSS-induced colitis mice was alleviated after treatment with exogenous Ang (1-7). In contrast, the colon tissue damage was significantly aggravated after Ang (1-7) was blocked by antagonist A779, Ang (1-7) specific receptor. Furthermore, in our previous study, we found an ACE2-Ang (1-7)-MAS axis in the small intestinal mucosa of rats. The expression of ACE2, Ang (1-7), and MAS in the ACE2 group was significantly higher than that in the model group, while the expression of Ang II was significantly downregulated. Gross, pathological, and electron microscopic results showed that the injury of intestinal mucosa was significantly reduced compared with that of the model group. The expression of

ACE2, Ang (1-7), and MAS in the MasR antagonistic group was significantly lower than that in the model group. In contrast, the expression of Ang II was significantly upregulated in the MasR antagonist group. Compared with the model group, the injury of intestinal mucosa in the MasR antagonistic group was more severe than that in the model group, which suggested that the ACE2-Ang (1-7)-MAS axis had a protective effect on NSAID-related small intestine injury. ACE2-Ang (1-7)-MAS may be a potential target for the prevention and treatment of NSAID-related small intestinal injury.

ACE2, which has the catalytic activity of carboxypeptidase, is less expressed in normal organisms than ACE, which is about 1/10 of ACE. Ang I and Ang II are the main substrates of ACE2. On the one hand, ACE2 can reduce the vasoconstriction and oxidative stress of Ang II by downregulating the level of Ang II; on the other hand, it can further antagonize the effect of Ang II by increasing the production of vacillating substance Ang (1-7) [22]. Ang (1-7) is the Ang II endogenous inhibitor. Previous studies have found that the level of ACE2 increases in many diseases, such as myocardial infarction, diabetes, kidney disease, and cirrhosis [23], thus suggesting that the RAS system is activated in the pathological state and the increase of ACE2 may be a stress response. In this study, we established colitis in mice using TNBS. These mice showed poor food intake, decreased activity, weight loss, loose stool, positive stool occult blood, and partial bloody stool. Moreover, the colonic tissue showed intestinal wall thickening, ulcer, necrosis, and other visible damage. In the TNBS group and the mica group, the score of macroscopic damage and histological damage was significantly higher compared to that in the control group. The expression level of IL-17A, Ang II, ACE2, and Ang (1-7) was significantly higher than that of the control group, indicating that Ang II, ACE2, and Ang (1-7) participated in the pathogenesis of colitis. High expression of Ang II can cause vasoconstriction of the intestinal mucosa, decrease of tissue blood supply, and damage of intestinal barrier function. At the same time, Ang II can also be used as an inflammatory factor to upregulate the level of IL-17A, further aggravating the inflammatory response, which may be an important pathogenesis of experimental colitis in mice.

Mica is a kind of natural layered mineral crystal, which is one of the silicate mineral drugs. Its main components are silicon dioxide and alumina. It has special physical properties, such as adsorbability, expansibility, plasticity, and ion-exchange property, so it can be adsorbed on the mucosal surface and enhance the function of the mucosal barrier. Previous studies indicated that mica could be used to treat diarrhea in children [24]. Mica can directly affect the mucosal surface, adsorb proinflammatory cytokines, promote mucus secretion, etc., which, in turn, reduce inflammatory cell infiltration and strengthen the mucosal barrier function [7]. Some studies [19, 25] have suggested that mica can also absorb proinflammatory factors, reduce intestinal mucosal permeability, and antagonize intestinal bacterial translocation. In our previous study [26], we found that the damage of colonic tissue in experimental colitis mice was significantly reduced after the intervention of mica microparticles, thus suggesting that mica can reduce the damage of colonic tissue in colitis mice.

In this study, we found that mica reduced weight loss, improved fecal characteristics, and reduced stool in the blood compared with those of the TNBS group. Moreover, the disease activity index was significantly lower than that of the TNBS group. The scores of macroscopic damage and histological damage were significantly reduced compared with those of the TNBS group, suggesting that mica intervention could significantly reduce the intestinal damage of the mice. Furthermore, we found that the expression of ACE2, Ang (1-7), and IL-10 in the colon tissue of the mica group was higher than that of the TNBS group. In comparison, the expression of Ang II and IL-17A was significantly lower, suggesting that mica can reduce inflammation and intestinal damage. Moreover, the correlation analysis showed that the expression of Ang II was positively correlated with the macroscopic damage score, histological damage score, and IL-17A and negatively correlated with IL-10. Ang II high expression can induce intestinal mucosa vasoconstriction, reduce tissue blood supply, and cause intestinal barrier function injury.

The expression of ACE2 and Ang (1-7) was negatively correlated with the macroscopic damage score, histological damage score, and IL-17A, but positively correlated with IL-10, showing that Ang II in experimental colitis mouse colon injury plays an essential role in the process. All these data indicate that the RAS system is involved in the development of experimental colitis in mice. During an early stage of colon injury, the body's self-defense mechanism is activated, ACE2 Ang-(1-7)-Mas axis expression level feedback to rising, to a certain extent can adversely affect Ang II proinflammatory role, chemotaxis raise of inflammatory cells and plays a role of negative regulating the release of inflammatory factor, its specific mechanism remains to be further researched. Mica on experimental colitis mouse colon injury has a protective effect; its mechanism in addition to adsorbing the inflammatory factor may also increase ACE2-Ang (1-7)-Mas axis, restrain Ang II 1 expression, and reduce inflammation reaction.

To sum up, our data suggested mica can alleviate TNBS-induced colitis in mice by regulating the inflammation process. Mica reduces Ang II and IL-17A and increases ACE2, IL-10, and Ang (1-7).

Abbreviations

IBD: Inflammatory bowel disease
RAS: Renin-angiotensin system
TNBS: 2,4,6-Trinitrobenzenesulfonic acid solution
Ang II: Angiotensin II
ACE2: Angiotensin-converting enzyme 2
Ang (1-7): Angiotensin 1-7.

Data Availability

All data, models, and code generated or used during the study appear in the submitted article.

Conflicts of Interest

The authors declare that they have no conflicts of interest.

Acknowledgments

This study was supported by the National Natural Science Foundation of China (Grant No. 81373877).

References

[1] G. G. Kaplan, "The global burden of IBD: from 2015 to 2025," *Nature Reviews. Gastroenterology & Hepatology*, vol. 12, no. 12, pp. 720–727, 2015.

[2] L. Prideaux, M. A. Kamm, P. P. De Cruz, F. K. L. Chan, and S. C. Ng, "Inflammatory bowel disease in Asia: a systematic review," *Journal of Gastroenterology and Hepatology*, vol. 27, no. 8, pp. 1266–1280, 2012.

[3] S. J. Forrester, G. W. Booz, C. D. Sigmund et al., "Angiotensin II signal transduction: an update on mechanisms of physiology and pathophysiology," *Physiological Reviews*, vol. 98, no. 3, pp. 1627–1738, 2018.

[4] M. Mastropaolo, M. G. Zizzo, M. Auteri et al., "Activation of angiotensin II type 1 receptors and contractile activity in human sigmoid colon *in vitro*," *Acta Physiologica (Oxford, England)*, vol. 215, no. 1, pp. 37–45, 2015.

[5] R. Ranjbar, M. Shafiee, A. R. Hesari, G. A. Ferns, F. Ghasemi, and A. Avan, "The potential therapeutic use of renin-angiotensin system inhibitors in the treatment of inflammatory diseases," *Journal of Cellular Physiology*, vol. 234, no. 3, pp. 2277–2295, 2018.

[6] M. Garg, S. G. Royce, C. Tikellis et al., "Imbalance of the renin-angiotensin system may contribute to inflammation and fibrosis in IBD: a novel therapeutic target?," *Gut*, vol. 69, no. 5, pp. 841–851, 2020.

[7] L. F. Li-na Meng, B. Lv, and W. Wu, "The protection of Mica on non-steroidal anti-inflammatory drug-related small intestine injury and the effect on TNF-α and NF-κB in rats," *Chinese Journal of integrated traditional and Western Medicine*, vol. 30, pp. 961–965, 2010.

[8] Y. Inokuchi, T. Morohashi, I. Kawana, Y. Nagashima, M. Kihara, and S. Umemura, "Amelioration of 2, 4, 6-trinitrobenzene sulphonic acid induced colitis in angiotensinogen gene knockout mice," *Gut*, vol. 54, no. 3, pp. 349–356, 2005.

[9] S. C. Liangjing Wang and J. Si, "The protection of Mica on non-steroidal anti-inflammatory drug-related small intestine injury and the effect on TNF-α and NF-κB in rats," *Chinese Journal of integrated traditional and Western Medicine*, vol. 30, pp. 961–965, 2010.

[10] M. Murano, K. Maemura, I. Hirata et al., "Therapeutic effect of intracolonically administered nuclear factor kappa B (p 65) antisense oligonucleotide on mouse dextran sulphate sodium (DSS)-induced colitis," *Clinical and Experimental Immunology*, vol. 120, no. 1, pp. 51–58, 2000.

[11] L. A. Dieleman, M. J. Palmen, H. Akol et al., "Chronic experimental colitis induced by dextran sulphate sodium (DSS) is characterized by Th1 and Th2 cytokines," *Clinical and Experimental Immunology*, vol. 114, no. 3, pp. 385–391, 1998.

[12] K. J. Maloy and F. Powrie, "Intestinal homeostasis and its breakdown in inflammatory bowel disease," *Nature*, vol. 474, no. 7351, pp. 298–306, 2011.

[13] T. Sato, A. Kadowaki, T. Suzuki et al., "Loss of apelin augments angiotensin II-induced cardiac dysfunction and pathological remodeling," *International Journal of Molecular Sciences*, vol. 20, no. 2, p. 239, 2019.

[14] J. R. Kemp, H. Unal, R. Desnoyer, H. Yue, A. Bhatnagar, and S. S. Karnik, "Angiotensin II-regulated microRNA 483-3p directly targets multiple components of the renin-angiotensin system," *Journal of Molecular and Cellular Cardiology*, vol. 75, pp. 25–39, 2014.

[15] P. Hallersund, A. Elfvin, H. F. Helander, and L. Fändriks, "The expression of renin-angiotensin system components in the human gastric mucosa," *Journal of the Renin-Angiotensin-Aldosterone System*, vol. 12, no. 1, pp. 54–64, 2010.

[16] K. Katada, N. Yoshida, T. Suzuki et al., "Dextran sulfate sodium-induced acute colonic inflammation in angiotensin II type 1a receptor deficient mice," *Inflammation Research*, vol. 57, no. 2, pp. 84–91, 2008.

[17] D. D. Lund, R. M. Brooks, F. M. Faraci, and D. D. Heistad, "Role of angiotensin II in endothelial dysfunction induced by lipopolysaccharide in mice," *American Journal of Physiology. Heart and Circulatory Physiology*, vol. 293, no. 6, pp. H3726–H3731, 2007.

[18] A. C. S. e. Silva, K. D. Silveira, A. J. Ferreira, and M. M. Teixeira, "ACE2, angiotensin-(1-7) and Mas receptor axis in inflammation and fibrosis," *British Journal of Pharmacology*, vol. 169, no. 3, pp. 477–492, 2013.

[19] R. A. Marangoni, A. K. Carmona, R. C. Passaglia, D. Nigro, Z. B. Fortes, and M. H. de Carvalho, "Role of the kallikrein-kinin system in Ang-(1-7)-induced vasodilation in mesenteric arterioles of Wistar rats studied in vivo-in situ," *Peptides*, vol. 27, no. 7, pp. 1770–1775, 2006.

[20] M. A. Khajah, M. M. Fateel, K. V. Ananthalakshmi, and Y. A. Luqmani, "Anti-inflammatory action of angiotensin 1-7 in experimental colitis," *PLoS One*, vol. 11, no. 3, article e0150861, 2016.

[21] T. R. Rodrigues Prestes, N. P. Rocha, A. S. Miranda, A. L. Teixeira, and E. S. A. C. Simoes, "The anti-inflammatory potential of ACE2/angiotensin-(1-7)/mas receptor axis: evidence from basic and clinical research," *Current Drug Targets*, vol. 18, no. 11, pp. 1301–1313, 2017.

[22] M. M. C. Arroja, E. Reid, L. A. Roy et al., "Assessing the effects of Ang-(1-7) therapy following transient middle cerebral artery occlusion," *Scientific Reports*, vol. 9, no. 1, p. 3154, 2019.

[23] Y. Ishiyama, P. E. Gallagher, D. B. Averill, E. A. Tallant, K. B. Brosnihan, and C. M. Ferrario, "Upregulation of angiotensin-converting enzyme 2 after myocardial infarction by blockade of angiotensin II receptors," *Hypertension*, vol. 43, no. 5, pp. 970–976, 2004.

[24] H. D. Dan Liang, L. Zhao, and L.-n. Meng, "The mechanism of small intestine injury and the prevention and treatment of mica by non-steroidal anti-inflammatory drugs," *Chinese Journal of Gastroenterology*, vol. 20, pp. 311–313, 2015.

[25] G. Chao and S. Zhang, "Therapeutic effects of muscovite to non-steroidal anti-inflammatory drugs-induced small intestinal disease," *International Journal of Pharmaceutics*, vol. 436, no. 1-2, pp. 154–160, 2012.

[26] M. W. Bibi Zhang, L. Lian, and L.-n. Meng, "Changes of Th17/Treg cells and protective effect of mica in mice with experimental colitis," *Chinese Journal of inflammatory bowel disease*, vol. 2, pp. 305–310, 2018.